AD-A099 988 ARMY MISSILE COMMAND REDSTONE ARSENAL AL ADVANCED S--ETC F/G 17/9
PERFORMANCE COMPARISON OF CELL AVERAGING AND 'GREATEST-OF' CONS--ETC(U)
FEB 81 N B LAWRENCE
UNCLASSIFIED DRSMI-RE-81-9-TR SBIE-AD-E950 131 NL

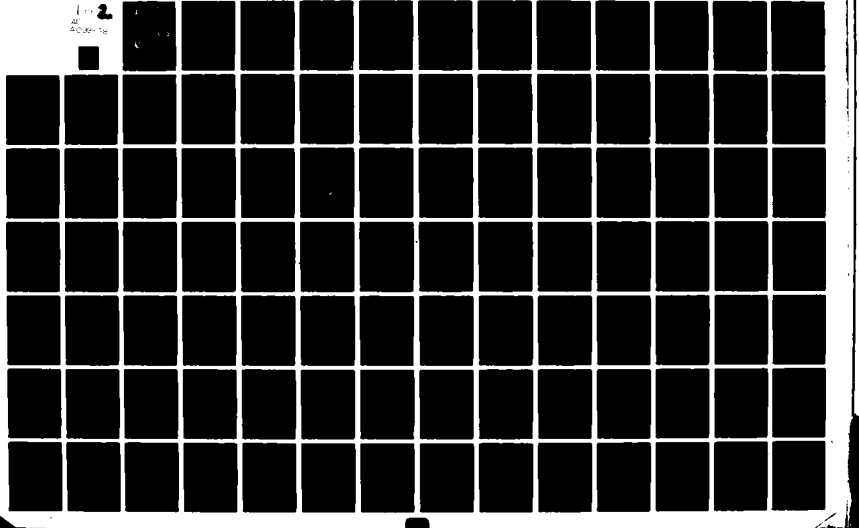

AD-E950131

(12) LEVEL III

AD A099988

TECHNICAL REPORT RE-81-9

PERFORMANCE COMPARISON OF CELL AVERAGING AND "GREATEST-OF" CONSTANT FALSE ALARM RATE (CFAR) METHODS

Neal B. Lawrence
Advanced Sensors Directorate
US Army Missile Laboratory

February 1981

U.S. ARMY MISSILE COMMAND
Redstone Arsenal, Alabama 35898

81 6 08 048

DISPOSITION INSTRUCTIONS

DESTROY THIS REPORT WHEN IT IS NO LONGER NEEDED. DO NOT RETURN IT TO THE ORIGINATOR.

DISCLAIMER

THE FINDINGS IN THIS REPORT ARE NOT TO BE CONSTRUED AS AN OFFICIAL DEPARTMENT OF THE ARMY POSITION UNLESS SO DESIGNATED BY OTHER AUTHORIZED DOCUMENTS.

TRADE NAMES

USE OF TRADE NAMES OR MANUFACTURERS IN THIS REPORT DOES NOT CONSTITUTE AN OFFICIAL INDORSEMENT OR APPROVAL OF THE USE OF SUCH COMMERCIAL HARDWARE OR SOFTWARE.

UNCLASSIFIED

SECURITY CLASSIFICATION OF THIS PAGE (When Data Entered)

REPORT DOCUMENTATION PAGE

READ INSTRUCTIONS BEFORE COMPLETING FORM

1. REPORT NUMBER: Technical Report RE-81-9	2. GOVT ACCESSION NO.: AD-A099988
3. RECIPIENT'S CATALOG NUMBER:	
4. TITLE (and Subtitle): PERFORMANCE COMPARISON OF CELL AVERAGING AND "GREATEST-OF" CONSTANT FALSE ALARM RATE (CFAR) METHODS	5. TYPE OF REPORT & PERIOD COVERED: Technical Report
	6. PERFORMING ORG. REPORT NUMBER:
7. AUTHOR(s): Neal B. Lawrence	8. CONTRACT OR GRANT NUMBER(s):
9. PERFORMING ORGANIZATION NAME AND ADDRESS: Commander, US Army Missile Command, Attn: DRSMI-RER, Redstone Arsenal, AL 35898	10. PROGRAM ELEMENT, PROJECT, TASK AREA & WORK UNIT NUMBERS:
11. CONTROLLING OFFICE NAME AND ADDRESS: Commander, US Army Missile Command, Attn: DRSMI-RER, Redstone Arsenal, AL 35898	12. REPORT DATE: February 1981
	13. NUMBER OF PAGES: 132
14. MONITORING AGENCY NAME & ADDRESS(if different from Controlling Office):	15. SECURITY CLASS. (of this report): Unclassified
	15a. DECLASSIFICATION/DOWNGRADING SCHEDULE:

16. DISTRIBUTION STATEMENT (of this Report)

Approved for public release; distribution is unlimited.

17. DISTRIBUTION STATEMENT (of the abstract entered in Block 20, if different from Report)

18. SUPPLEMENTARY NOTES

19. KEY WORDS (Continue on reverse side if necessary and identify by block number)

Radar
Radar Signal Processing
Constant False Alarm Rate (CFAR)
Cell Averaging
Greatest-Of
Probability of False Alarm
Probability of Detection

20. ABSTRACT (Continue on reverse side if necessary and identify by block number)

Radar system detection procedures involve the comparison of a received signal to a threshold value. A fixed threshold is not successful in controlling the false alarms because of changing interference conditions such as noise, clutter, and jammers. Consequently, an adaptive threshold is frequently used to establish a constant false alarm rate (CFAR). The maximum likelihood cell averaging approach is one of the adaptive procedures. The

(continued)

DD FORM 1 JAN 73 1473 EDITION OF 1 NOV 65 IS OBSOLETE

UNCLASSIFIED

SECURITY CLASSIFICATION OF THIS PAGE (When Data Entered)

20. Abstract (continued)

cell averaging CFAR is of major importance because it has superior performance in homogeneous Gaussian noise. Unfortunately, nonhomogeneous interference such as that produced at chaff and clutter edges will degrade the performance of the cell averaging CFAR. The search for a CFAR method which can control the false alarms resulting from clutter edges has produced a modification to the cell averaging approach which is known as the "greatest-of" CFAR.

The objective of this effort was to compare the performance of the cell averaging and "greatest-of" CFAR methods for different processor configurations (i.e., detector laws, wordlengths CFAR window width, etc.) and environmental conditions (i.e., homogeneous noise, nonhomogeneous interference, interfering target, etc.). The performance comparison was made based on probabilities of false alarm and probabilities of detection determined by a Monte Carlo simulation.

This report contains a review of a fixed threshold analysis, a review of the theoretical analysis of three CFAR techniques: cell averaging, "greatest-of," and log/CFAR, a performance comparison of the cell averaging and "greatest-of" CFAR techniques, and a summary of the results with recommendations for future effort.

Three significant results were obtained. The performance of the two CFAR methods is independent of the detector, i.e., square law or linear. The cell averaging gives better detection performance in an interfering target environment, while the "greatest-of" provides better false alarm regulation in a nonhomogeneous interference environment.

TABLE OF CONTENTS

TABLE OF CONTENTS (cont'd)

LIST OF TABLES

LIST OF TABLES (cont'd)

LIST OF FIGURES

LIST OF FIGURES (cont'd)

LIST OF FIGURES (cont'd)

LIST OF SYMBOLS

CFAR	Constant false alarm rate
$\overline{\Delta}$dB	Average signal-to-noise difference in decibels
dB	Decibels
K	Cell averaging CFAR constant
K_G	"Greatest-of" CFAR constant
N	Number of CFAR reference cells or window size
N_I, N_Q	In-phase and quadrature channel noise components
P	IF signal peak
PFA	Probability of false alarm
$\overline{PFA}_{CA}$	Cell averaging CFAR average PFA
$\overline{PFA}_G$	"Greatest-of" CFAR average PFA
$\overline{PFA}_D$	Design average PFA
$\overline{PFA}_P$	Prototype average PFA
PD	Probability of detection
$\overline{PD}_{CA}$	Cell averaging CFAR average PD
$\overline{PD}_G$	"Greatest-of" CFAR average PD
$\overline{PD}_P$	Prototype average PD
pdf	Probability density function
S_I, S_Q	In-phase and quadrature channel signal components
SNR	Signal-to-noise ratio
σ^2	Gaussian noise variance
u, u_1, u_2	Independent uniform random variables

LIST OF SYMBOLS (cont'd)

x_I, x_Q	In-phase and quadrature channel video
x	IF signal-to-noise ratio
$\bar{x}$	Average IF signal-to-noise ratio
y	Square Law detector output
y_i	Detector output for cell i
y_o	Detector output for cell o or cell of interest
Y_{th}	Fixed or adaptive threshold value for square law detector system
Y_G	"Greatest-of" CFAR threshold value
z	Linear detector output
Z_{th}	Fixed threshold value for linear detector system
σ^o	Clutter backscatter coefficient

CHAPTER I. INTRODUCTION

1.0 Background

The basic operation of a radar is the transmission and reception of electrical energy. The received signal or radar return is composed of target, noise, jammer and/or clutter energy. For a ground-based air defense radar, the target is an aircraft, missile, etc.; clutter is ground, trees, rain or chaff; and jammers are electrical energy transmission devices. Whereas proper radar design will reduce the effects of clutter and jammers while enhancing the target, a signal processor is normally required to provide target enhancement while rejecting interference. Additional interference, i.e., thermal noise from system electronic components, increases the total interference power which the processor must reduce.

A typical quadrature channel radar digital signal processor is shown in Figure 1. The mixers and the lowpass filters are used to translate the intermediate frequency bandpass radar signal to in-phase and quadrature channel baseband signals. After the signals are digitized by the analog-to-digital converters, the clutter power is reduced by clutter rejection filters, commonly referred to as moving target indicators (MTI). Once the clutter power is reduced below the thermal ncise level, the signal-to-noise (and/or jammer) ratio is improved by some type of coherent integrator, for instance, a fast Fourier transformer. With the clutter rejected and the signal-to-noise ratio increased, the amplitude of each range/doppler cell is extracted. These detected outputs are sent to a decision element.

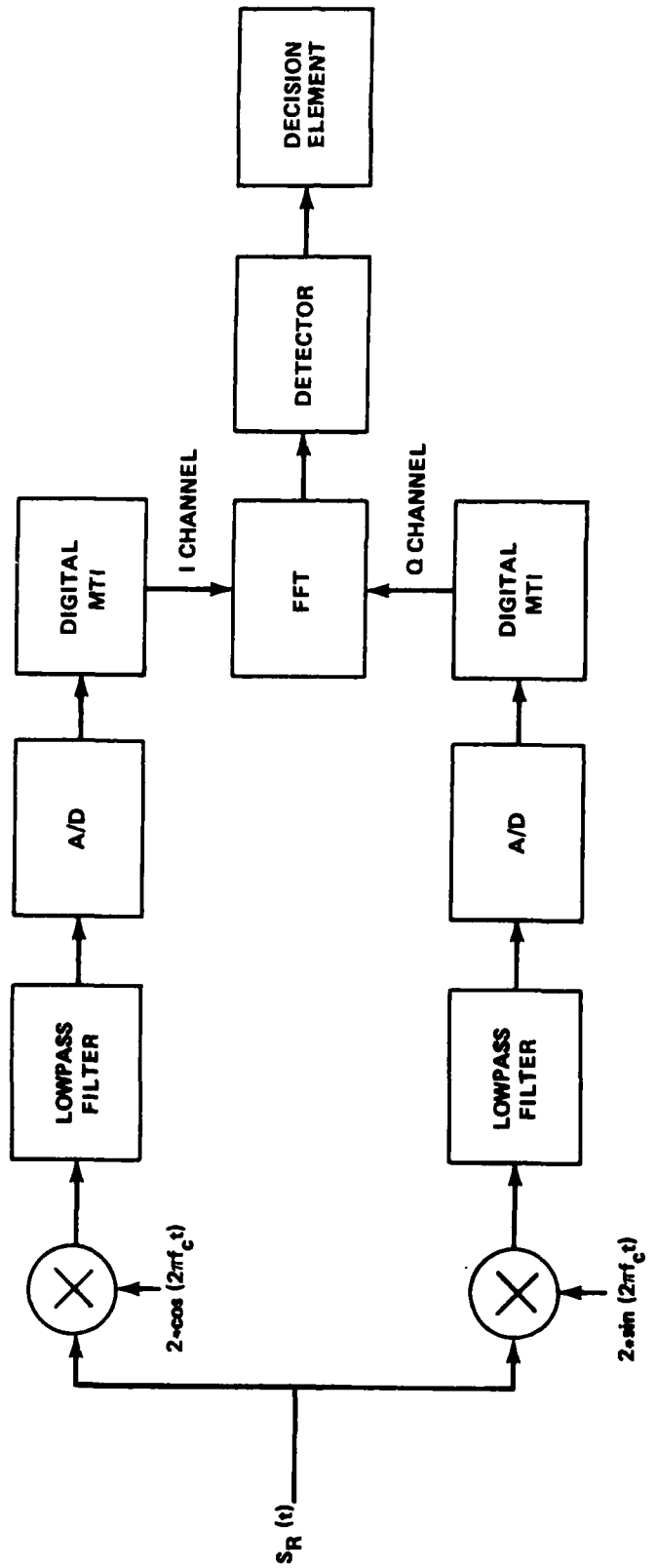

Figure 1. Quadrature Channel Digital Signal Processor Configuration

The function of the decision element is to produce an output or target report only if a target is present, i.e., a detection. If no target is present and an output is reported, this is a false alarm which the decision element should minimize. Typically, the probability of detection should be greater than 50 percent while the false alarm rate, or probability of false alarm, would be between 10^{-3} and 10^{-9}.

Basically, the decision element compares a threshold (which is a function of the system probability of false alarm requirement) to the detector outputs. A target report is issued if the threshold is exceeded.

If a fixed threshold decision element is used, the false alarm rate is extremely sensitive to small changes in the average value of the energy from all sources of interference. This sensitivity is easily seen in Figure 2. If the threshold is set for a probability of false alarm of 10^{-8}, an increase of only 3 dB in total interference power density corresponds to a 10^{4} increase in the probability of false alarm. This increase would put an unreasonable demand on the radar data processor. Therefore, an adaptive threshold decision element is required to provide acceptable target detectability while maintaining a constant false alarm rate (CFAR).

The processing principles used to counteract the variations in the output interference level are referred to as constant false alarm rate (CFAR) or adaptive detection processing techniques. The most common approach to the design of such CFAR processors is to sample the background interference in the time-and/or-frequency domain around the current range and doppler cell, then utilize the samples to estimate

the unknown statistical parameters of the interference. This estimate is used to maintain a CFAR by control of the threshold level.

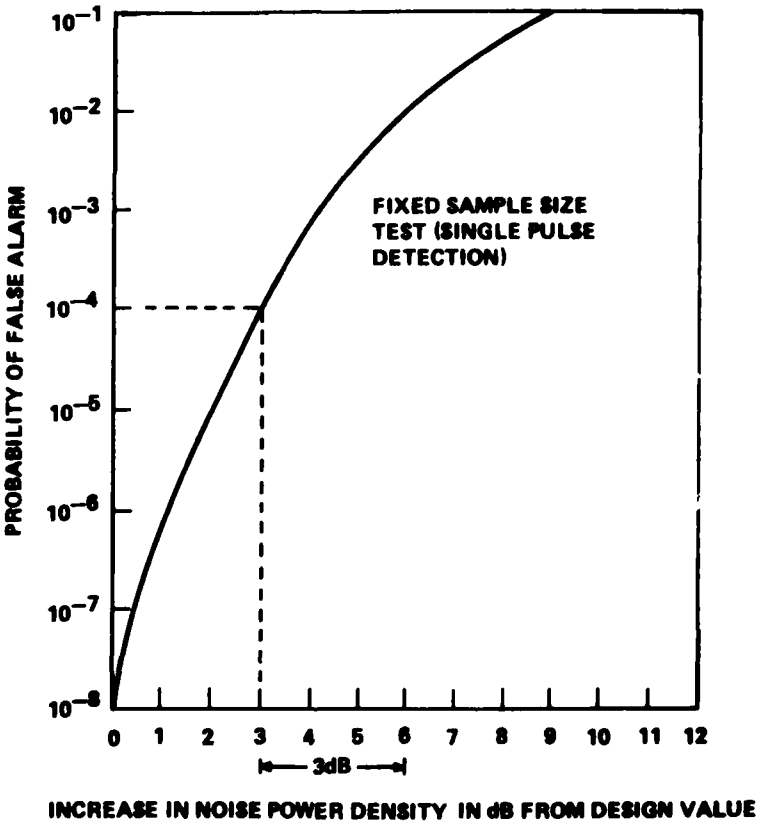

Figure 2. False Alarm Probability for Fixed Threshold Detection

1.1 Purpose

The purpose of this study is to compare the performance of two commonly known CFAR techniques, the cell averaging and the "greatest-of." The performance comparison will be based on detection probabilities and false alarm probabilities obtained from a Monte Carlo simulation of the two techniques. The performance of the processors will be determined for different target models, clutter environments, detector laws, wordlengths, and interfering target power levels. The simulation will be utilized for verification of theoretical performance results

and determination of performance results not obtainable by present analytical methods.

1.2 Content

Chapter II reviews the theoretical analysis of a fixed threshold processor. Probability density functions at the detector output are derived for noise only and target plus noise for both a linear and a square law detector. Two target models are used, a steady or nonfluctuating target and a Swerling I target. The probability of false alarm for each detector is determined by using the noise only probability density functions. The probability of detection is determined for each detector and a steady target, and for the square law detector and a Swerling I target.

Chapter III contains a theoretical analysis of three commonly known adaptive threshold or CFAR techniques. The CFAR techniques are cell averaging, "greatest-of," and log. Each technique is described and various performance equations are derived or given. Probability of false alarm and probability of detection equations are derived for the cell averaging and "greatest-of" CFAR methods.

Chapter IV describes the Monte Carlo simulation developed for a performance comparison of the cell averaging and the "greatest-of" CFAR techniques. Mathematical models of the targets, noise and clutter are given. Implementation of the two CFAR techniques is presented. Finally, the determination of the probabilities of false alarm and probabilities of detection for both CFAR processors is discussed.

Chapter V presents a performance comparison of the two CFAR processors based on the false alarm and detection probabilities obtained from the Monte Carlo simulation. The comparisons include different

detector laws, clutter environments, quantization wordlengths, and interfering target power levels.

Chapter VI contains the summary, conclusions, and recommendations for future work.

CHAPTER II. FIXED THRESHOLD PERFORMANCE ANALYSIS

2.0 Introduction

The radar statistical detection problem in noise is one of choosing between signal and noise at the radar processor output or noise alone; that is, when the processor output voltage is described by v(t), one wants to test per range cell between H_0 (noise alone) or H_1 (signal plus noise) as follows:

$$H_0: \quad v(t) = n(t)$$
$$H_1: \quad v(t) = s(t) + n(t) \ . \tag{2.1}$$

The fixed threshold analysis assumes that the decision element is preceded by a prewhitening or clutter rejection filter, such as an MTI.

The decision element in Figure 1 tests the processed video to determine whether a signal is present (H_1) or not present (H_0). For a specified voltage level or threshold, the decision element reports a target if the amplitude of the video is greater than the threshold, and reports no target if the video amplitude is less than the threshold.

It is possible that processed video which contains only noise can exceed the threshold generating a false target report or false alarm. By increasing the threshold the number of false alarms diminishes. However, the chances of detecting a target also decrease. Consequently the threshold setting is made as low as possible, consistent with a tolerable false alarm rate with which the system can operate.

In a given system the fixed threshold would be determined by establishing a tolerable false alarm rate based on overall system

considerations. Having determined the threshold setting, the probability of detecting a desired target can be calculated.

This chapter will discuss the probability density functions (pdf) at the output of the detector for both a square law and a linear detector with noise only and signal plus noise inputs. The signal or target models used were a nonfluctuating or steady target [1] and a Swerling I target [2]. Expressions are given for the probability of false alarm and the probability of detection associated with the pdf.

2.1 Noise Only

This section gives the pdf and probability of false alarm expressions for the single pulse amplitude detected noise only cases. The detectors considered are the linear and square law detectors.

2.1.1 Linear Detector

A linear detector extracts the envelope of the video and is given as

$$z = \sqrt{x_I^2 + x_Q^2} \ , \tag{2.2}$$

where x_I is the in-phase video, x_Q is the quadrature video, and z is the detector output.

If x_I and x_Q are independent zero mean Gaussian random variables and homogeneous, i.e., they have the same variance, σ^2, the pdf of z is

$$p(z) = \frac{z}{\sigma^2} \exp[-z^2/2\sigma^2] \ . \tag{2.3}$$

This pdf is the well known Rayleigh distribution.

Assuming a fixed threshold, Z_{th}, the probability of false alarm is

$$PFA = \int_{Z_{th}}^{\infty} p(z)dz = \int_{Z_{th}}^{\infty} \frac{z}{\sigma^2} \exp[-z^2/2\sigma^2]dz \ ,$$

by a change of variables

$$w = z^2 \qquad dw = 2zdz$$

$$W_{th} = Z_{th}^2$$

then

$$PFA = \int_{Z_{th}^2}^{\infty} \frac{1}{2\sigma^2} \exp[-w/2\sigma^2]dw = \exp\left[-Z_{th}^2/2\sigma^2\right] . \tag{2.4}$$

This equation can be used to determine a threshold given a desired probability of false alarm, i.e.,

$$Z_{th} = [-\ln(PFA)2\sigma^2]^{\frac{1}{2}} . \tag{2.5}$$

2.1.2 Square Law Detector

A square law detector produces an output which is proportional to the square of the video envelope and is given by

$$y = x_I^2 + x_Q^2 , \tag{2.6}$$

where x_I is the in-phase video, x_Q is the quadrature video, and y is the detector output.

If x_I and x_Q are independent zero mean Gaussian random variables and homogeneous, i.e., they have the same variance, σ^2, the pdf of y is

$$p(y) = \frac{1}{2\sigma^2} \exp[-y/2\sigma^2] . \tag{2.7}$$

The pdf is the well known exponential distribution.

Assuming a fixed threshold, Y_{th}, the probability of false alarm is

$$PFA = \int_{Y_{th}}^{\infty} p(y)dy = \exp\left[-Y_{th}/2\sigma^2\right] . \tag{2.8}$$

This equation can be used to determine a threshold given a desired probability of false alarm, i.e.,

$$Y_{th} = [-\ln(PFA)2\sigma^2] . \tag{2.9}$$

2.2 Target Plus Noise

This section gives the pdf and probability of detection expressions for the single pulse amplitude detected target plus noise cases. The target will be either a nonfluctuating or steady target or a Swerling I target.

At this point, it is desirable to discuss the definition of intermediate frequency (IF) signal-to-noise ratio, x, commonly found in radar literature. The basic writings of Marcum [1], Swerling [2], and Rice [3] used the following:

$$x = \frac{\text{Average Signal Power at IF}}{\text{Average Noise Power at IF}} = \frac{P^2}{2\sigma^2} \tag{2.10}$$

where the received target is $P\cos(2\pi ft + \theta)$ whose IF average power is $P^2/2$.

For simplicity, it can be assumed that any quadrature channel processing, such as a clutter rejection filter, will not affect the signal-to-noise ratio. Hence the IF signal-to-noise ratio and the detector input signal-to-noise ratio are the same.

2.2.1 Steady Target

A steady target [1] is defined as a target where the signal-to-noise ratio for one pulse describes the signal-to-noise ratio of any pulse of a train under consideration. Hence, the pdf is

$$p(x) = P^2/2\sigma^2 \ , \tag{2.11}$$

where P is the IF signal peak.

2.2.1.1 Linear Detector

The pdf of a single steady target plus noise variate, z, after linear detection is derived in Appendix A:

$$p(z) = \frac{z}{\sigma^2} \exp\left[-\frac{z^2 + P^2}{2\sigma^2}\right] I_o\left(\frac{zP}{\sigma^2}\right) , \tag{2.12}$$

where P is the peak signal voltage prior to detection, σ^2 is again the same variance, and I_o is the modified Bessel function of the first kind of zero order [4].

The probability of detection is given by

$$PD = \int_{Z_{th}}^{\infty} p(z)dz = \int_{Z_{th}}^{\infty} \frac{z}{\sigma^2} \exp\left[-\frac{z^2 + P^2}{2\sigma^2}\right] I_o\left(\frac{zP}{\sigma^2}\right) dz \ . \tag{2.13}$$

This equation is of the form of a Q-function [4]

$$Q(b,c) = \int_c^{\infty} a \exp\left[-\frac{a^2 + b^2}{2}\right] I_o(ab)da \tag{2.14}$$

and thus Equation (2.13) can be written as

$$PD = Q(b,c) \ , \tag{2.15}$$

where $b = P/\sigma$ and $c = Z_{th}/\sigma$.

2.2.1.2 Square Law Detector

The pdf of a single steady target plus noise variate, y, of a square law amplitude detector is

$$p(y) = \frac{1}{2\sigma^2} \exp\left[-\frac{y + P^2}{2\sigma^2}\right] I_o\left(\frac{\sqrt{2y}P}{\sigma^2}\right) \tag{2.16}$$

which is obtained from Equation (2.12) by a change of variables.

The probability of detection for the square law detector is the same as for the linear detector given in Equation (2.15), i.e.,

$$PD = Q(b,c) \ , \tag{2.17}$$

where $b = P/\sigma$ and $c = \sqrt{Y_{th}}/\sigma$.

2.2.2 Swerling I Target

A Swerling I target [2] is defined as samples which are correlated within a pulse group but are independent on a scan-to-scan basis (slowly fading). This case is applicable to many radar targets since they tend not to be independent from pulse to pulse, but independent from scan to scan due to target position change.

The pdf for a single sample signal-to-noise ratio, x, is

$$w(x,\bar{x}) = \frac{1}{\bar{x}} \exp\left[-\frac{x}{\bar{x}}\right] , \tag{2.18}$$

where $\bar{x} = \overline{p^2}/2\sigma^2$ is the average signal-to-noise ratio.

2.2.2.1 Linear Detector

The mathematical analysis of a Swerling I target plus noise and a linear detector is difficult and no analysis was found in the literature.

2.2.2.2 Square Law Detector

The pdf for a single Swerling I target plus noise square law detector output variate, y, is derived in Appendix A and is given as

$$p(y) = \frac{1}{2\sigma^2\ (1+\bar{x})} \exp\left[-\frac{y}{2\sigma^2\ (1+\bar{x})}\right] u(y) \ . \tag{2.19}$$

The probability of detection is given by

$$PD = \int_{Y_{th}}^{\infty} p(y)dy = \int_{Y_{th}}^{\infty} \frac{1}{2\sigma^2 (1+\bar{x})} \exp\left[-\frac{y}{2\sigma^2 (1+\bar{x})}\right] dy$$

$$= \exp\left[-Y_{th}/2\sigma^2 (1+\bar{x})\right] . \qquad (2.20)$$

Substituting Equation (2.8) yields

$$PD = PFA^{\frac{1}{1+\bar{x}}} . \qquad (2.21)$$

2.3 Conclusions

A fixed threshold decision element is normally used to specify radar system performance. Due to the complex equations obtained when a linear detector and/or a steady target is used, the performance will normally be based on a Swerling I target model and a square law detector. This assumption does not cause any significant problems. The Swerling I target model is a realistic model for many radar targets and the square law and linear detector have, as shown by Marcum [1], essentially the same detection performance for a single pulse.

In an actual radar system, the use of a fixed threshold would require having a priori knowledge of the thermal noise variance, σ^2, to maintain a desired probability of false alarm. For example, if PFA = 10^{-6}, then from Equation (2.8)

$$Y_{th} = -\ln(PFA)2\sigma^2 = 27.63\sigma^2 . \qquad (2.22)$$

Hence Y_{th} is a function of the input noise variance, σ^2. As shown in Chapter I, the probability of false alarm is strongly affected by a change in σ^2.

Even if exact knowledge of the thermal noise were available, the total system interference variance can change due to residual clutter not cancelled by the prewhitening filter or jammers. Therefore, an adaptive technique for determining the threshold is required. These techniques are referred to as constant false alarm rate (CFAR) processors or adaptive detection processors.

CHAPTER III. ADAPTIVE THRESHOLD ANALYSIS

3.0 Introduction

This chapter reviews the theoretical analysis of three commonly found CFAR processors: cell averaging, "greatest-of," and log. Basically, these processors sample the background interference in the time domain around a cell, i.e., a range cell of interest, and then utilize the samples to estimate the unknown statistical parameters of the interference. This estimate is used to determine a threshold for the cell of interest.

The estimated threshold's probability density functions are given, and equations for the probability of false alarm and probability of detection are derived for the cell averaging and "greatest-of" CFAR techniques. The analysis assumes a square law detector and a Swerling I target for reasons stated in Chapter II.

Only a limited analysis of the log CFAR is presented due to a lack of available analytical results. An equivalence to the cell averaging technique is discussed.

As in the fixed threshold analysis, the CFAR processor analysis will be based on white Gaussian noise interference which is a result of the prewhitening or clutter rejection filter.

3.1 Cell Averaging CFAR Analysis

This procedure (Figure 3) forms the threshold Y_{th} by scaling the average value of N square law detected reference cell outputs of the quadrature channels, I and Q, i.e.,

$$Y_{th} = \frac{K}{N} \sum_{n=1}^{N} y_n = \frac{K}{N} \sum_{n=1}^{N} \left(x_I^2 + x_Q^2\right)_n = \frac{K}{N} \sum_{n=1}^{2N} (x_{IQ})_n \tag{3.1}$$

where the last summation results since it is equivalent to summing 2N statistically independent, squared, zero mean Gaussian random variables x_{IQ}. It is assumed that the referenced cells are homogeneous, i.e., each $(x_{IQ})_n$ has the same variance, σ^2. Consequently the distribution for $NY_{th}/K\sigma^2$ will have a chi-square pdf with 2N degrees of freedom. The pdf for Y_{th} is obtained by changing variables on the chi-square pdf [5]. Thus

$$p(Y_{th}) = \left(\frac{N}{2K}\right)^N \frac{1}{\sigma^2\,(N-1)!} \left(\frac{Y_{th}}{\sigma^2}\right)^{N-1} \exp\left[-Y_{th}N/(2\sigma^2K)\right] u(Y_{th}) . \tag{3.2}$$

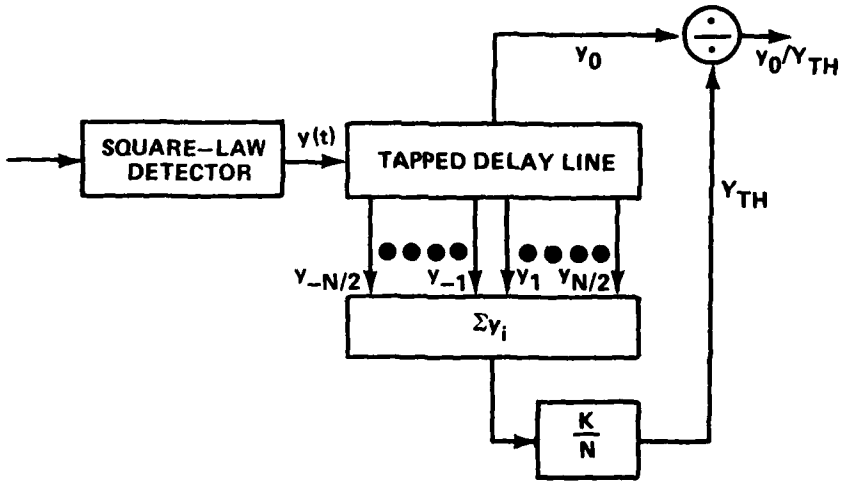

Figure 3. Block Diagram of a Conventional Cell Averaging CFAR Processor

This equation can be used with the fixed threshold PFA of Equation (2.8) to obtain the expected PFA when the cell averaging CFAR controls the threshold, i.e.,

$$\overline{PFA}_{CA} = E\{PFA\} = \int_{-\infty}^{\infty} \exp\left[-Y_{th}/2\sigma^2\right] p(Y_{th}) dY_{th}$$

$$= \left(\frac{N}{K}\right)^N \frac{1}{(N-1)!} \frac{1}{2\sigma^2} \int_0^{\infty} \exp\left[-Y_{th}/2\sigma^2\right] \left(\frac{Y_{th}}{2\sigma^2}\right)^{N-1} \exp\left[-NY_{th}/2K\sigma^2\right] dY_{th} .$$

Letting $a = Y_{th}/(2\sigma^2)$ gives

$$\overline{PFA}_{CA} = \left(\frac{N}{K}\right)^N \frac{1}{(N-1)!} \int_0^{\infty} a^{N-1} \exp[-a(N/K+1)] da . \qquad (3.3)$$

Letting $a = b/(N/K+1)$ yields

$$\overline{PFA}_{CA} = \left(\frac{N}{K}\right)^N \frac{1}{(N-1)!} \int_0^{\infty} \frac{b^{N-1}}{\left(\frac{N}{K}+1\right)^{N-1}} \exp[-b] \frac{db}{\frac{N}{K}+1}$$

$$= \left(\frac{N}{K}\right)^N \frac{1}{(N-1)!} \frac{1}{\left(\frac{N}{K}+1\right)^N} \int_0^{\infty} b^{N-1} \exp[-b] db$$

$$\overline{PFA}_{CA} = \left(1 + \frac{N}{K}\right)^{-N} .$$

This allows the CFAR threshold constant, K, to be determined from the desired average probability of false alarm, $\overline{PFA}_{CA}$, i.e.,

$$K = N\left[\left(\frac{1}{\overline{PFA}_{CA}}\right)^{1/N} - 1\right] . \qquad (3.4)$$

It is easily seen that the average probability of false alarm is not dependent on the noise variance. Hence, the Gaussian noise level does not have to be known to maintain CFAR. Nitzberg [6] called this an unknown level CFAR, but it is commonly known as a range cell averaging CFAR.

The expected value of the probability of detection $\overline{PD}_{CA}$ for the Swerling I target can be determined by the same procedure, i.e.,

$$\overline{PD}_{CA} = E\{PD\} = \int_{-\infty}^{\infty} PD\ p(Y_{th})dY_{th}$$

$$= \int_{-\infty}^{\infty} \exp\left[-Y_{th}/2\sigma^2(1+\bar{x})\right] p(Y_{th})dY_{th} \qquad (3.5)$$

$$\overline{PD}_{CA} = \left(1 + \frac{K}{N(1+\bar{x})}\right)^{-N} .$$

Substituting Equation (3.3) yields

$$\overline{PD}_{CA} = \left[\frac{1 + \bar{x}}{\bar{x} + \overline{PFA}_{CA}^{-1/N}}\right]^N$$

where $\bar{x}$ is the average IF signal-to-noise ratio.

This result can be used to plot $\overline{PD}_{CA}$ versus $\bar{x}$ with $\overline{PFA}_{CA}$ and N as parameters. A typical curve is shown in Figure 4.

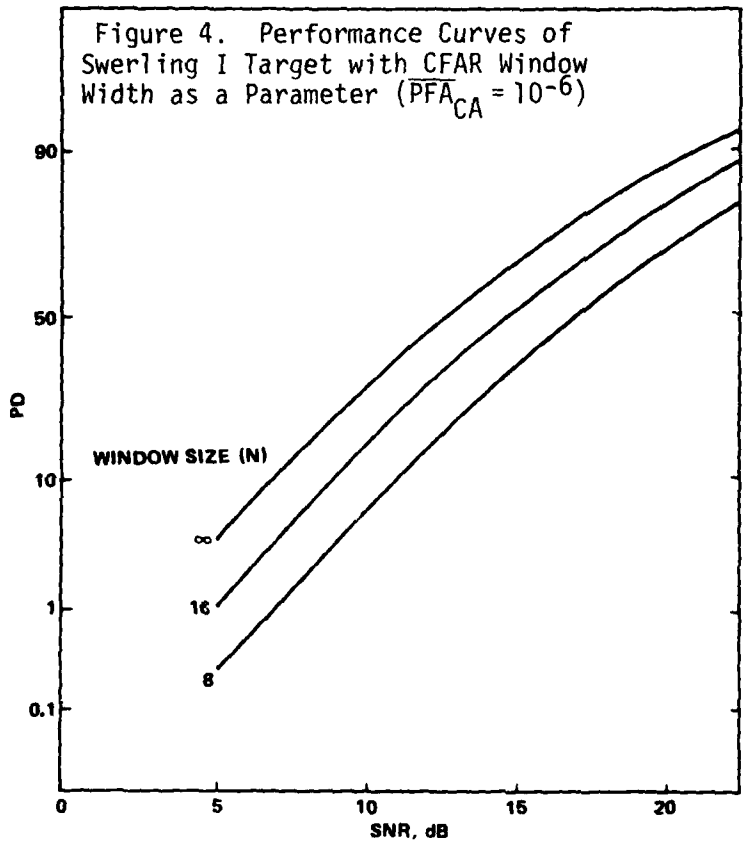

Figure 4. Performance Curves of Swerling I Target with CFAR Window Width as a Parameter ($\overline{PFA}_{CA} = 10^{-6}$)

Since the fixed threshold performance curves are extensively tabulated [7], a general cell averaging CFAR signal-to-noise loss curve is desirable. The loss is given by the equation from Moore [8],

$$L = -10 \log \left[\frac{\left[\frac{-R/N}{\log \frac{1 + \bar{x}_{CA}}{\bar{x}_{CA} + 10^{R/N}}} \right] - 1}{\bar{x}_{CA}} \right] \tag{3.6}$$

where R corresponds to the exponential in the $\overline{PFA}_{CA}$, i.e., $\overline{PFA}_{CA} = 10^{-R}$, N is the number of reference cells, and $\bar{x}_{CA}$ is cell averaging signal-to-noise ratio necessary to give the same PD at $\bar{x}$ for a fixed threshold detector. This loss is shown in Figure 5.

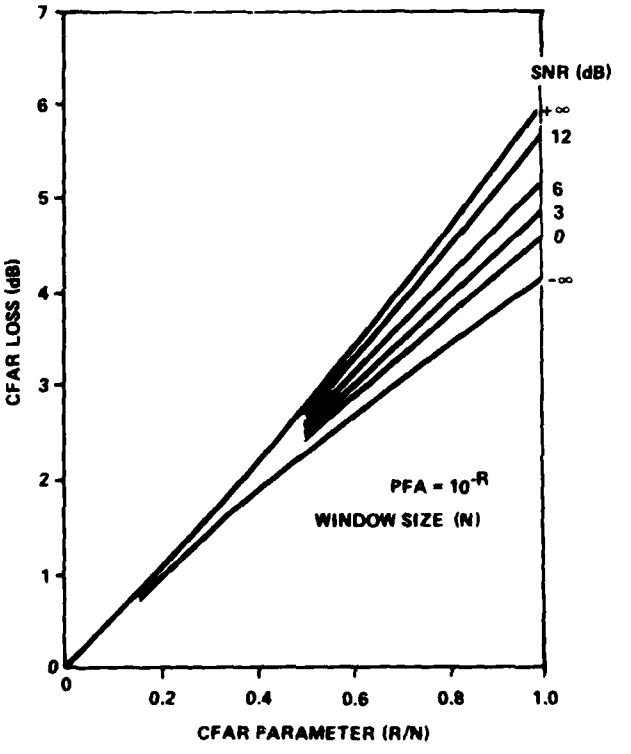

Figure 5. Cell Averaging CFAR Loss

3.2 "Greatest-Of" CFAR Analysis

In this method (Figure 6), the reference cells are divided into two subsets of size N/2. The cell averaging method is used to determine a threshold for each of the reference cell subsets. One subset is located before the reference cell of interest and the other after the reference cell of interest. The "greatest-of" CFAR threshold is obtained by selecting the largest value from the two subset thresholds, i.e.,

$$Y_1 = \frac{K_G}{N/2} \sum_{n=1}^{N/2} y_n$$

$$Y_2 = \frac{K_G}{N/2} \sum_{n=-1}^{-N/2} y_n$$

$$Y_G = \text{MAX}\,[Y_1, Y_2]\ . \qquad (3.7)$$

The G subscripts for "greatest-of" are used so that there is a distinction from the cell averaging processor.

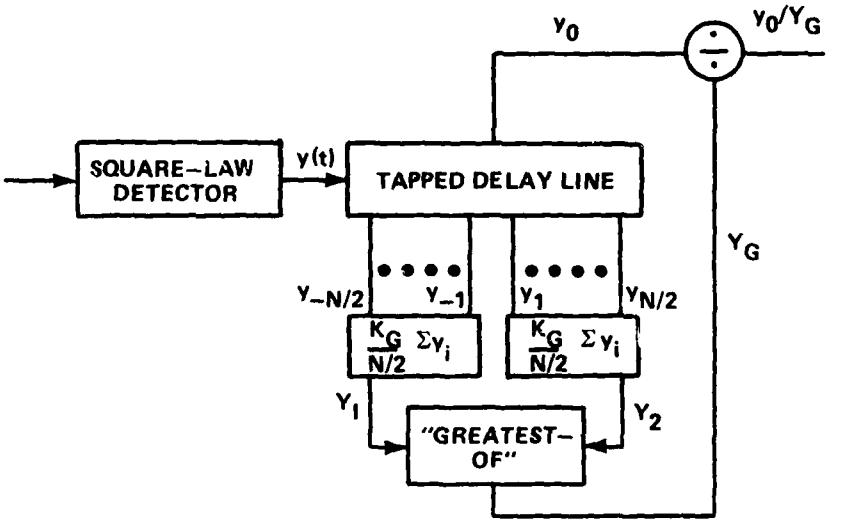

Figure 6. Block Diagram of a "Greatest-of" CFAR Processor

Since Y_1 and Y_2 are determined by the cell averaging method, then $NY_1/(2K_G\sigma^2)$ and $NY_2/(2K_G\sigma^2)$ are chi-square distributions with N degrees of freedom. Consequently, the pdf for Y_1 (or Y_2) can be obtained from Equation (3.2).

By replacing Y with Y_1 (or Y_2) and N with N/2, i.e., for Y_1

$$p(Y_1) = \left(\frac{N/2}{K_G}\right) \frac{1}{2\sigma^2} \frac{1}{(N/2 - 1)!} \left(\frac{Y_1}{2\sigma^2}\right)^{N/2 - 1} \exp\left[-\frac{N}{2K_G} \frac{Y_1}{2\sigma^2}\right] u(Y_1). \tag{3.8}$$

Papoulis [9] gives an expression for finding a pdf of the maximum of two random variables, cf., Equation (7-15), p. 193,

$$\begin{aligned} p_G(Y_G) &= 2F(Y)p(Y)\Big|_{Y=Y_G} \\ &= 2F_Y(Y_G)p_Y(Y_G) \end{aligned} \tag{3.9}$$

where the cumulative distribution function for Y_1 and Y_2 is represented by $F(\cdot)$.

The average probability of false alarm for the "greatest-of" CFAR is derived in Appendix A and is given by

$$\overline{PFA}_G = \frac{2\ \overline{PFA}_p}{\left(\frac{N}{2} - 1\right)!\left(1 + \overline{PFA}_p{}^{-2/N}\right)^{N/2}} \sum_{n=0}^{N/2 - 1} \frac{\left(n + \frac{N}{2} - 1\right)!}{n!\left(1 + \overline{PFA}_p{}^{2/N}\right)^n} \tag{3.10}$$

where $\overline{PFA}_p$ is called the prototype section PFA and is equal to

$$\overline{PFA}_p = \left(1 + \frac{K_G}{N/2}\right)^{-N/2} . \tag{3.11}$$

Note that this is an expression for a cell averaging CFAR which uses N/2 reference cells.

It is possible to solve for K_G in terms of $\overline{PFA}_P$ as in Equation (3.4) with N replaced by N/2, but K_G is not easily related to $\overline{PFA}_G$. However, the results of Equation (3.10) can be plotted as shown in Figure 7, then used to obtain the threshold constant. For example, if it is desired to establish $\overline{PFA}_G = 10^{-6}$ with N = 32, then from Figure 7, $\overline{PFA}_P = 1.75 \times 10^{-5}$. Consequently, K_G is calculated to be 15.73 and would be used in the Y_1 and Y_2 determinations in order to establish $\overline{PFA}_G = 10^{-6}$.

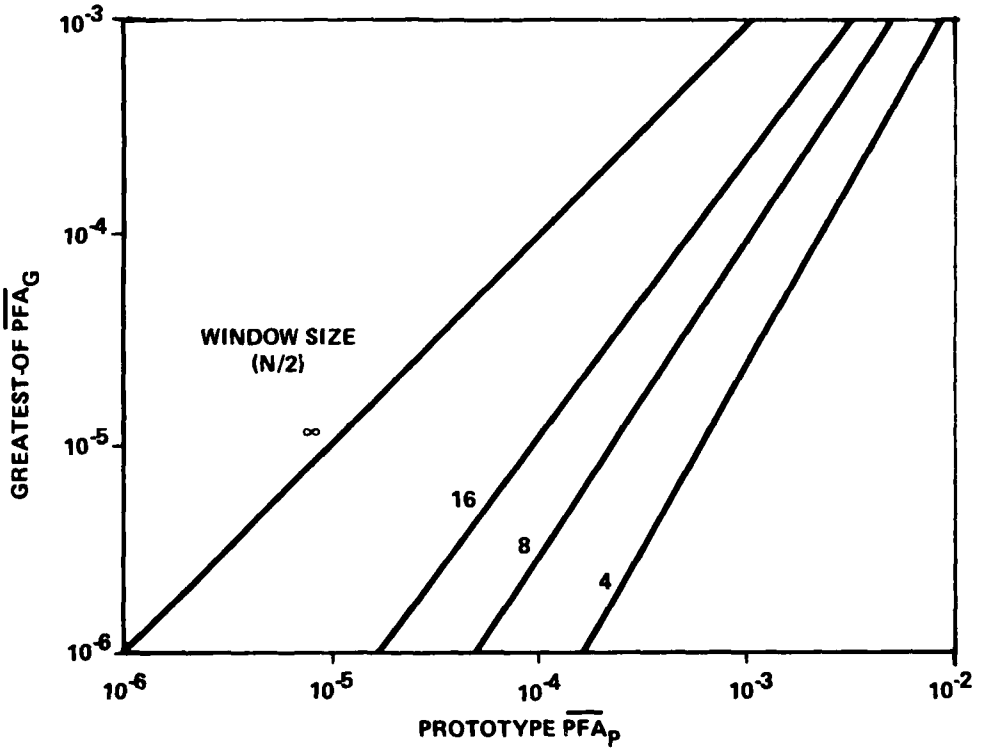

Figure 7. GO CFAR False Alarm Characteristics

Similar results derived in Appendix A hold for the probability of detection

$$\overline{PD}_G = \int_0^\infty PD\ P_G(Y_G)dY_G$$

$$= \frac{2\ \overline{PD}_P}{\left(\frac{N}{2} - 1\right)!\left(1 + \overline{PD}_P{}^{-2/N}\right)^{N/2}} \sum_{n=0}^{N/2-1} \frac{\left(n + \frac{N}{2} - 1\right)!}{n!\left(1 + \overline{PD}_P{}^{-2/N}\right)^n} \qquad (3.12)$$

where the prototype section $\overline{PD}_P$ is

$$\overline{PD}_P = \left(1 + \frac{2K_G}{N(1 + \bar{x})}\right)^{-N/2} = \left(\frac{\bar{x} + \overline{PFA}_P{}^{-2/N}}{1 + \bar{x}}\right)^{-N/2} . \qquad (3.13)$$

This represents the performance of a cell averaging CFAR with N/2 reference cells. Once $\overline{PFA}_P$ has been found (as from Figure 7), then $\overline{PD}_P$ can be calculated from Equation (3.13) and $\overline{PD}_G$ from Equation (3.12). It would be highly desirable to determine the signal-to-noise ratio loss for the "greatest-of" CFAR as compared to the ideal fixed threshold. Unfortunately, the complexity of Equation (3.12) prevents such an analysis.

Analysis of the "greatest-of" CFAR has been performed [8, 10, 11, 13]. One advantage of the "greatest-of" CFAR is discussed in References 8, 10, and 11, that is, the improved regulation of false alarms obtained for range extended clutter when compared to a cell averaging CFAR. Range extended clutter, discussed further in Chapters IV and V, is the weather or chaff clutter not rejected by the clutter filter and occupying some of the CFAR reference cells.

3.3 Log CFAR Analysis

This system (Figure 8) forms an estimate for the threshold as

$$V_T = K \prod_{j=1}^{N} y_j{}^{1/N} = K\left[\prod_{j=1}^{N} y_j\right]^{1/N} \qquad (3.14)$$

An equivalent method, Figure 9, for processing is to use a log detector at the input such that

$$\log V_T = \sum_{j=1}^{N} \frac{1}{N} \log y_j + \log K \tag{3.15}$$

is formed and $\log y_o$ is compared to this threshold.

The expected value of the estimate is determined to be

$$E\{V_T\} = K\left(E\left[y_j^{1/N}\right]\right)^N = 2K\sigma_j^2\left[\Gamma\left(\frac{1}{N} + 1\right)\right]^N . \tag{3.16}$$

The gamma function will become approximately equal to 1 for large N since $\Gamma(1)=1$. Thus the expected value of the threshold will become

$$\lim_{N \to \infty} E\{V_T\} = \lim_{N \to \infty} 2K\sigma_j^2\left[\Gamma\left(\frac{1}{N} + 1\right)\right]^N = 2K\sigma_j^2 \tag{3.17}$$

which is equal to $2K\sigma_o^2$ for homogeneous noise. Therefore a reasonable estimate can be formed by using the log CFAR algorithm.

Whereas a detailed mathematical analysis has not been performed, Hansen and Ward [12] have performed a Monte Carlo analysis of the log CFAR. Nitzberg [6], concerning a similar algorithm called the geometric-mean CFAR, has determined the probability of detection when an assumption is made about the noise distribution in the auxiliary cells, viz., the geometric-mean assumption.

In comparing the log CFAR and the cell averaging CFAR, Hansen and Ward [12] have proposed an empirically determined formula for the relationship between the number of reference samples required by the two detectors in order for their CFAR losses to be identical:

$$N_{log} = 1.65\, N_{CA} - 0.65 . \tag{3.18}$$

The main advantage of the log CFAR is the increased dynamic range available due to the log detector.

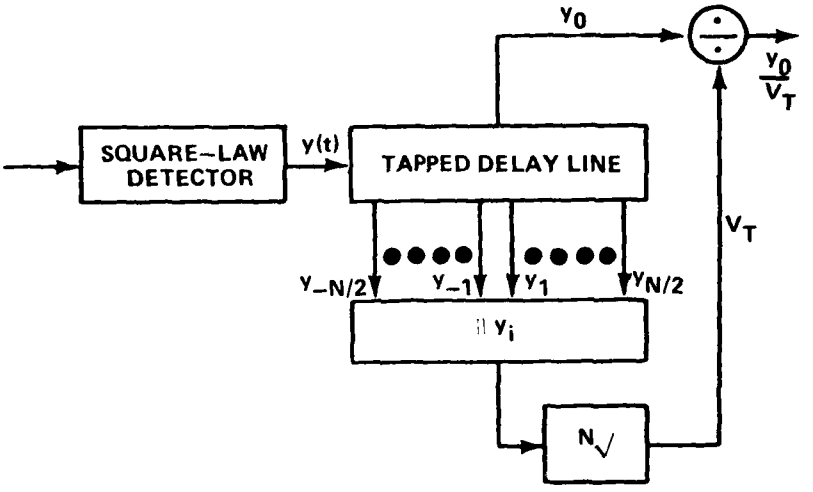

Figure 8. Block Diagram of Cell Averaging Log/CFAR Processor

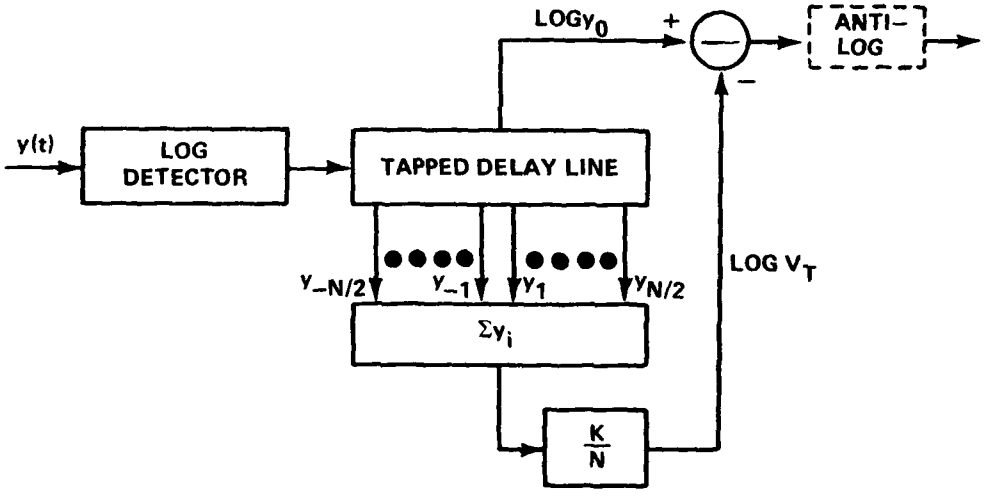

Figure 9. Equivalent Block Diagram of Cell Averaging Log/CFAR Processor

3.4 Summary

The cell averaging CFAR has been utilized extensively in radar signal processors due to its capability in homogeneous noise and its well understood and analyzed performance.

The log CFAR is simply a cell averaging CFAR following a log detector which provides performance equivalent to the cell averaging CFAR if the number of cells is sufficient. The log CFAR has been used extensively due to its dynamic range capability.

The "greatest-of" CFAR has not been used extensively, due partly to the original belief that it had approximately a 1 dB loss over the cell averaging CFAR, e.g., Hansen [10]. Recent work by Moore [8], Moore and Lawrence [11] and Hansen and Sawyer [13] has shown only a 0.2 dB difference in the two processors. Hence, the "greatest-of" CFAR, whose main advantage is the improved false alarm regulation in extended clutter [8, 11] should have increased utilization in radar processors.

CHAPTER IV. DESCRIPTION OF SIMULATION

4.0 Introduction

The cell averaging CFAR and the "greatest-of" CFAR are two commonly used techniques. Analysis of the cell averaging CFAR has been extensively performed [10, 14-16], but only limited analysis of the "greatest-of" CFAR has been performed [8, 11, 13].

The main thrust of this study is to determine the performance of the two CFAR processors by development of a simulation and utilization of Monte Carlo techniques. The performance results obtained are used to compare the two techniques. This chapter gives a description of the simulation.

4.1 Simulation Description

A block diagram of the simulation is shown in Figure 10.

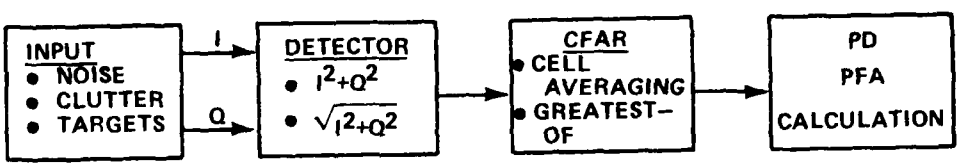

Figure 10. Block Diagram of CFAR Simulation

First, synthetic video composed of a combination of target, noise and clutter is generated for a quadrature channel processor. The amplitude is extracted by an exact square law or linear detector. The detected output is compared against a threshold determined by either a cell averaging CFAR or a "greatest-of" CFAR using other detected outputs.

If the detector output exceeds the threshold, a target detection is reported. If the output is interference only, this is a false alarm; if the output contains signal, this is a detection. A detection and false alarm count are maintained for both processors. Finally, after a number of Monte Carlo trials the detection and false alarm counts are used to calculate a probability of detection and a probability of false alarm for each processor.

4.2 Synthetic Video

This section discusses the target models, noise, and clutter used in the simulation.

4.2.1 Target Models

Two target models were used in the simulation: a steady or non-fluctuating target [1] and a Swerling I target [2].

The steady target is defined as a target where the signal-to-noise ratio for one pulse describes the signal-to-noise ratio of any pulse of a train under consideration. A steady target is modeled in the I and Q channels by

$$S_I = P\cos(\theta)$$
$$S_Q = P\sin(\theta) \qquad (4.1)$$

where P is the IF peak signal voltage and θ is a uniformly distributed random phase angle.

A Swerling I target is defined as samples which are correlated within a pulse train but are independent on a scan-to-scan basis (slowly fading). This case is applicable to many radar targets, since they tend not to be independent from pulse to pulse, but due to target position change, independent from scan to scan. The probability density function for one sample, x, is

$$w(x,\bar{x}) = \frac{1}{\bar{x}} \exp\left[-\frac{x}{\bar{x}}\right] \tag{4.2}$$

where $\bar{x} = \overline{P^2}/2\sigma^2$ is the average signal-to-noise ratio. Since the power distribution of a Swerling I target is the well known exponential, then the amplitude distribution is Rayleigh and the Swerling I target models in the I and Q channels are given by

$$\begin{aligned} S_I &= P\sqrt{-2\ln u_1}\cos(2\pi u_2) \\ S_Q &= P\sqrt{-2\ln u_1}\sin(2\pi u_2) \end{aligned} \tag{4.3}$$

where u_1 and u_2 are independent uniformly distributed variates from 0 to 1.

4.2.2 Noise Model

The system noise will be zero mean Gaussian noise whose pdf is given by

$$p(v) = \frac{1}{\sqrt{2\pi\sigma^2}} \exp[-v^2/2\sigma^2] \tag{4.4}$$

where σ^2 is the variance.

There is a procedure for generating uncorrelated Gaussian samples called the direct method [17]. In this procedure, pairs of independent samples (u_1, u_2) are drawn from a uniform distribution (0 to 1), then transformed as

$$\begin{aligned} v_1 &= \sqrt{-2\ln u_1}\cos(2\pi u_2) \\ v_2 &= \sqrt{-2\ln u_2}\sin(2\pi u_2) \end{aligned} \tag{4.5}$$

where v_1, v_2 are the uncorrelated samples of the Gaussian distribution. From Equation (4.5), u_1 and u_2 may be expressed as functions of v_1 and v_2

$$u_1 = \exp\left[-\frac{v_1^2 + v_2^2}{2}\right]$$

$$u_2 = \frac{1}{2\pi} \arctan\left(\frac{v_2}{v_1}\right) . \tag{4.6}$$

The independence of v_1 and v_2 can be shown as follows:

$$p_1(v_1, v_2) = p_2(u_1, u_2)|J| \tag{4.7}$$

where $|J|$ = absolute value of the Jacobian of the transformation, but, since $p_2(u_1, u_2) = p(u_1)\, p(u_2) = 1$,

$$p_1(v_1, v_2) = |J| \tag{4.8}$$

where

$$|J| = \frac{d(u_1,u_2)}{d(v_1,v_2)} = \begin{vmatrix} \frac{du_1}{dv_1} & \frac{du_1}{dv_2} \\ \frac{du_2}{dv_1} & \frac{du_2}{dv_2} \end{vmatrix} \tag{4.9}$$

and

$$p_1(v_1,v_2) = \begin{vmatrix} -x_1 \exp\left[-\frac{\left(v_1^2 + v_2^2\right)}{2}\right] & -x_2 \exp\left[-\frac{\left(v_1^2 + v_2^2\right)}{2}\right] \\ \frac{1}{2\pi} \frac{1}{\left(1 + \frac{v_2^2}{v_1^2}\right)\left(-\frac{v_2}{v_1^2}\right)} & \frac{1}{2\pi} \frac{1}{\left(1 + \frac{v_2^2}{v_1^2}\right)\left(\frac{1}{v_1}\right)} \end{vmatrix} \tag{4.10}$$

The above expression reduces to

$$p_1(v_1,v_2) = \frac{1}{2\pi} \exp\left[-\frac{v_1^2 + v_2^2}{2}\right] = \left(\frac{1}{\sqrt{2\pi}} \exp\left[-\frac{v_1^2}{2}\right]\right)\left(\frac{1}{\sqrt{2\pi}} \exp\left[-\frac{v_2^2}{2}\right]\right) \tag{4.11}$$

$$p_1(v_1,v_2) = |J| = p_1(v_1)p_1(v_2) . \tag{4.12}$$

Hence, v_1 and v_2 are independent Gaussian variables.

The variance of v_1 and v_2 is

$$\overline{v_1^2} = \overline{v_2^2} = 1 \ . \tag{4.13}$$

Hence, the Gaussian noise is modeled in the I and Q channels as

$$N_I = \sigma v_1$$
$$N_Q = \sigma v_2 \tag{4.14}$$

where v_1 and v_2 are defined in Equation (4.5) and σ is the standard deviation in each channel and at IF.

4.2.3 Clutter Models

Two clutter models were included in the simulation: nonhomogeneous interference and Weibull [18] distributed clutter.

The nonhomogeneous interference is clutter where the power density varies as a function of range, i.e., chaff or weather clutter which is distributed in range. The clutter power appears as a step function with a clutter edge [14] as shown in Figure 11.

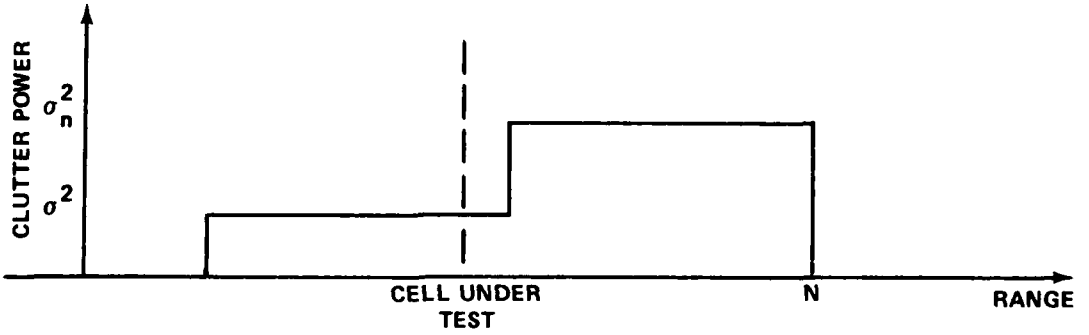

Figure 11. Clutter Edge Model

The clutter is assumed to be Gaussian in each range cell and the clutter powers in the N CFAR reference cells are related by a ratio τ_n such that

$$\tau_n = \frac{\sigma_n^2}{\sigma^2}; \quad n = 1, 2, \ldots N \tag{4.15}$$

where σ^2 is the clutter power in the cell of interest and σ_n^2 is the clutter power in the n_{th} reference cell.

In Reference 18, Boothe has shown that the spatial distribution of the ground clutter backscatter coefficient, σ^o, for various types of terrain fit quite well with a Weibull pdf. The Weibull pdf is given by

$$p(\sigma^o) = \frac{b(\sigma^o)^{b-1}}{a} \exp\left[-\frac{(\sigma^o)^b}{a}\right] \tag{4.16}$$

where b = 1/A (A = Weibull slope parameter) and

$$a = \frac{(\sigma_m^o)^b}{\ln 2} \tag{4.17}$$

where σ_m^o = median value of Weibull pdf. Typical values of the clutter slope parameter (A) and median backscatter coefficient (σ_m^o) are given in Reference 18.

A single Weibull sample, σ^o, can be generated by

$$\sigma^o = \frac{\sigma_m^o}{(\ln 2)^A} [-\ln(u)]^A \tag{4.18}$$

where u is a uniformly distributed random variate. Due to the quadrature channel processing, two independent Weibull samples, σ_I^o and σ_Q^o, must be generated.

Hence, the Weibull pdf is given in the I and Q channels as

$$\sigma_I^o = \frac{\sigma_m^o}{(\ln 2)^A} [-\ln(u_1)]^A \cos(2\pi u_2)$$

$$\sigma_Q^o = \frac{\sigma_m^o}{(\ln 2)^A} [-\ln(u_1)]^A \sin(2\pi u_2) \tag{4.19}$$

where u_1 and u_2 are independent samples drawn from a uniform distribution (0,1).

4.3 Detector Laws

The square law detector output is given by

$$y = I^2 + Q^2 \tag{4.20}$$

where I and Q are the video in the in-phase and quadrature channels, i.e., signal plus interference, respectively.

The linear detector output is given by

$$z = \sqrt{I^2 + Q^2} \tag{4.21}$$

where I and Q are as above.

4.4 CFAR Processors

Two constant false alarm rate processors are modeled in the simulation.

4.4.1 Cell Averaging CFAR

The cell averaging CFAR will form a threshold Y_{th} by scaling the average value of N detected reference cell outputs of the quadrature channels, i.e.,

$$Y_{th} = \frac{K}{N} \sum_{n=1}^{N} y_n \tag{4.22}$$

where the y_n's are the detector outputs, n is the reference cell index and K is the scaling constant. The actual model is implemented as shown in Figure 3, that is,

$$Y_{th} = \frac{K}{N}\left[\sum_{n=-1}^{-N/2} y_n + \sum_{n=1}^{N/2} y_n\right] \tag{4.23}$$

where y_o, the cell of interest, is not included in the threshold determination.

4.4.2 "Greatest-Of" CFAR

The "greatest-of" CFAR will form a threshold Y_G by using the cell averaging CFAR processor on two sets of N/2 detected reference cell outputs and will select the largest value obtained. The "greatest-of" processor is simulated as

$$Y_1 = \frac{K_G}{N/2} \sum_{n=-1}^{-N/2} y_n$$

$$Y_2 = \frac{K_G}{N/2} \sum_{n=1}^{N/2} y_n \qquad (4.24)$$

and

$$Y_G = \text{MAX}\,[Y_1, Y_2]$$

where K_G is the "greatest-of" scaling constant. Again y_o, the cell of interest, is not included in the threshold determination.

4.5 PFA and PD Determinations

The probabilities of false alarm are determined from detector outputs which contain noise and/or interference only. A threshold for the cell of interest is calculated by the cell averaging CFAR processor using other detector outputs. The magnitude of the cell of interest is compared to the threshold and, if it is larger, a false alarm is reported. In the simulation, a false alarm counter (FAC) is initialized to zero at the beginning of a Monte Carlo sequence, then FAC is incremented by one for each false alarm reported. Finally, the average probability of false alarm is determined as

$$\overline{PFA}_{CA} = \frac{FAC}{NMON} \qquad (4.25)$$

where NMON is the number of Monte Carlo trials. The average probability of false alarm, $\overline{PFA}_G$, for the "greatest-of" CFAR is determined by the same procedure.

The probabilities of detection are determined from detector outputs which contain targets. The same procedure is used as in the PFA determination; however, a target detection counter (TDC) is incremented for each threshold that is exceeded by the magnitude of the cell of interest in which a target resides. Then the average probability of detection is determined as

$$\overline{PD}_{CA} = \frac{TDC}{NMON} . \tag{4.26}$$

The average probability of detection, $\overline{PD}_G$, for the "greatest-of" is determined in a similar manner.

4.6 Summary

A simulation has been developed which can be used to determine the cell averaging CFAR and "greatest-of" CFAR performance for different environmental conditions, targets and detectors. The probability of false alarm and the probability of detection results obtained can be used to verify the theoretical performance equations and to compare the relative performance of the two processors.

CHAPTER V. RESULTS

5.0 Introduction

The simulation described in Chapter IV was developed to compare the performance of the cell averaging and "greatest-of" CFAR processors. The utilization of a simulation allows determination of the processors' performance for the different targets, detectors and clutter environments simulated. The probabilities of false alarm and probabilities of detection are the basis for comparing the two CFAR processors. The desired probability of false alarm in radars is normally quite small, i.e., 10^{-3} to 10^{-9}. Thus, it is difficult to verify the probability of false alarm using a computer simulation due to the amount of computer time required to complete a sufficient number of Monte Carlo passes, i.e., 10^{5} or more. This difficulty was overcome by programming the simulation on an array processor. The array processor is a high speed arithmetic unit designed for scientific applications. A brief discussion of the array processor is given in Appendix D.

5.1 Probability of False Alarm Results

To compare the two CFAR techniques it is necessary to design them to maintain the same average probability of false alarm in homogeneous noise, i.e., $\overline{PFA}_G = \overline{PFA}_{CA}$.

For the cell averaging CFAR it is only required to specify the desired average probability of false alarm, $\overline{PFA}_{CA}$, and the number of reference cells N, and by using Equation (3.4) to determine the threshold constant K.

For the "greatest-of" CFAR the design procedure is somewhat complicated. The threshold constant K_G is determined by a computer program which iterates $\overline{PFA}_P$ in Equation (3.10) until the desired value for the $\overline{PFA}_G$ is obtained. Then this value of $\overline{PFA}_P$ and the number of reference cells N is used in Equation (3.11) to determine K_G.

Hence, theoretically $\overline{PFA}_{CA} = \overline{PFA}_G$ for the same number of reference cells in homogeneous noise.

The design probabilities of false alarm of 10^{-3}, 10^{-4}, and 10^{-5} were chosen because they are commonly found values and because the Gaussian random number generator lacks distribution tails necessary for a false alarm rate $<10^{-5}$. The CFAR window widths N were chosen to be 8, 16, and 32, since digital hardware is normally implemented in powers of two. The probabilities of false alarm for the cell averaging and "greatest-of" CFAR obtained by the Monte Carlo simulation are given in Table 1.

Table 1. CFAR Processor Probabilities of False Alarm

$\overline{PFA}_D$	N	$\overline{PFA}_{CA}$	$\overline{PFA}_P$	$\overline{PFA}_G$
10^{-3}	8	0.113-2	0.877-2	0.106-2
	16	0.110-2	0.507-2	0.107-2
	32	0.104-2	0.318-2	0.103-2
10^{-4}	8	0.121-3	0.223-2	0.123-3
	16	0.104-3	0.104-2	0.110-3
	32	0.110-3	0.532-3	0.124-3
10^{-5}	8	0.106-4	0.599-3	0.770-5
	16	0.134-4	0.230-3	0.144-4
	32	0.115-4	0.940-4	0.115-4

The number of Monte Carlo runs used to determine the results in Table 1 were 10^5, 10^6, and 10^7 for the probabilities of false alarm

10^{-3}, 10^{-4}, and 10^{-5}, respectively. The number of Monte Carlo runs required to give a priori probabilities PFA and PD for a specified range of the estimated parameters is calculated in Appendix C.

5.2 Probability of Detection Results

The performance curves in Figures 12 through 23 were determined by the Monte Carlo simulation. The curves are plotted as probability of detection versus input signal-to-noise ratio. The cell averaging CFAR performance curves are given in Figures 12 through 14 for a steady target and in Figures 15 through 17 for a Swerling I target. A square law detector is used. The "greatest-of" CFAR performance curves are given in Figures 18 through 20 for a steady target and in Figures 21 through 23 for a Swerling I target. Again, a square law detector is used.

The design false alarm probabilities of 10^{-3}, 10^{-4}, and 10^{-5} are shown on the plots while the actual average false alarm probabilities are given in Table 1.

The theoretical probability of detection equations have been determined for the cell averaging CFAR with a steady target and a Swerling I target and for the "greatest-of" CFAR with a Swerling I target only. These equations are shown below.

The theoretical PD for a square law detected steady target and cell averaging CFAR is derived in Reference 14 and is given as

$$\overline{PD} = 1 - \frac{g^2}{g^2 + 1} \sum_{m=o}^{N-1} \frac{\exp[-a^2/(g^2 + 2)]}{m!} \left(\frac{2}{g^2 + 2}\right)^m L_m(e), \quad (5.1)$$

where $g = K\sqrt{2/N}$ is the input signal-to-noise ratio, $e = a^2g^2/[2(g^2 + 2)]$ and $L_m(e)$ are Laguerre polynomials with the properties

$$L_o(e) = 1, \; L_1(e) = 1 + e, \; L_{m+1}(e) = (e + 2m + 1)L_m(e) - m^2L_{m-1}(e). \quad (5.2)$$

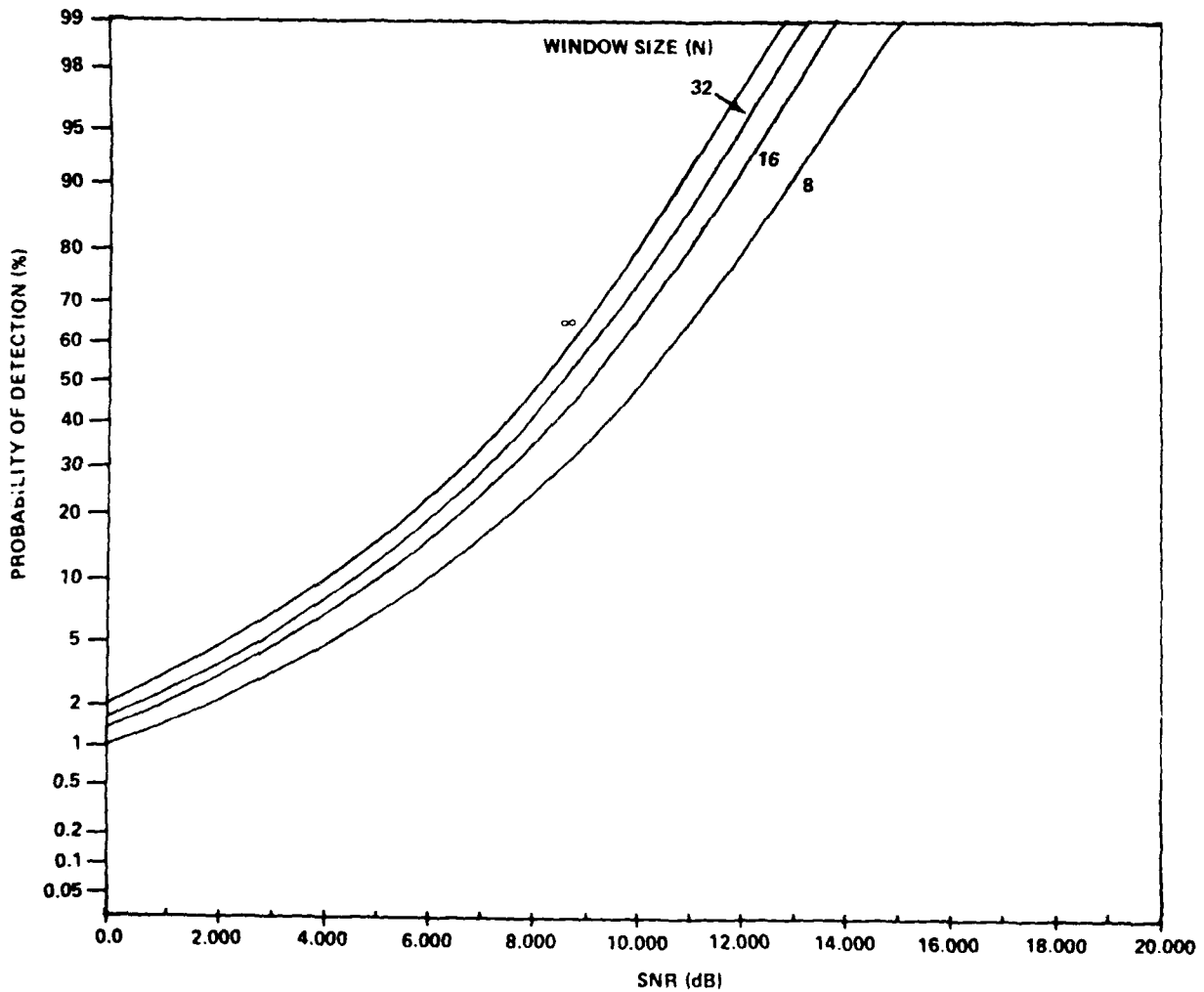

Figure 12. Cell Averaging CFAR Performance Curves ($\overline{PFA}_D = 10^{-3}$, Steady Target, Square Law Detector)

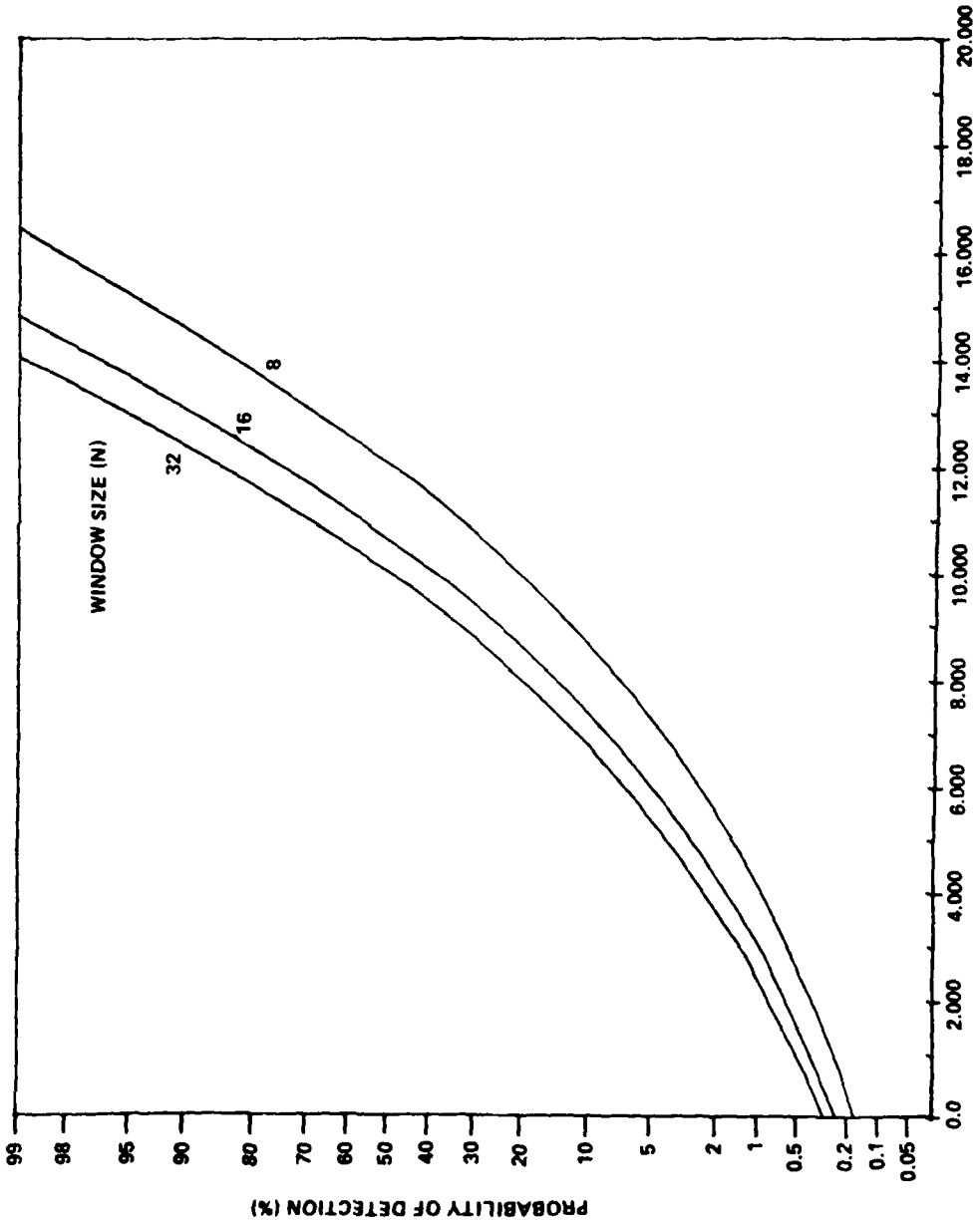

Figure 13. Cell Averaging CFAR Performance Curves ($\overline{PFA}_D = 10^{-4}$, Steady Target, Square Law Detector)

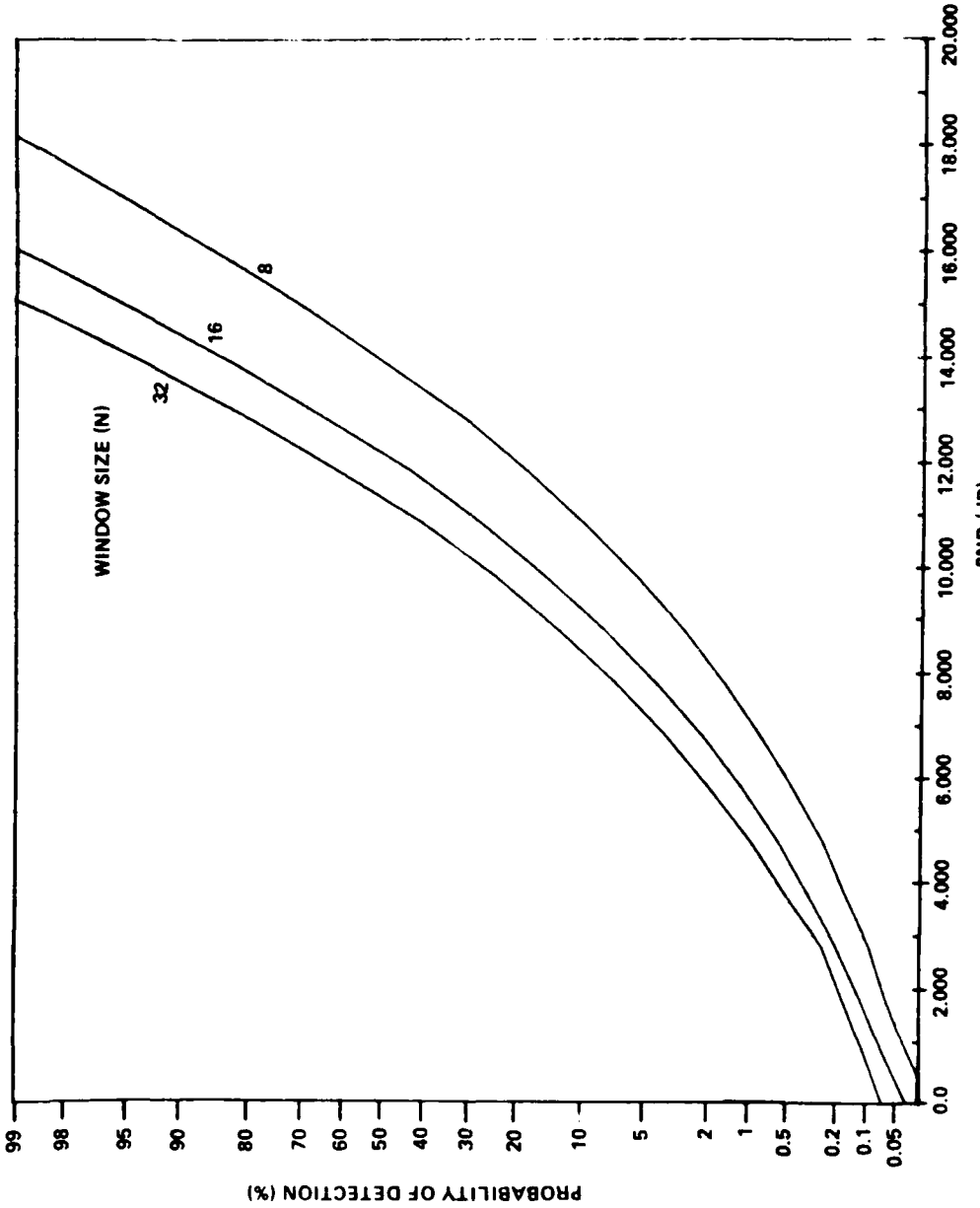

Figure 14. Cell Averaging CFAR Performance Curves ($\overline{PFA}_D = 10^{-5}$, Steady Target, Square Law Detector)

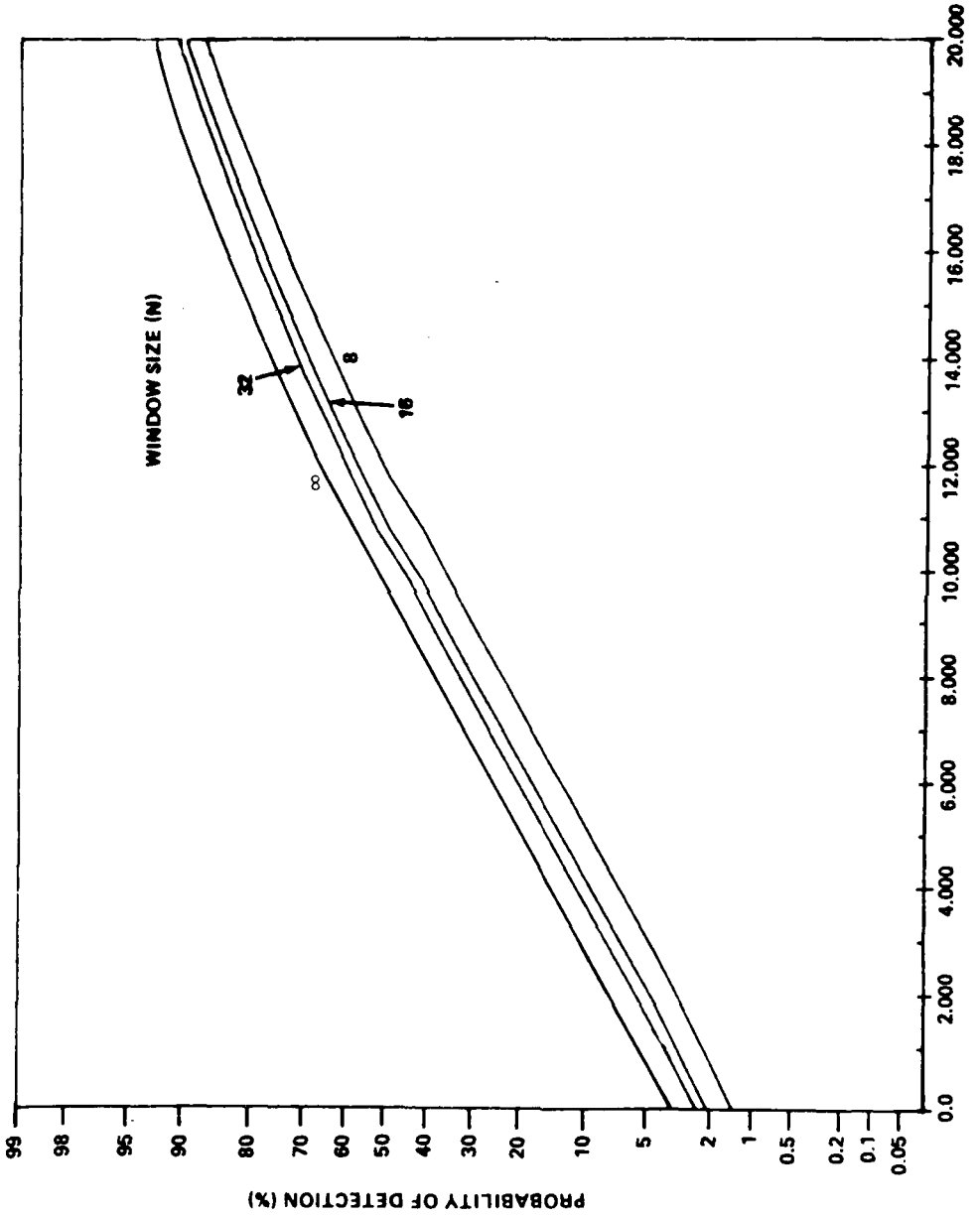

Figure 15. Cell Averaging CFAR Performance Curves ($\overline{PFA}_D = 10^{-3}$, Swerling I Target, Square Law Detector)

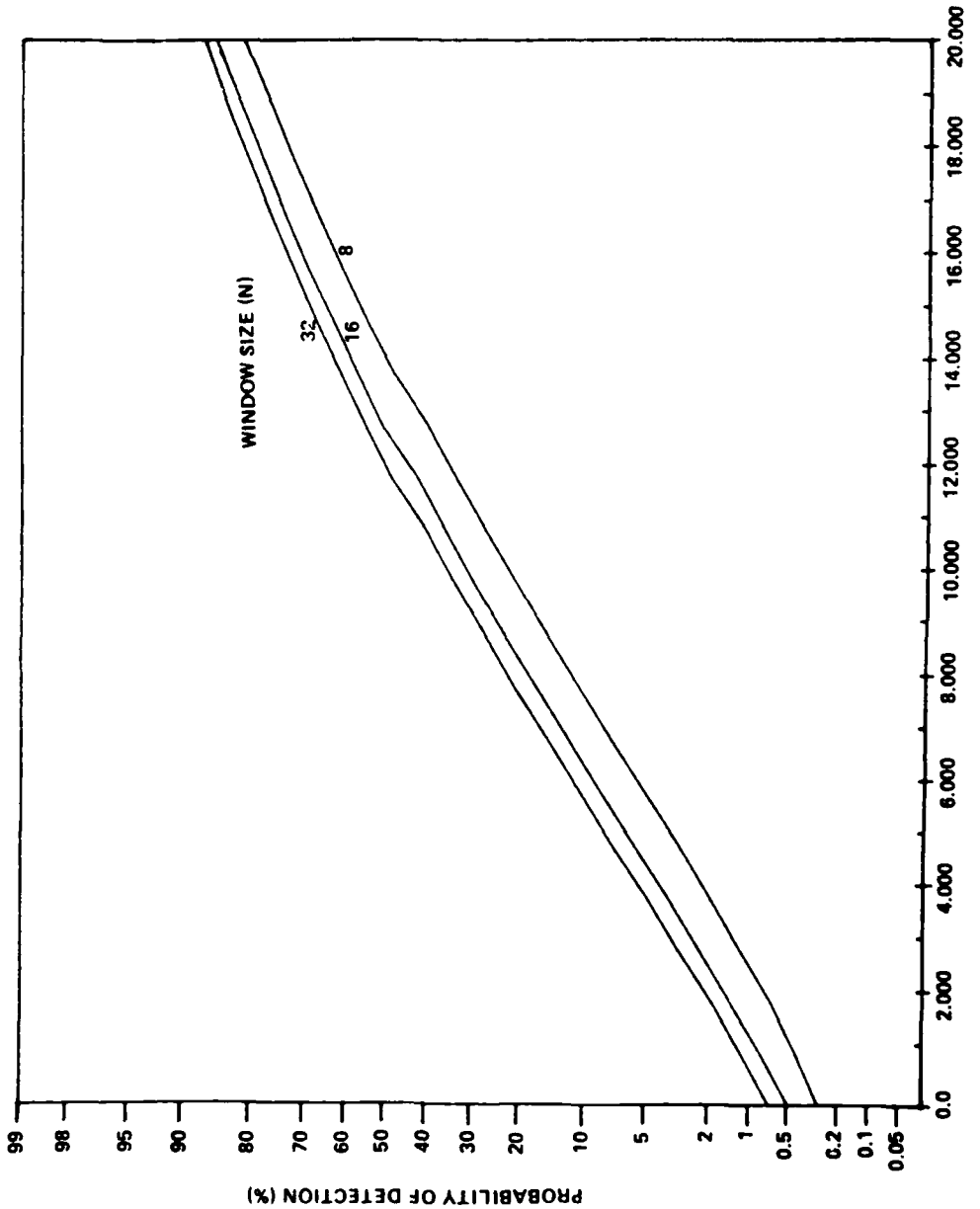

Figure 16. Cell Averaging CFAR Performance Curves ($\overline{PFA}_D = 10^{-4}$, Swerling I Target, Square Law Detector)

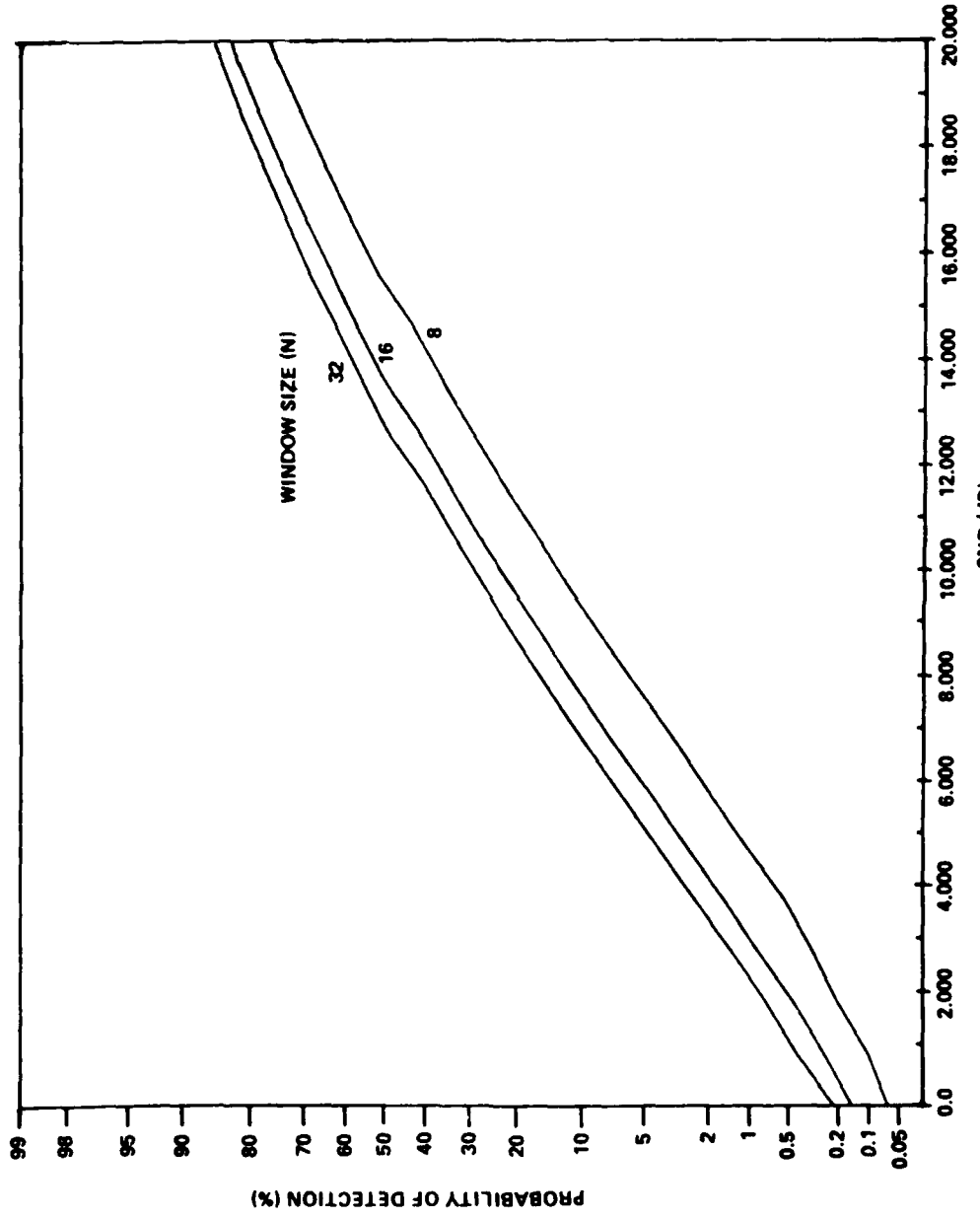

Figure 17. Cell Averaging CFAR Performance Curves ($\overline{PFA}_D = 10^{-5}$, Swerling I Target, Square Law Detector)

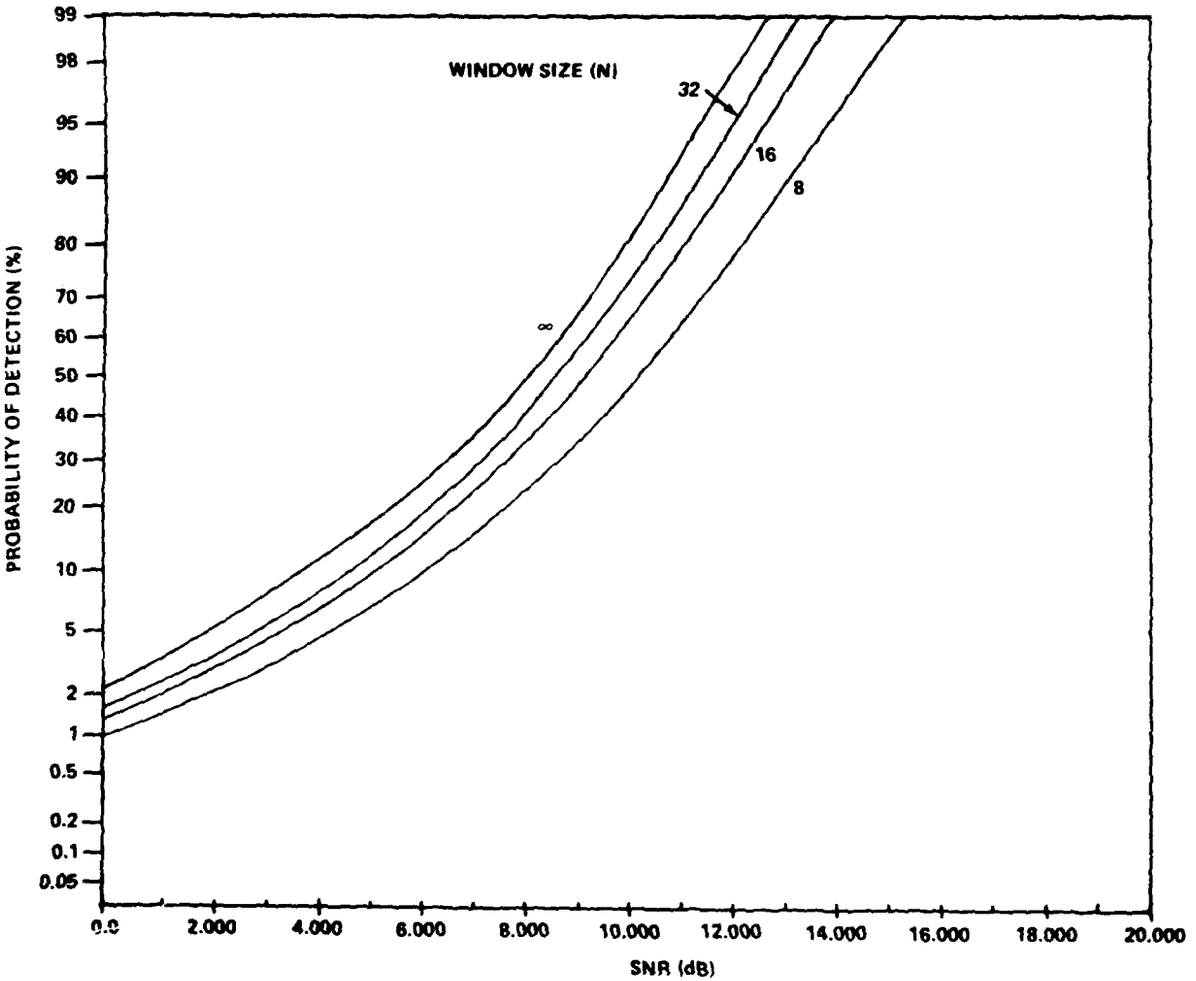

Figure 18. "Greatest-Of" Performance Curves ($\overline{PFA}_D = 10^{-3}$, Steady Target, Square Law Detector)

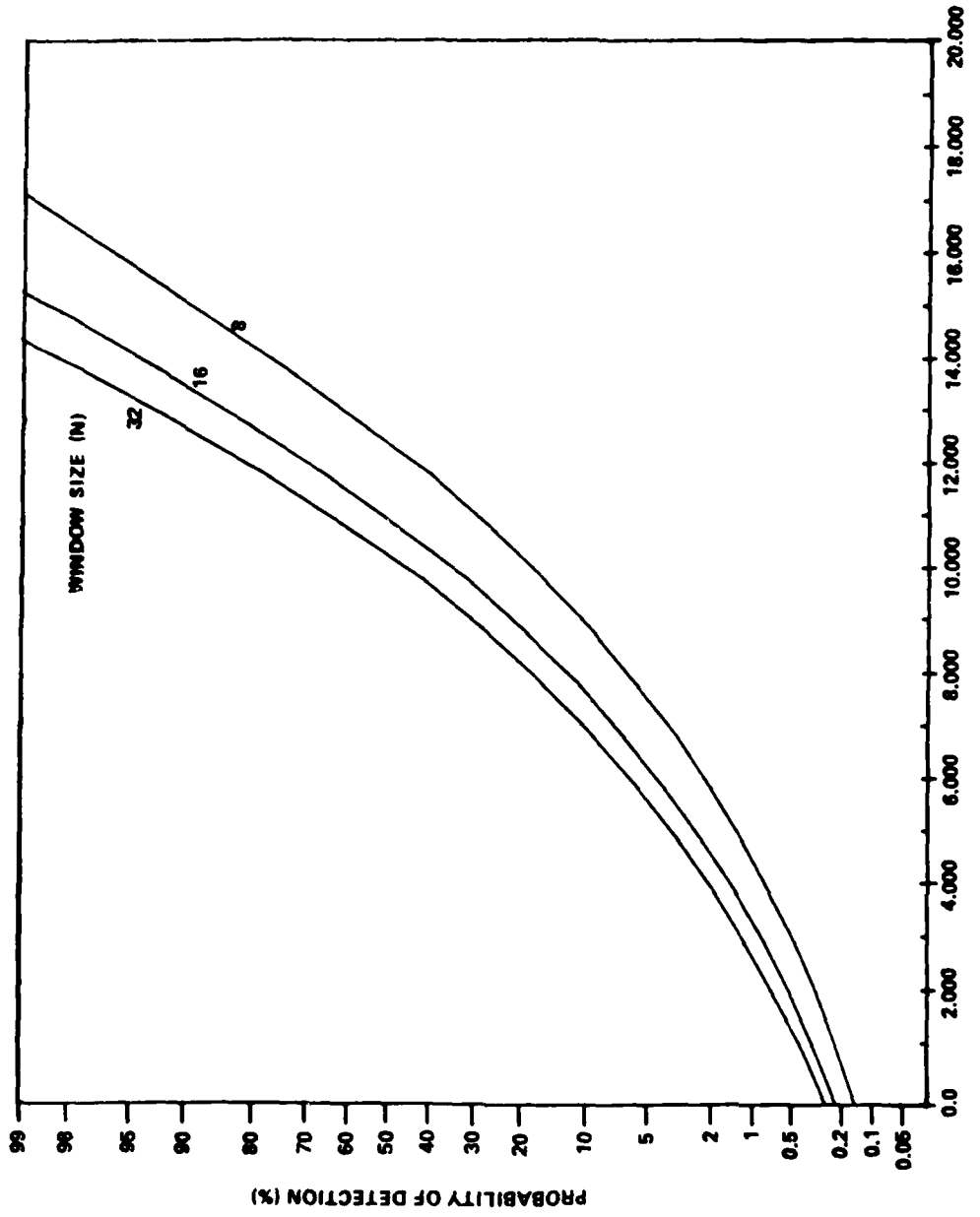

Figure 19. "Greatest-Of" Performance Curves ($\overline{PFA}_D = 10^{-4}$, Steady Target, Square Law Detector)

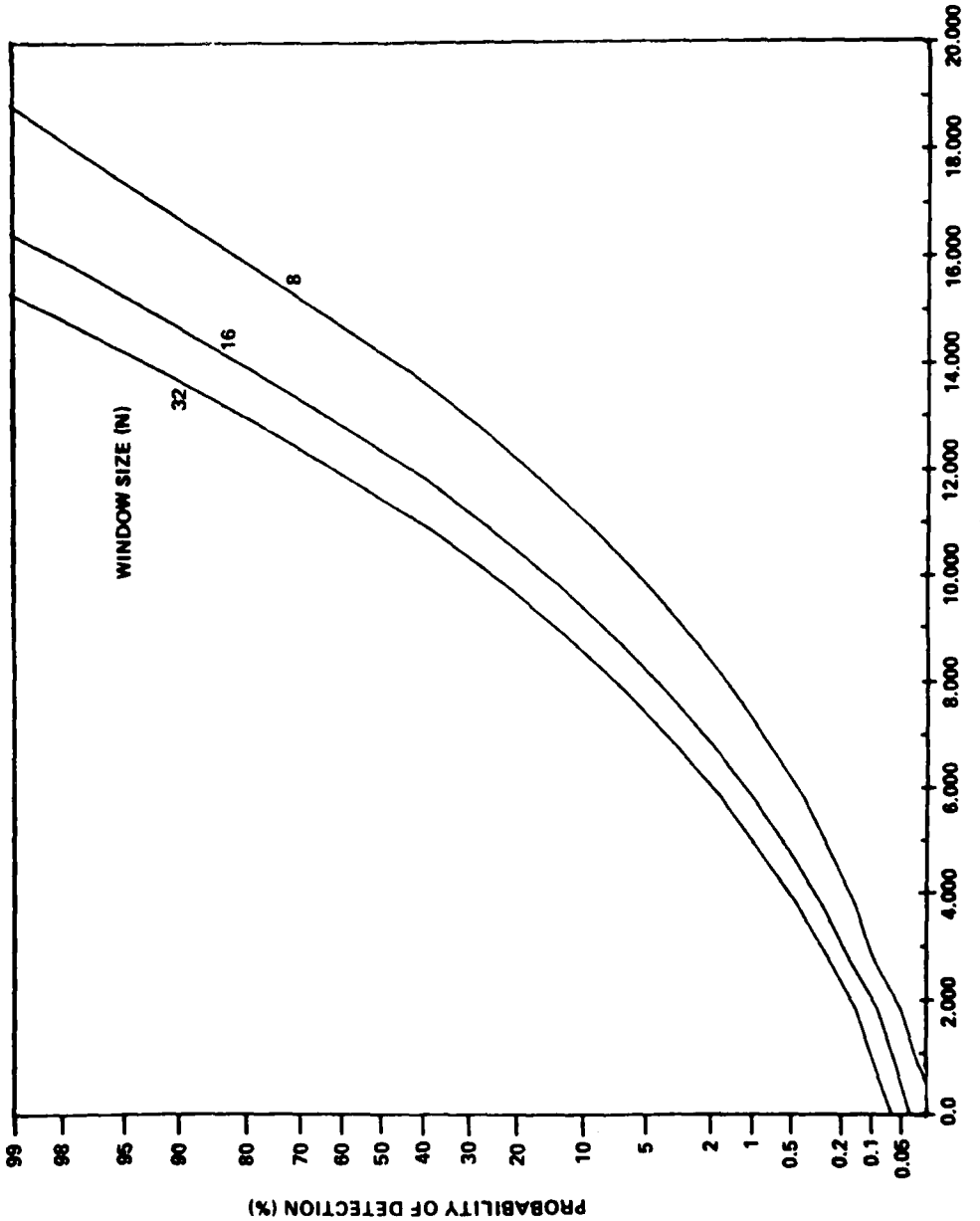

Figure 20. "Greatest-Of" Performance Curves ($\overline{PFA}_D = 10^{-5}$, Steady Target, Square Law Detector)

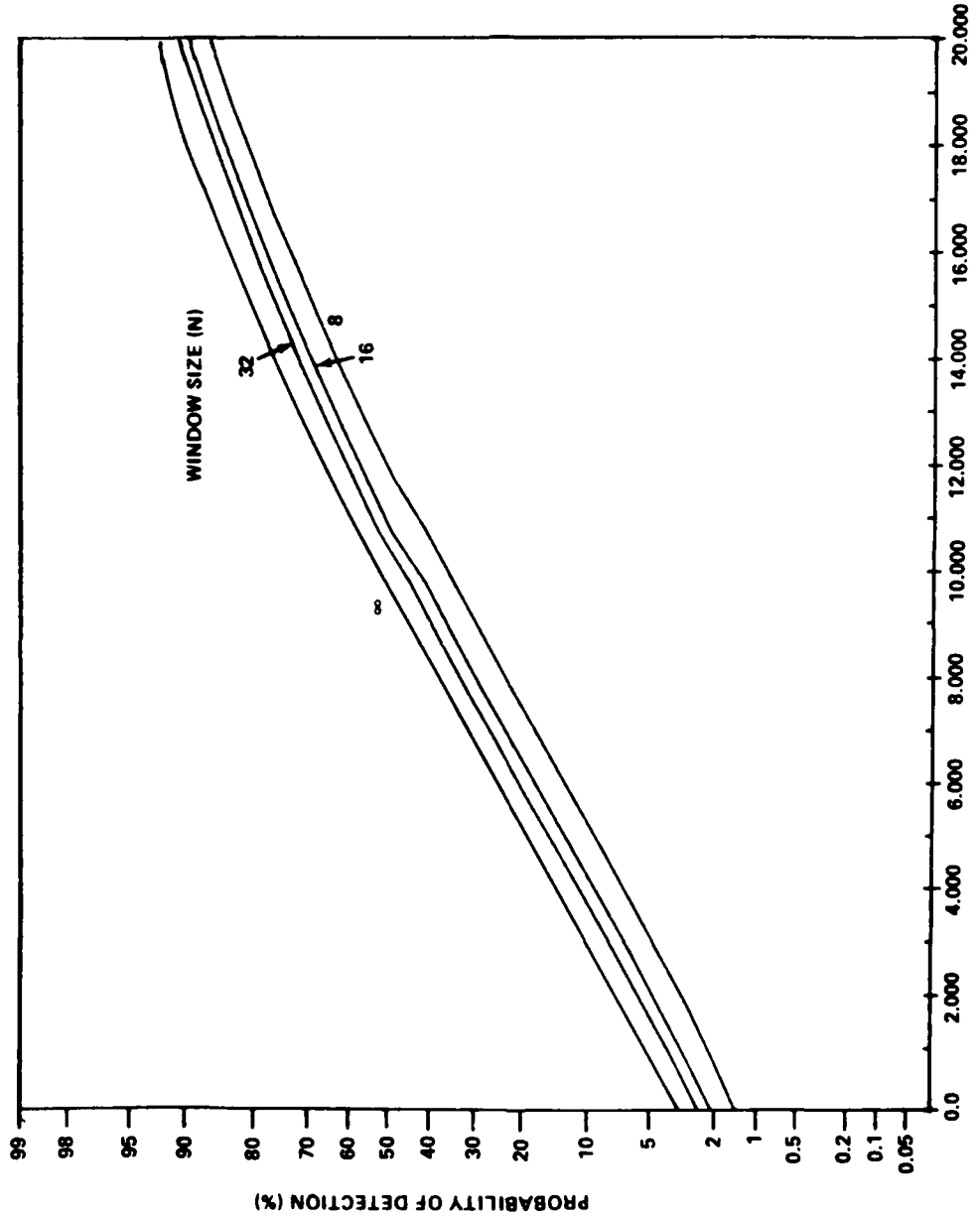

Figure 21. "Greatest-Of" Performance Curves ($\overline{PFA}_D = 10^{-3}$, Swerling I Target, Square Law Detector)

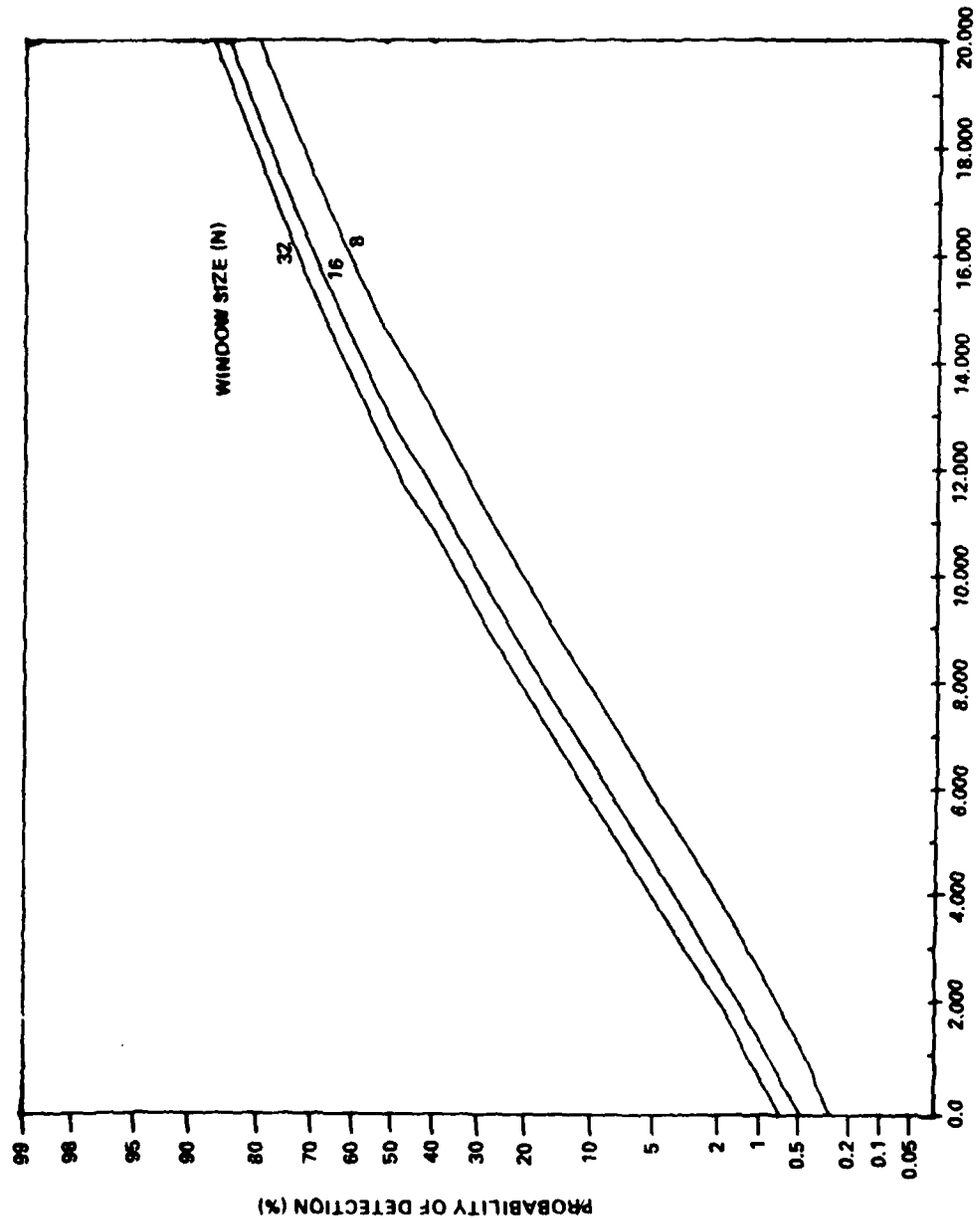

Figure 22. "Greatest-Of" Performance Curves ($\overline{PFA}_D = 10^{-4}$, Swerling I Target, Square Law Detector)

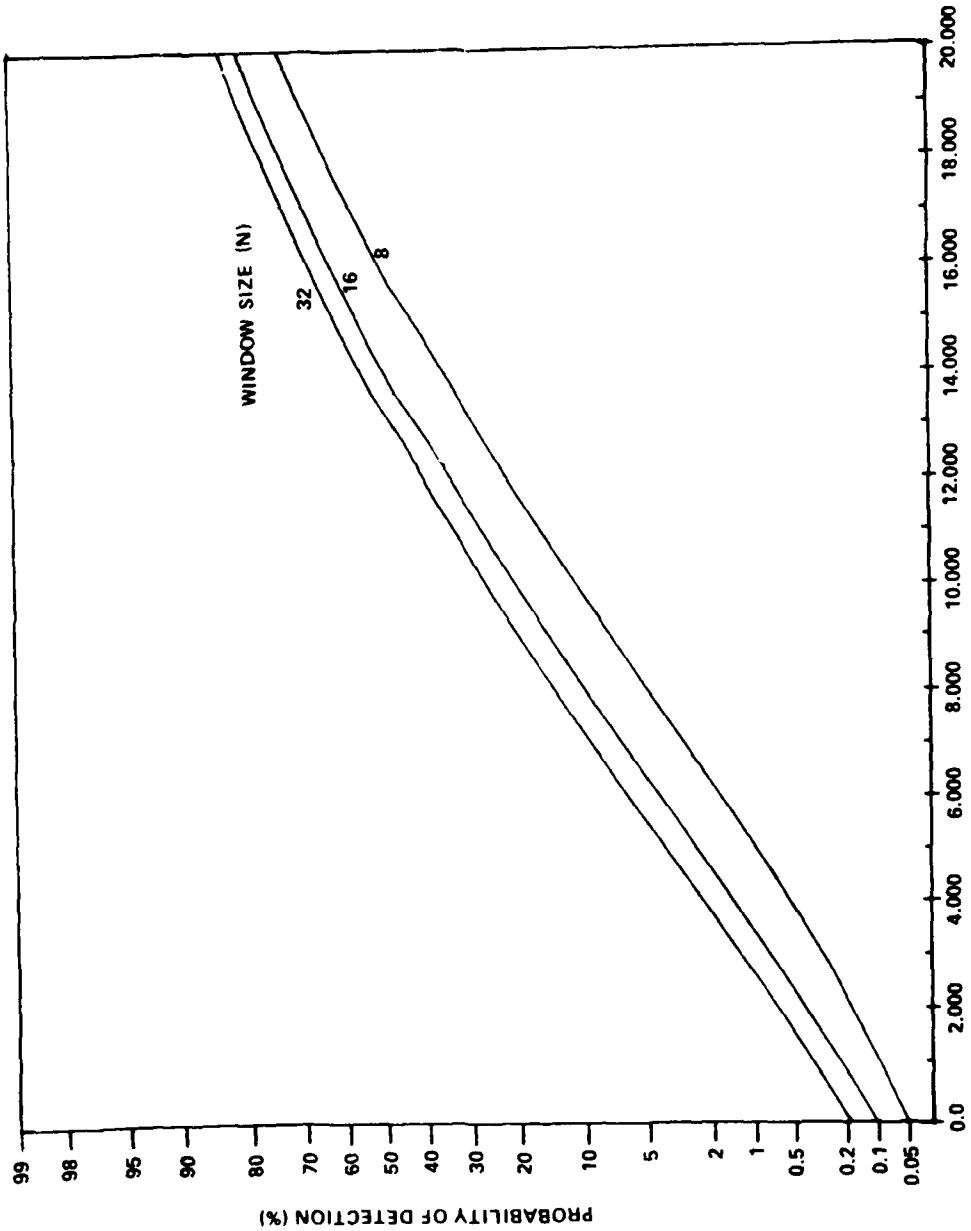

Figure 23. "Greatest-Of" Performance Curves ($\overline{PFA}_D = 10^{-5}$, Swerling I Target, Square Law Detector)

The theoretical PD for a square law detected Swerling I target using cell averaging CFAR is given in Equation (3.5) and repeated here.

$$\overline{PD}_{CA} = \left[1 + \frac{K}{N(1+\bar{x})}\right]^{-N} \tag{5.3}$$

where N is number of reference cells, $\bar{x}$ is the input signal-to-noise-ratio, and K is the threshold constant.

The theoretical PD for a square law detected Swerling I target and "greatest-of" CFAR is given in Equation (3.12) and repeated here.

$$\overline{PD}_G = \frac{2\overline{PD}_p}{\left(\frac{N}{2}-1\right)!\left(1+\overline{PD}_p{}^{-2/N}\right)^{N/2}} \sum_{n=0}^{N/2-1} \frac{\left(n+\frac{N}{2}-1\right)!}{n!\left(1+\overline{PD}_p{}^{-2/N}\right)^{n}} \tag{5.4}$$

where the prototype $\overline{PD}_p$ is

$$\overline{PD}_p = \left[1 + \frac{2K_G}{N(1+\bar{x})}\right]^{-N/2} \tag{5.5}$$

where N is the number of reference cells and K_G is the "greatest-of" threshold constant.

The probability of detection curves for an ideal threshold, i.e., a fixed threshold system where the noise power is known, are given in Meyer and Mayer [7]. Ideal threshold curves are plotted in Figures 12, 15, 18, and 21. The curves on Figures 12 and 18 were extracted from page 126 of Reference 7, while the curves on Figures 15 and 21 were extracted from page 218 of Reference 7. For the Swerling I target results the curve could be generated using Equation (2.20).

5.3 Probability of Detection Comparison

The performance curves, Figures 24 through 29, provide a comparison of the cell averaging and "greatest-of" CFAR probabilities of detection. They are replots of Figures 17 through 28 where the cell

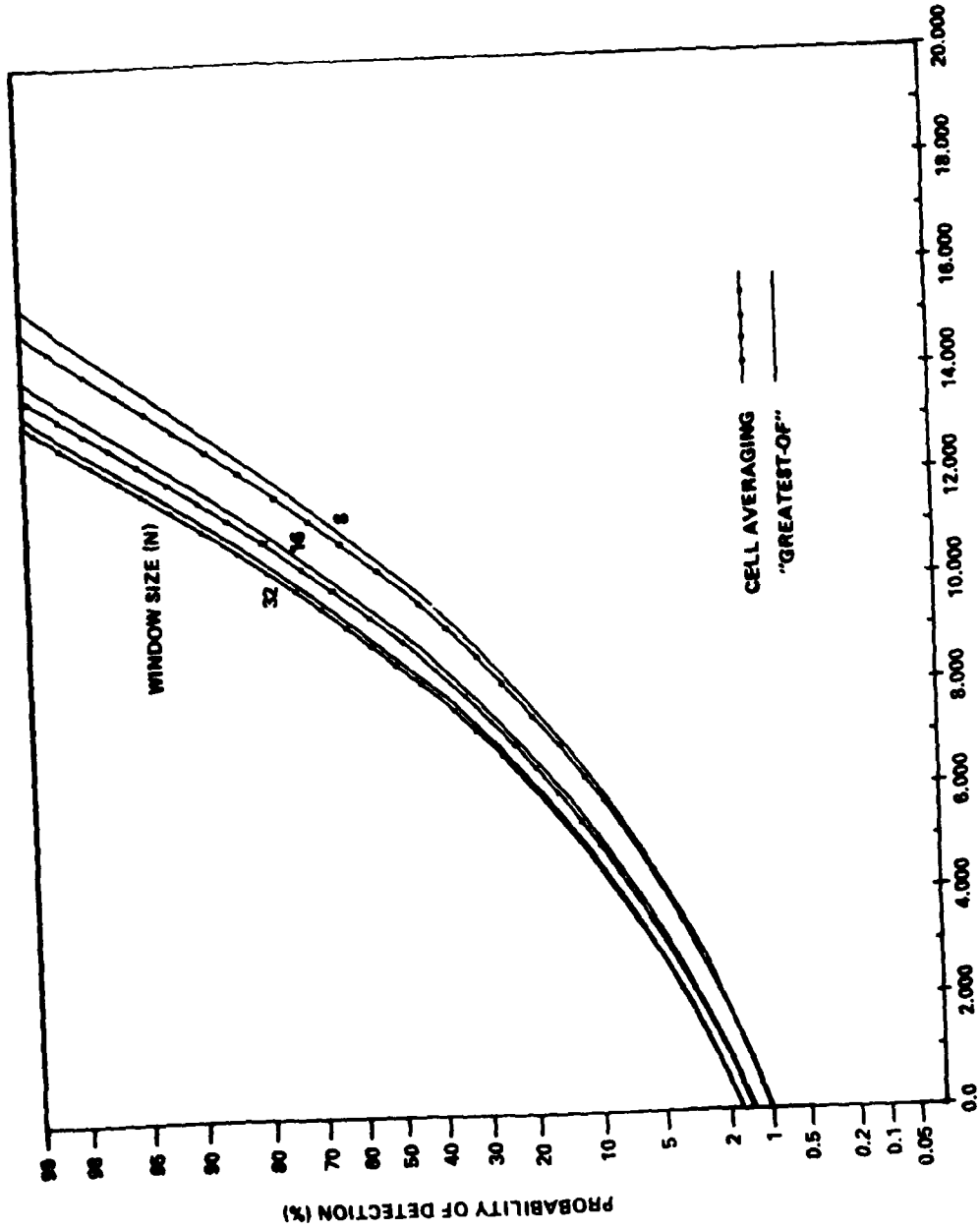

Figure 24. Performance Comparison of Cell Averaging and "Greatest-Of" ($\overline{PFA}_D = 10^{-3}$, Steady Target, Square Law Detector)

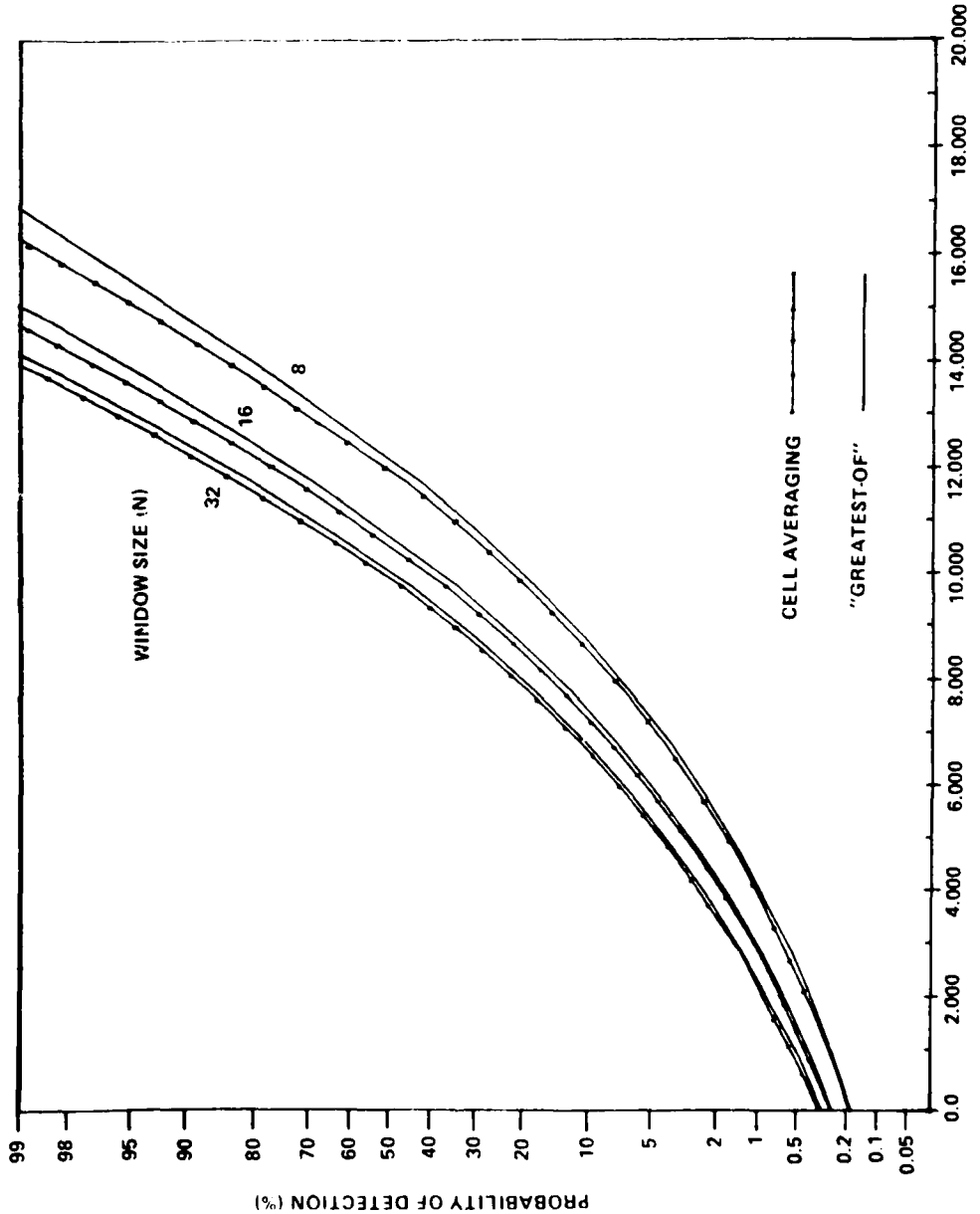

Figure 25. Performance Comparison of Cell Averaging and "Greatest-Of" ($\overline{PFA}_D = 10^{-4}$, Steady Target, Square Law Detector)

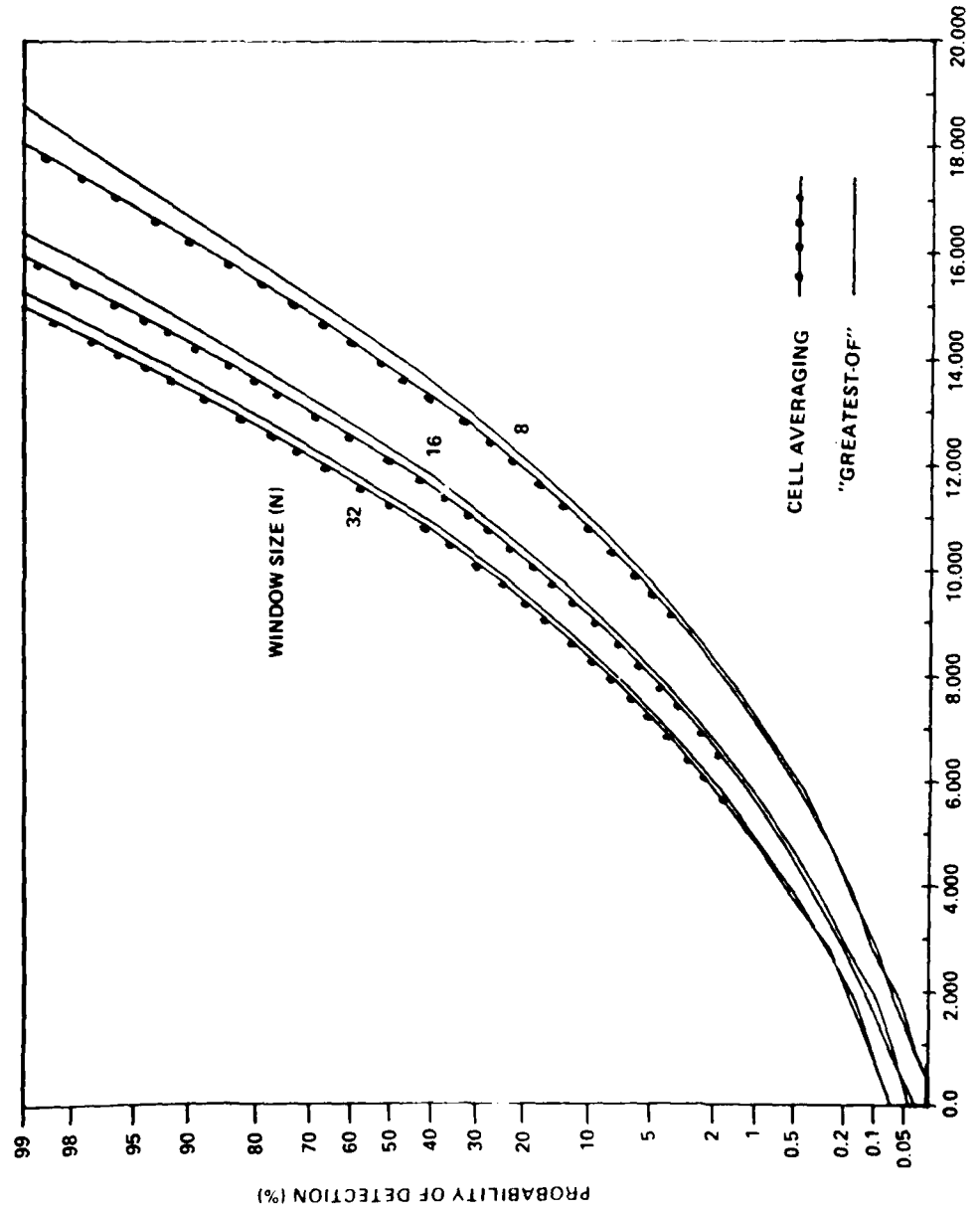

Figure 26. Performance Comparison of Cell Averaging and "Greatest-Of" ($\overline{PFA}_D = 10^{-5}$, Steady Target, Square Law Detector)

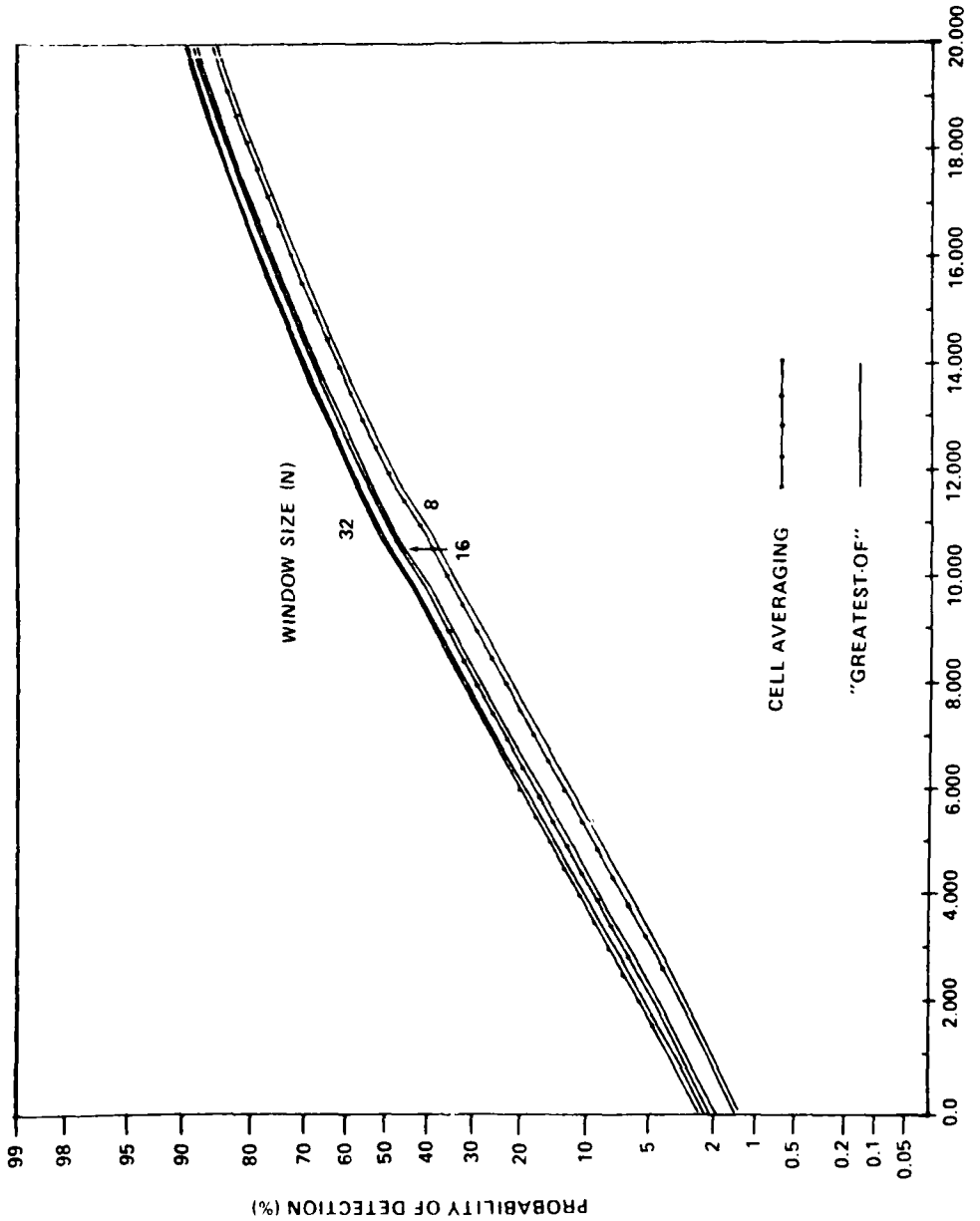

Figure 27. Performance Comparison of Cell Averaging and "Greatest-Of" ($\overline{PFA}_D = 10^{-3}$, Swerling I Target, Square Law Detector)

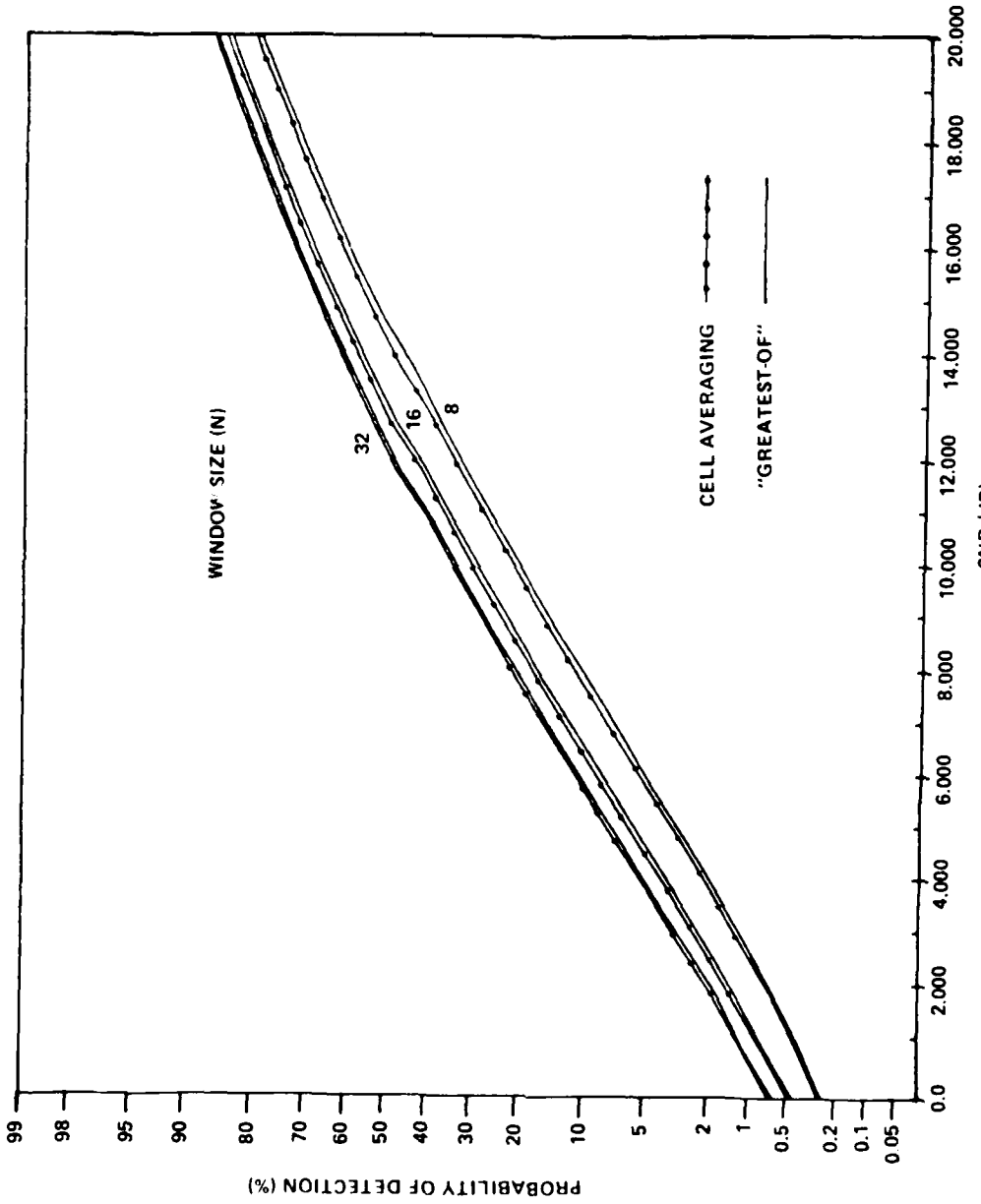

Figure 28. Performance Comparison of Cell Averaging and "Greatest-Of" ($\overline{PFA}_D = 10^{-4}$, Swerling I Target, Square Law Detector)

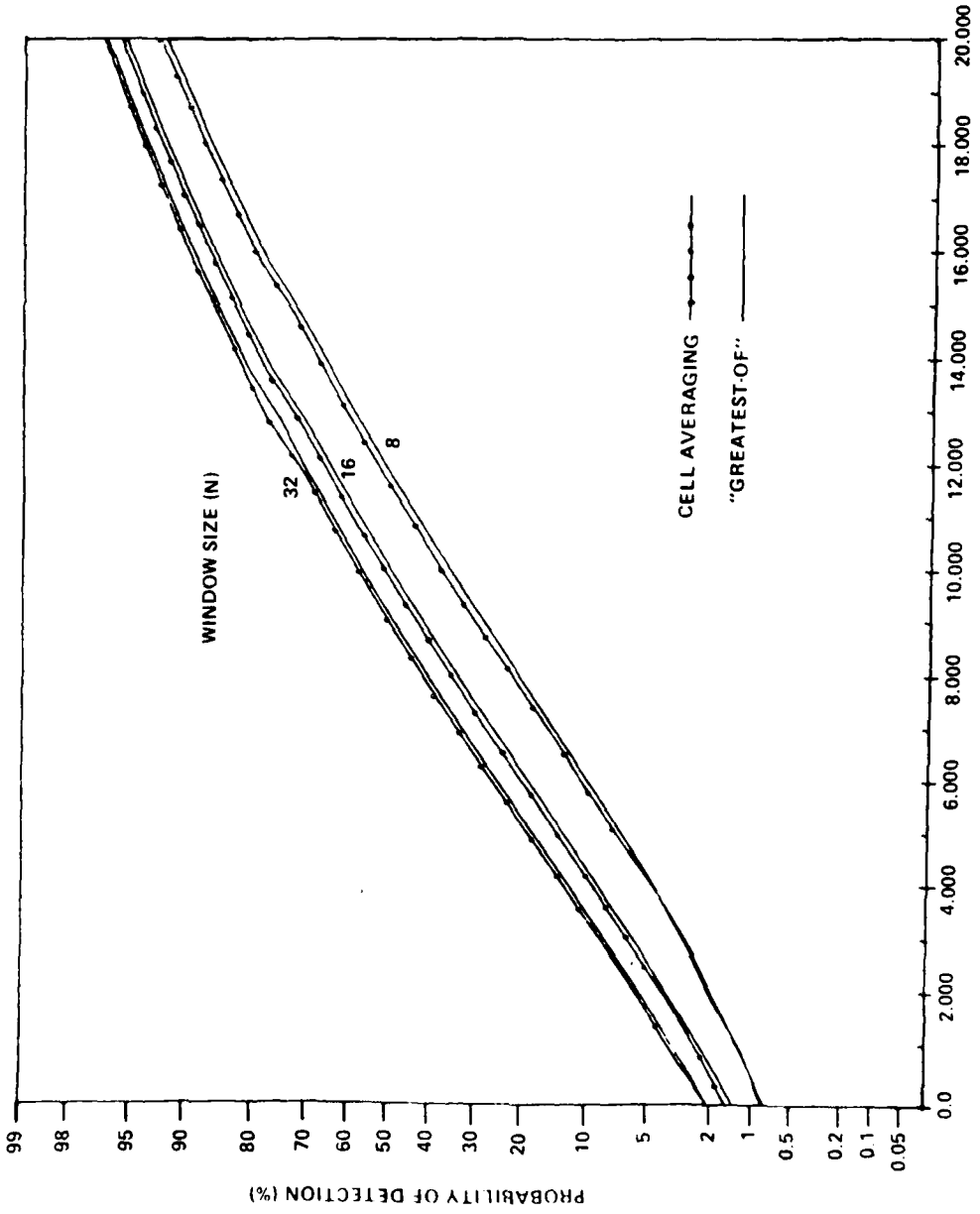

Figure 29. Performance Comparison of Cell Averaging and "Greatest-Of" ($\overline{PFA}_D = 10^{-5}$, Swerling I Target, Square Law Detector)

averaging and "greatest-of" CFAR probabilities of detection curves are combined for a particular design probability of false alarm and target model. The actual probabilities of false alarm are given in Table 1.

It can be seen that the cell averaging CFAR has better detection performance in homogeneous noise than the "greatest-of" CFAR. For the target model of greater interest, i.e., the Swerling I target, the detection performance of the two processors is almost equivalent.

Since the Monte Carlo simulation determines probabilities of detection, a more meaningful comparison could be made using signal-to-noise ratios. Using Equation (3.5), the input signal-to-noise ratio for the cell averaging CFAR and a Swerling I target is

$$\bar{x}_{CA} = \frac{1 - \sqrt[N]{\overline{PD}_{CA}}\ \overline{PFA}_{CA}^{-1/N}}{\sqrt[N]{\overline{PD}_{CA}} - 1} \tag{5.6}$$

where N is the number of reference cells, $\overline{PFA}_{CA}$ is the average probability of false alarm, and $\overline{PD}_{CA}$ is the average probability of detection. Hence, given an average probability of detection, average probability of false alarm, and CFAR window width, the input signal-to-noise ratio for the cell averaging CFAR can be determined.

To compare the two CFAR techniques, an average signal-to-noise difference $\bar{\Delta}$dB was calculated as follows. For a particular $\overline{PFA}_D$, i.e., 10^{-3}, 10^{-4}, or 10^{-5}, CFAR window width N, i.e., 8, 16, or 32, and the Monte Carlo determined $\overline{PD}$'s, i.e., $\overline{PD}_{CA}$ or $\overline{PD}_G$, the corresponding cell averaging CFAR input signal-to-noise ratio for both CFAR techniques was determined using Equation (5.6). That is, the input signal-to-noise ratio $x_{CA}(j)$ for the cell averaging is calculated as

$$\bar{x}_{CA}(j) = \frac{1 - \sqrt[N]{\overline{PD}_{CA}(j)}\ \overline{PFA}_D^{-1/N}}{\sqrt[N]{\overline{PD}_{CA}(j)} - 1} \tag{5.7}$$

and the input SNR, $\bar{x}_G(j)$, for the "greatest-of" is calculated as

$$\bar{x}_G(j) = \frac{1 - \sqrt[N]{\overline{PD}_G(j)}\ \overline{PFA}_D^{-1/N}}{\sqrt[N]{\overline{PD}_G(j)} - 1} \tag{5.8}$$

where j is an index for the 21 Monte Carlo obtained probabilities of detection corresponding to each of the 21 input signal-to-noise ratios, i.e., from 0 dB to 20 dB in increments of 1 dB.

After converting $\bar{x}_{CA}(j)$ and $\bar{x}_G(j)$ to decibels, an average signal-to-noise difference is calculated as

$$\bar{\Delta}dB = \sum_{j=1}^{21} \frac{\bar{x}_{CA}(j) - \bar{x}_G(j)}{21} . \tag{5.9}$$

The results, given in Table 2, indicate a range of average signal-to-noise differences for the Swerling I target as 0.115 dB to 0.215 dB. These results are comparable to analytical results of [8] and [13].

Table 2. Signal-to-Noise Ratio Comparison of Cell Averaging and "Greatest-Of" CFAR Processors

$\overline{PFA}_D$	N	$\bar{\Delta}$dB
10^{-3}	8	0.206
	16	0.175
	32	0.115
10^{-4}	8	0.215
	16	0.190
	32	0.142
10^{-5}	8	0.192
	16	0.205
	32	0.150

5.4 Detector Law Performance Comparison

The recent introduction of digital technology to radar signal processing has necessitated the use of linear detectors for amplitude extraction. This is a result of the bit growth associated with a squaring function, i.e., for B bit input the output requires 2·B bits.

It is further noted that an exact linear detector is the square root of a square law detector. Hence, the actual detector used is an approximation to the exact linear detector. A number of these algorithms have been designed and normally take advantage of the divide by two which results from right shifts of digital words. Two commonly found algorithms are

$$R = \text{MAX}\ (|I|,|Q|) + \frac{1}{2}\ \text{MIN}\ (|I|,|Q|) \tag{5.10}$$

and

$$R = \text{MAX}\ (|I|,|Q|) + \frac{1}{4}\ \text{MIN}\ (|I|,|Q|) \tag{5.11}$$

where R is detector output and $|I|$ and $|Q|$ are the absolute values of the in-phase and quadrature inputs. Since there are a number of detector approximation algorithms, no processor analysis is performed using these algorithms.

The performance curves given in Figures 30 through 37 were obtained for the cell averaging and "greatest-of" CFAR processors using exact square law and linear detection. Again the probabilities of detection obtained by the Monte Carlo simulation are plotted versus the input signal-to-noise ratio. The results obtained for a particular CFAR technique and both detectors are plotted together.

It can be seen that the performance of the square law detector is superior to that of the linear detector for any combination of target

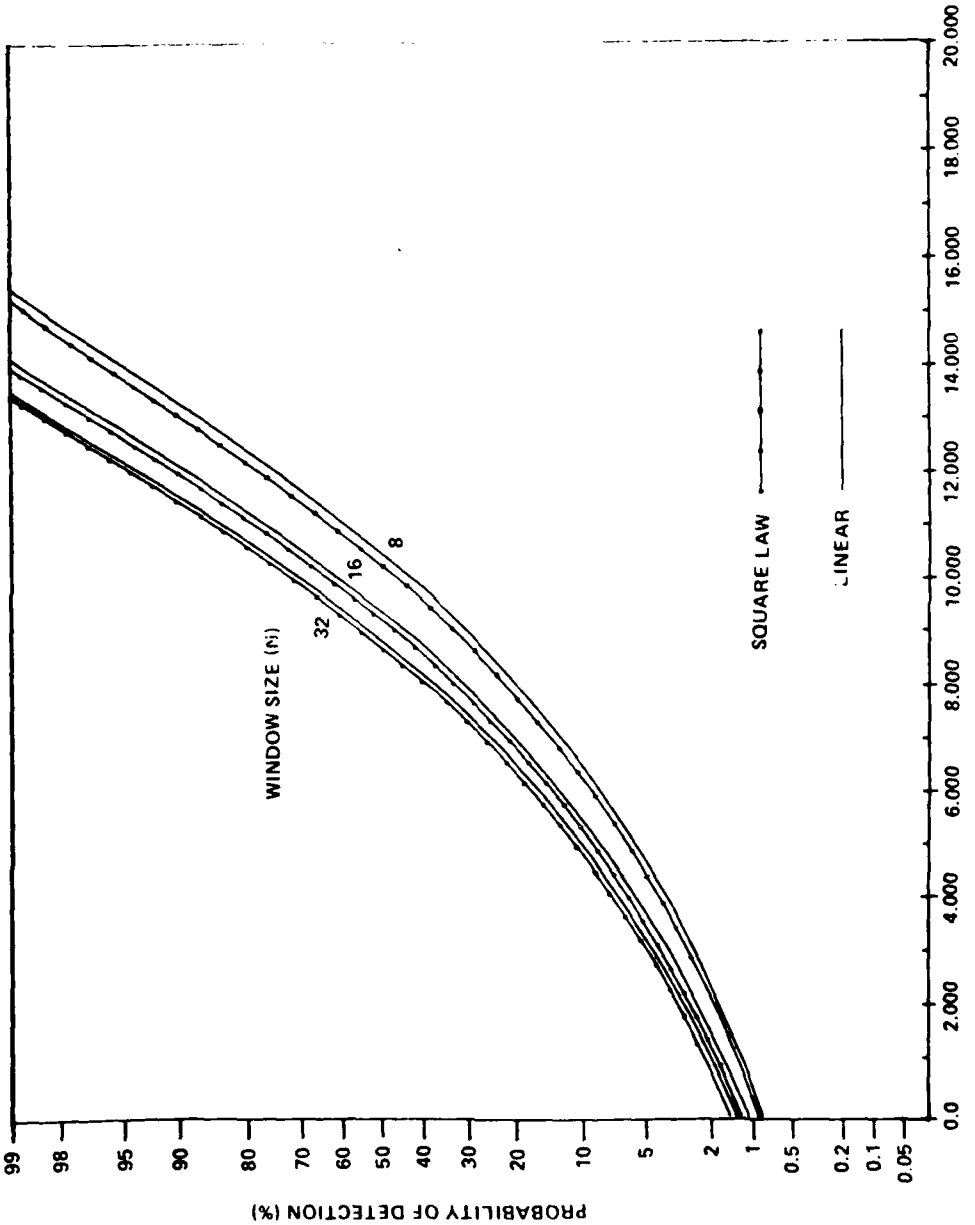

Figure 30. Performance Comparison of Detector Laws for Cell Averaging ($\overline{PFA}_D = 10^{-3}$, Steady Target)

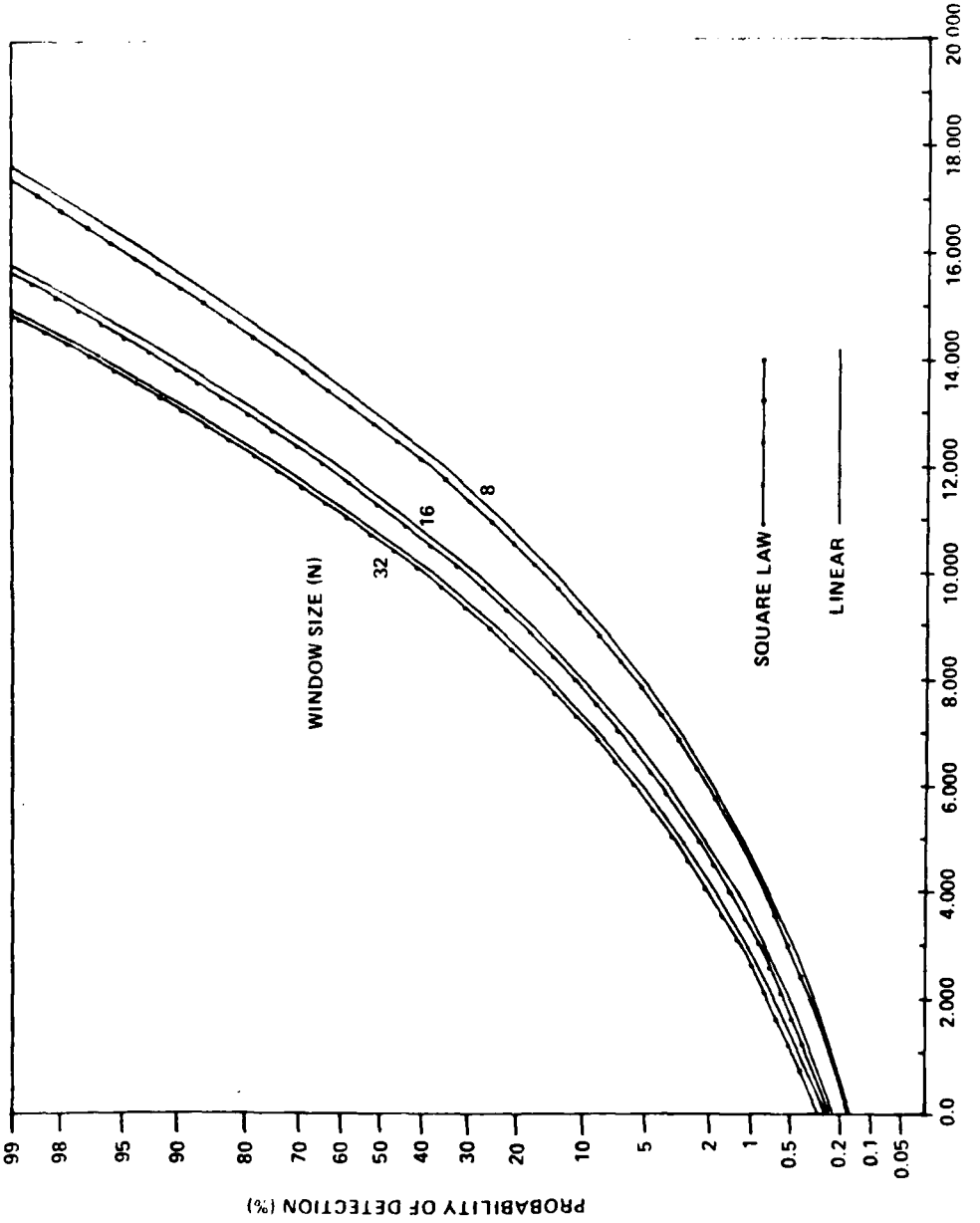

Figure 31. Performance Comparison of Detector Laws for Cell Averaging ($\overline{PFA}_D = 10^{-4}$, Steady Target)

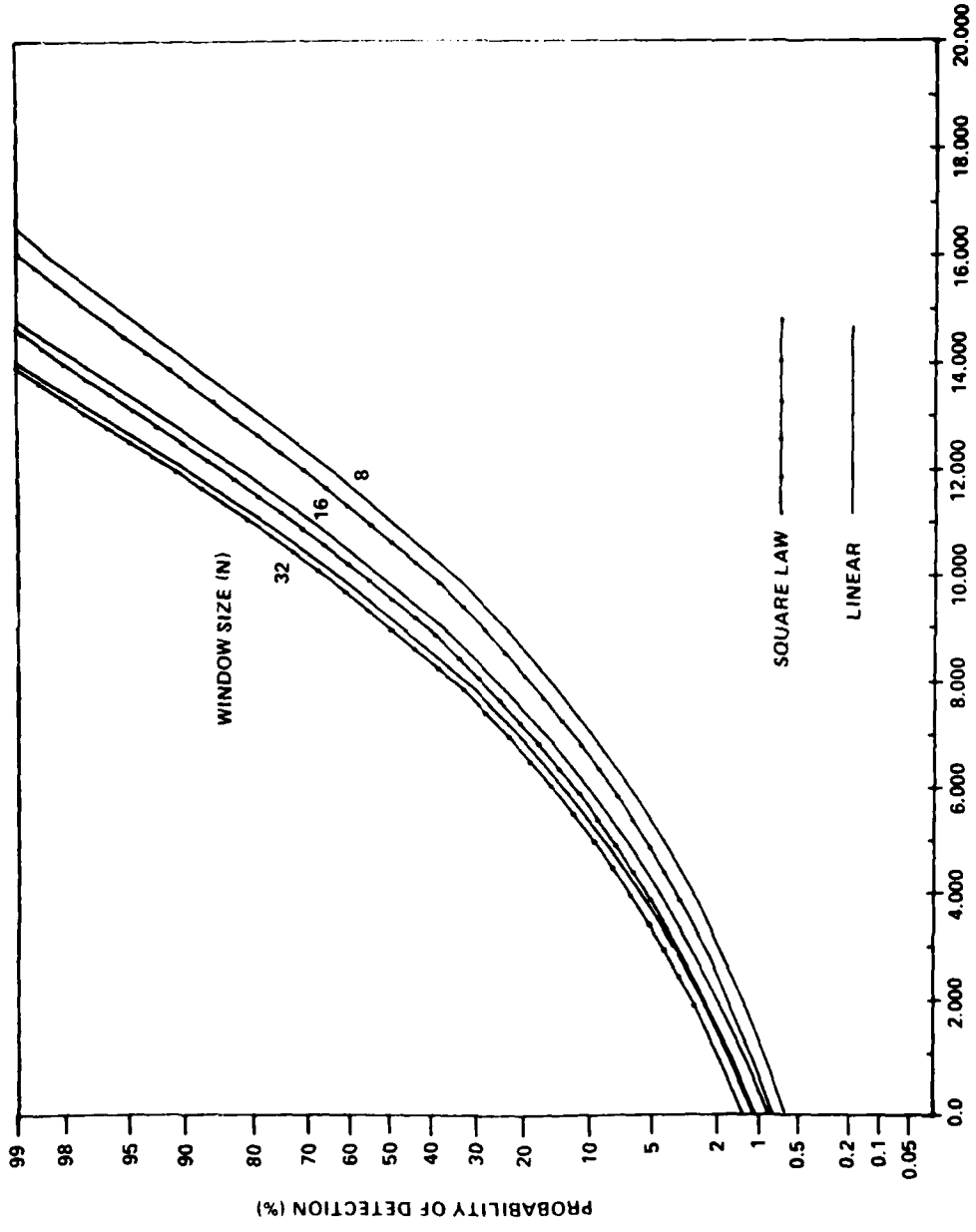

Figure 32. Performance Comparison of Detector Laws for "Greatest-Of" ($\overline{PFA}_D = 10^{-3}$, Steady Target)

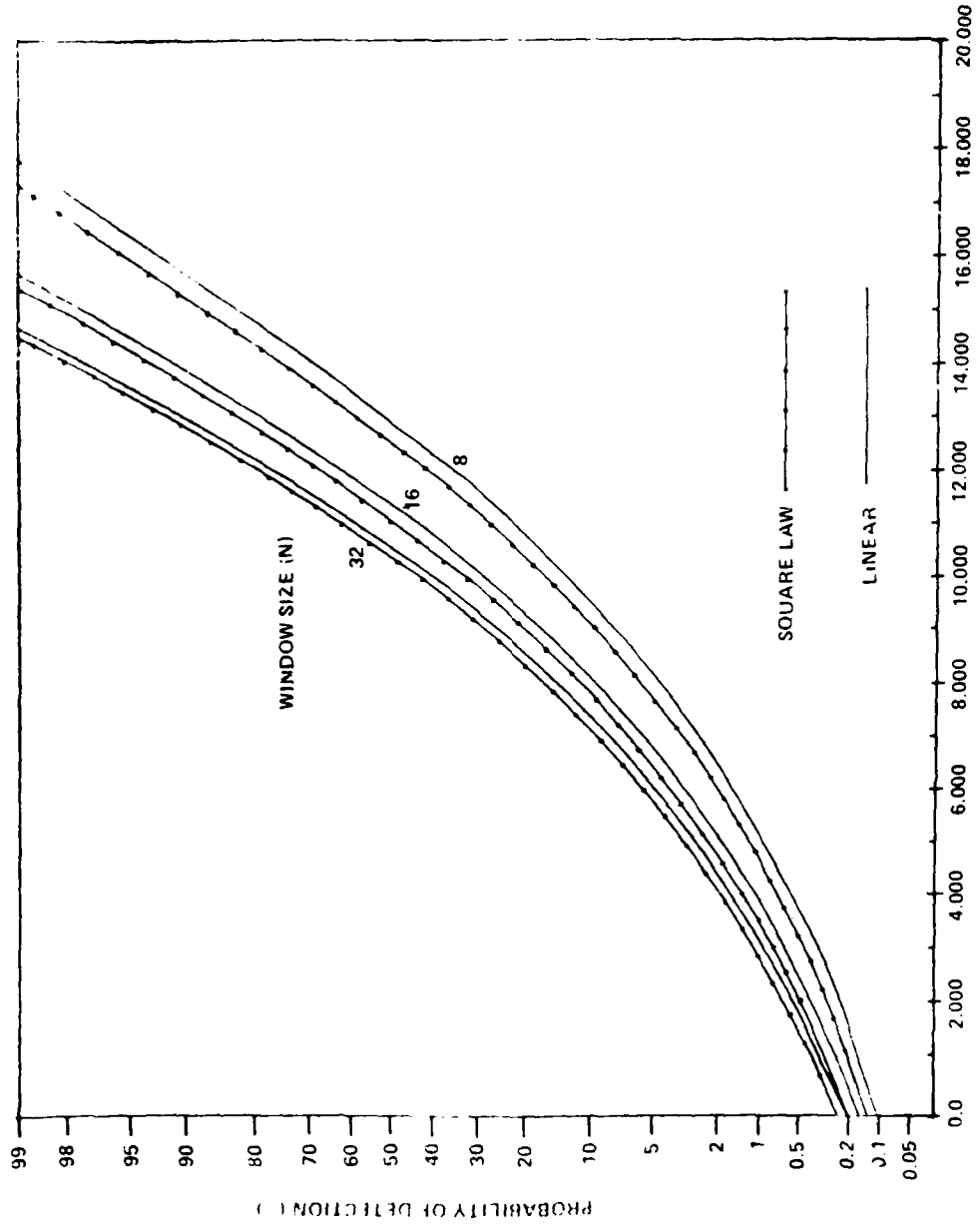

Figure 33. Performance Comparison of Detector Laws for "Greatest-Of" ($\overline{PFA}_D = 10^{-4}$, Steady Target)

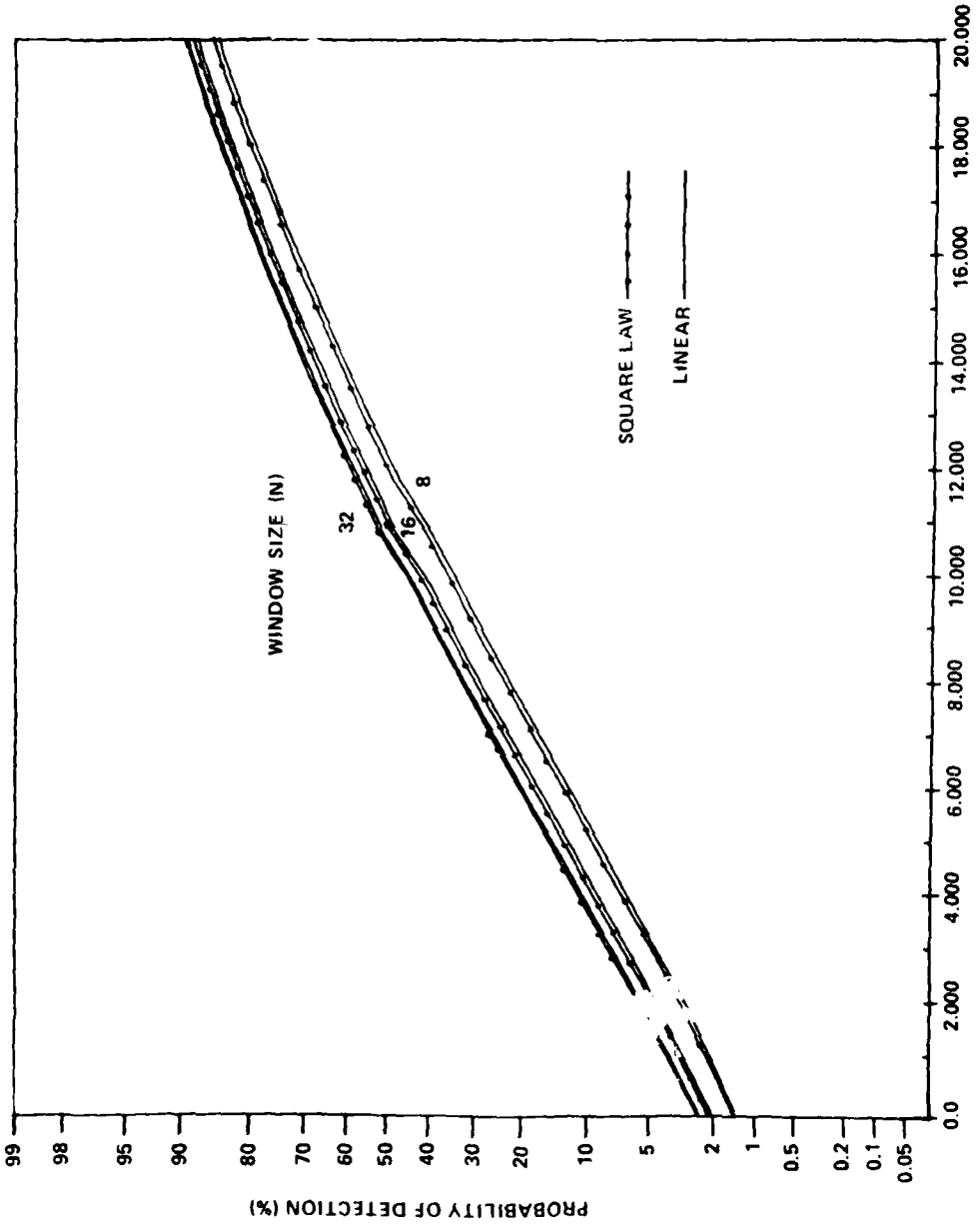

Figure 34. Performance Comparison of Detector Laws for Cell Averaging ($\overline{PFA}_D = 10^{-3}$, Swerling I Target)

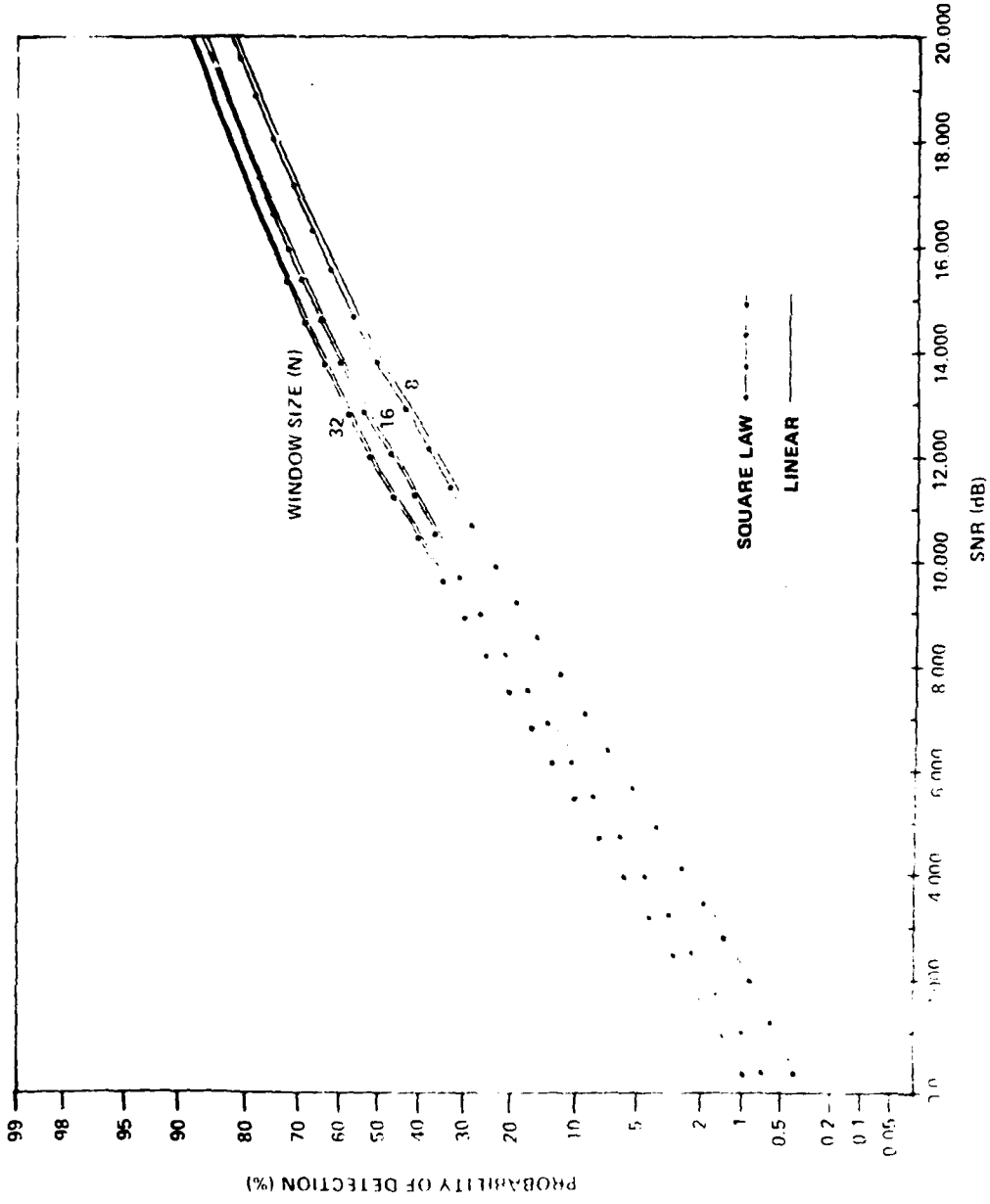

Figure 35. Performance Comparison of Detector Laws for Cell Averaging ($\overline{PFA}_D = 10^{-4}$, Swerling I Target)

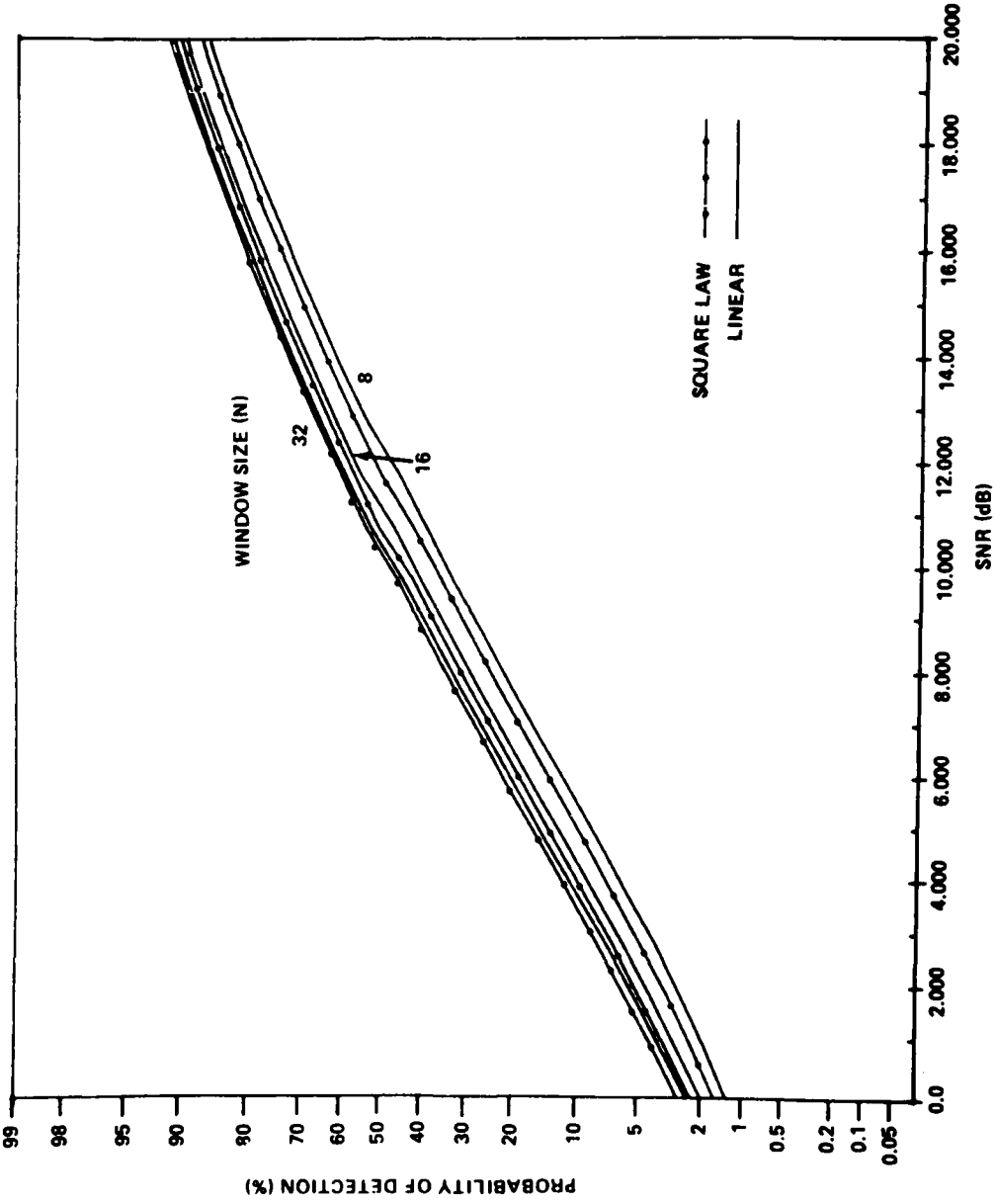

Figure 36. Performance Comparison of Detector Laws for "Greatest-Of" ($\overline{PFA}_D = 10^{-3}$, Swerling I Target)

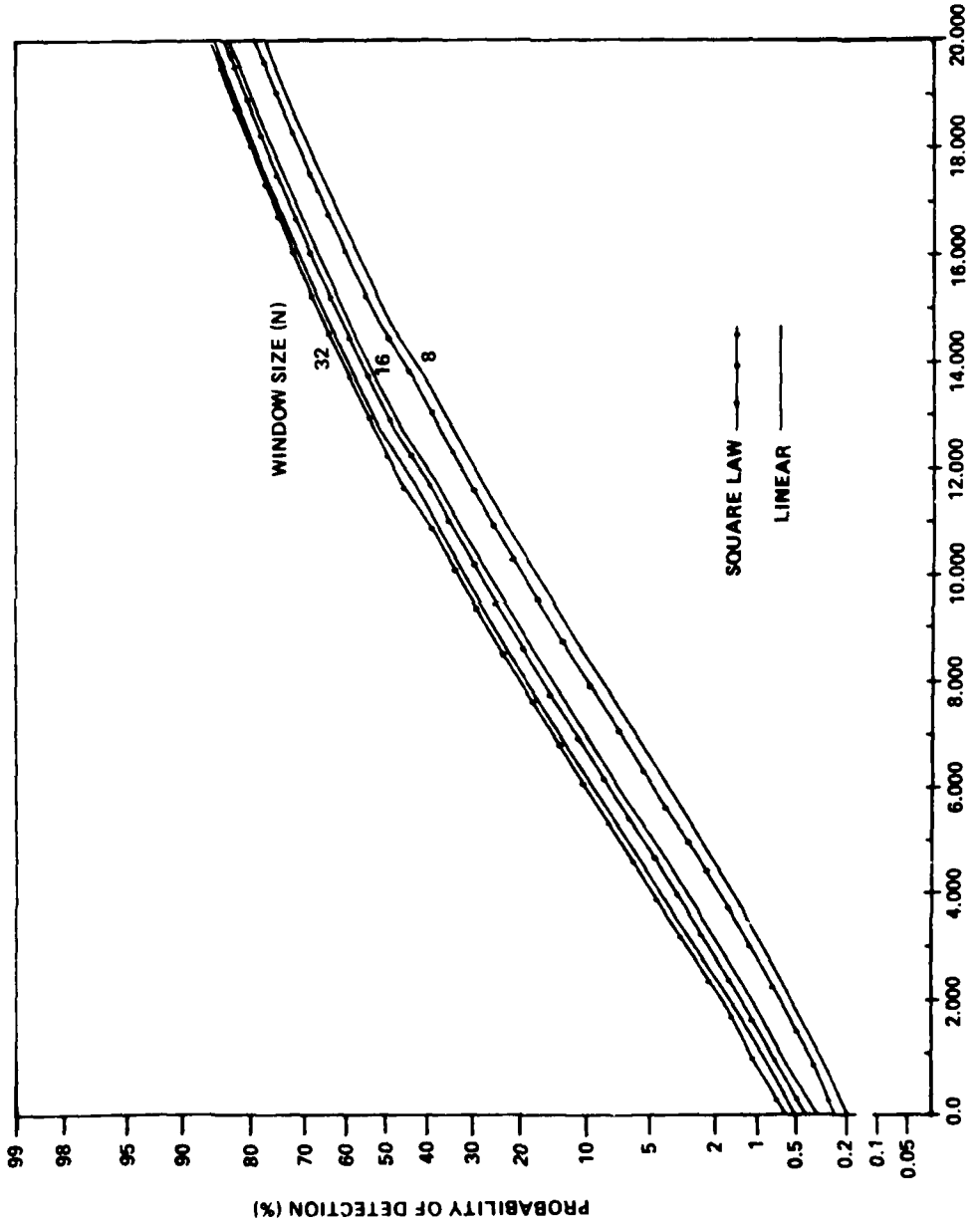

Figure 37. Performance Comparison of Detector Laws for "Greatest-Of" ($\overline{PFA}_D = 10^{-4}$, Swerling I Target)

model, average probability of false alarm and window width, for either CFAR technique. For the target of greatest interest, i.e., the Swerling I target, the detection difference between using a square law or a linear detector is small.

The actual $\overline{PFA}$s determined by the Monte Carlo simulation for the linear detector system are given in Table 3.

Table 3. Linear Detector Probabilities of False Alarms

$\overline{PFA}_D$	N	$\overline{PFA}_{CA}$	$\overline{PFA}_G$
10^{-3}	8	0.114-2	0.98-3
	16	0.112-2	0.89-3
	32	0.98-3	0.89-3
10^{-4}	8	0.125-3	0.10-3
	16	0.99-4	0.93-4
	32	0.103-3	0.99-4

Average signal-to-noise ratio differences $\overline{\Delta}$dB are calculated for a particular CFAR procedure and the probabilities of detection obtained for the two detectors. A positive $\overline{\Delta}$dB indicates a superior performance for the square law detector. The average signal-to-noise ratio differences $\overline{\Delta}$dB are given in Table 4 for a cell averaging CFAR and a Swerling I target and in Table 5 for a "greatest-of" CFAR and Swerling I target. The results indicate that the difference in the performance obtained for either detector and 32 reference cells is at most 0.22 dB. Hence, most results obtained for a square law system could be used for a linear detector system as well. This is an important conclusion since the theoretical analysis of the CFAR processors is obtainable only for a square law detector, and analysis costs are reduced by not having to simulate both detectors.

Table 4. Signal-to-Noise Ratio Comparison for Different Detector Laws and a Cell Averaging CFAR

$\overline{PFA}_D$	N	$\overline{\Delta}$dB
10^{-3}	8	0.240
	16	0.183
	32	0.142
10^{-4}	8	0.210
	16	0.172
	32	0.148

Table 5. Signal-to-Noise Ratio Comparison for Different Detector Laws and a "Greatest-of" CFAR

$\overline{PFA}_D$	N	$\overline{\Delta}$dB
10^{-3}	8	0.45
	16	0.30
	32	0.22
10^{-4}	8	0.43
	16	0.29
	32	0.21

5.5 Clutter Edge Performance Comparison

One problem which must be solved by adaptive detection techniques is the regulation of false alarms in nonhomogeneous interference. For radar this would be chaff or weather clutter distributed in range. The boundary of this interference, i.e., the clutter edge (Figure 11) will move into (or out of) the reference cells as the range cell of interest approaches (or leaves) the clutter area. Generally, the signal-to-interference ratio in the clutter area is low and the probability of detection is small. Hence, the deviation of the false alarm rate from the originally designed rate is of greater importance.

It will be assumed that the range extent of the clutter will be sufficient to eventually cover all of the CFAR range cells, i.e., the reference cells and the cell of interest. The clutter will be described mathematically as white Gaussian noise with the ratio of the reference cell noise variance to the cell-of-interest noise variance as

$$\tau_n = \frac{\sigma_n^2}{\sigma^2}, \quad n = 1, 2, \ldots N . \tag{5.12}$$

It has been shown [19] that for the cell averaging CFAR

$$\overline{PFA}_{CA} = \prod_{n=1}^{N} \left(1 + \tau_n \frac{K}{N}\right)^{-1} . \tag{5.13}$$

For the condition where the clutter occupies $N_1 \leq N/2$ reference cells, then $\tau_n = \sigma_c^2/\sigma^2 = \tau_c$. In each of these cells and $\tau_n = 1$ for non-clutter cells, it follows that

$$\overline{PFA}_{CA} = \overline{PFA}_D^{\frac{N-N_1}{N}} \left[1 + \tau_c \left(\overline{PFA}_D^{-1/N} - 1\right)\right]^{-N_1} \tag{5.14}$$

where $\overline{PFA}_D$ is the homogeneous interference design value.

For $N/2 \leq N_1 < N$, then the cell of interest will also contain the clutter and $\tau_n = 1$ for the clutter covered cells. The uncovered cells will have $\tau_n = \sigma^2/\sigma_c^2 = 1/\tau_c$. Thus

$$\overline{PFA}_{CA} = \left[1 + \frac{\overline{PFA}_D^{-1/N} - 1}{\tau_c}\right]^{-(N-N_1)} \left(\overline{PFA}_D\right)^{N_1/N} . \tag{5.15}$$

Theoretical results for the "greatest-of" CFAR in nonhomogeneous interference have been performed only for restrictive cases [11]. The Monte Carlo simulation allows not only for verification of cell averaging

theoretical results but also determination of the "greatest-of" performance.

Performance comparison curves are shown in Figures 38 through 43. These curves give the probabilities of false alarm versus the number of cells covered by the clutter for the cell averaging and "greatest-of" CFAR processors. The plots contain the cell averaging theoretical analysis and the Monte Carlo results. There are two regions divided by the cell of interest.

In region one, where the clutter edge enters either CFAR processor window, the probability of false alarm is smaller than the originally designed probability of false alarm. Hence, this region is not important since both processors will maintain the false alarm rate below the design false alarm rate. For this region the PFAs determined by the simulation produce erroneous or no results for probabilities of false alarm less than 10^{-5}. However, the cell averaging theoretical results, Equation (5.14), are plotted.

In region two, where the clutter is in the cell of interest and there are at least N/2 + 1 reference cells, the probability of false alarm is now greater than the design probability of false alarm for both processors. The worst case for both processors is when the cell of interest and N/2 + 1 reference cells are covered. The actual probabilities of false alarm are given in Table 6.

It is readily observed that both CFAR processors cannot maintain the design probability of false alarm in certain clutter edge conditions. However, the "greatest-of" CFAR is less sensitive to this environment. From Table 6 the probabilities of false alarm for the cell averaging CFAR are a factor of 1.4 to 7.4 higher than the

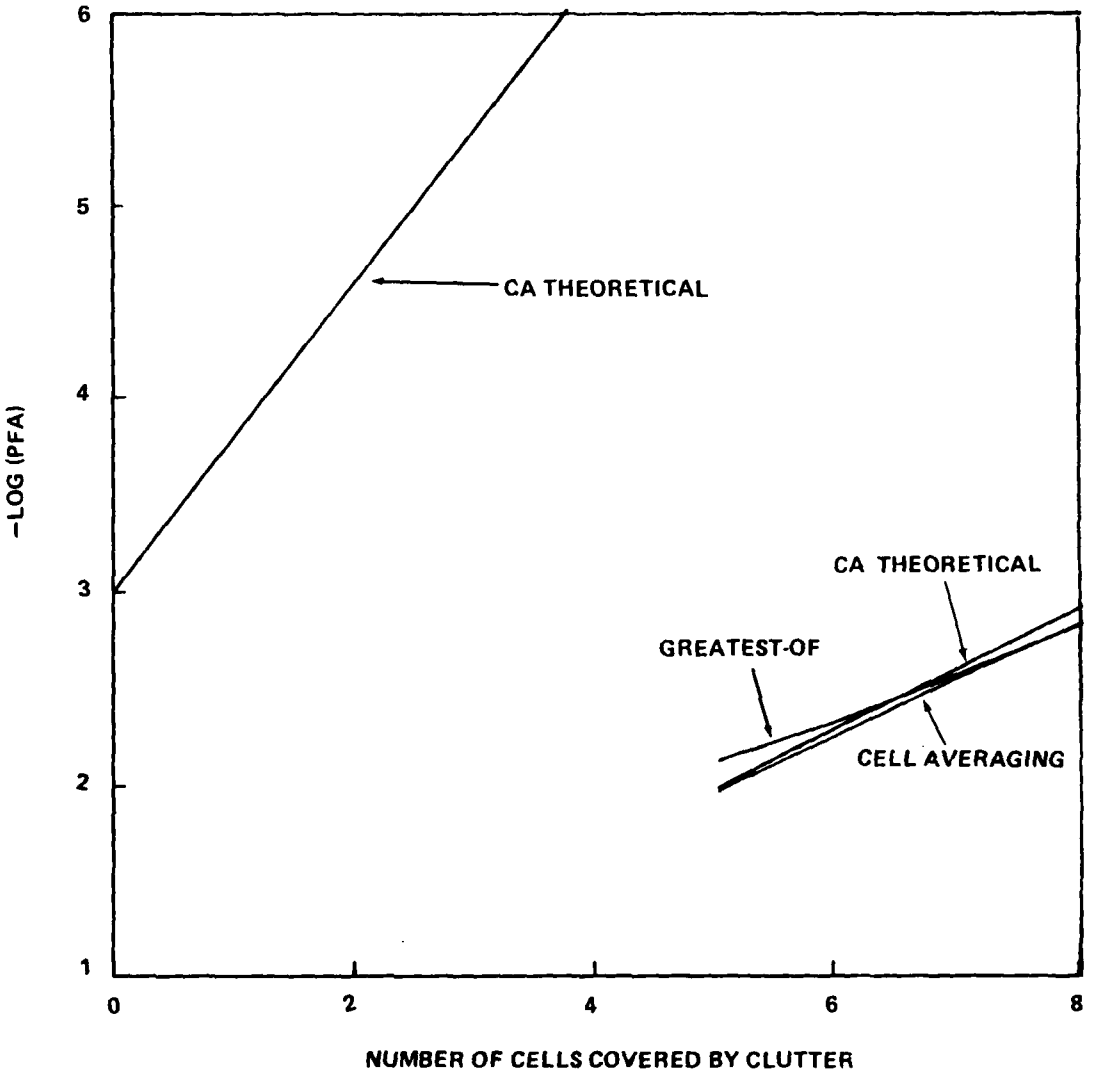

Figure 38. Clutter Edge Effects on Probability of False Alarm (N=8, τ_c = 10, $\overline{PFA}_D = 10^{-3}$)

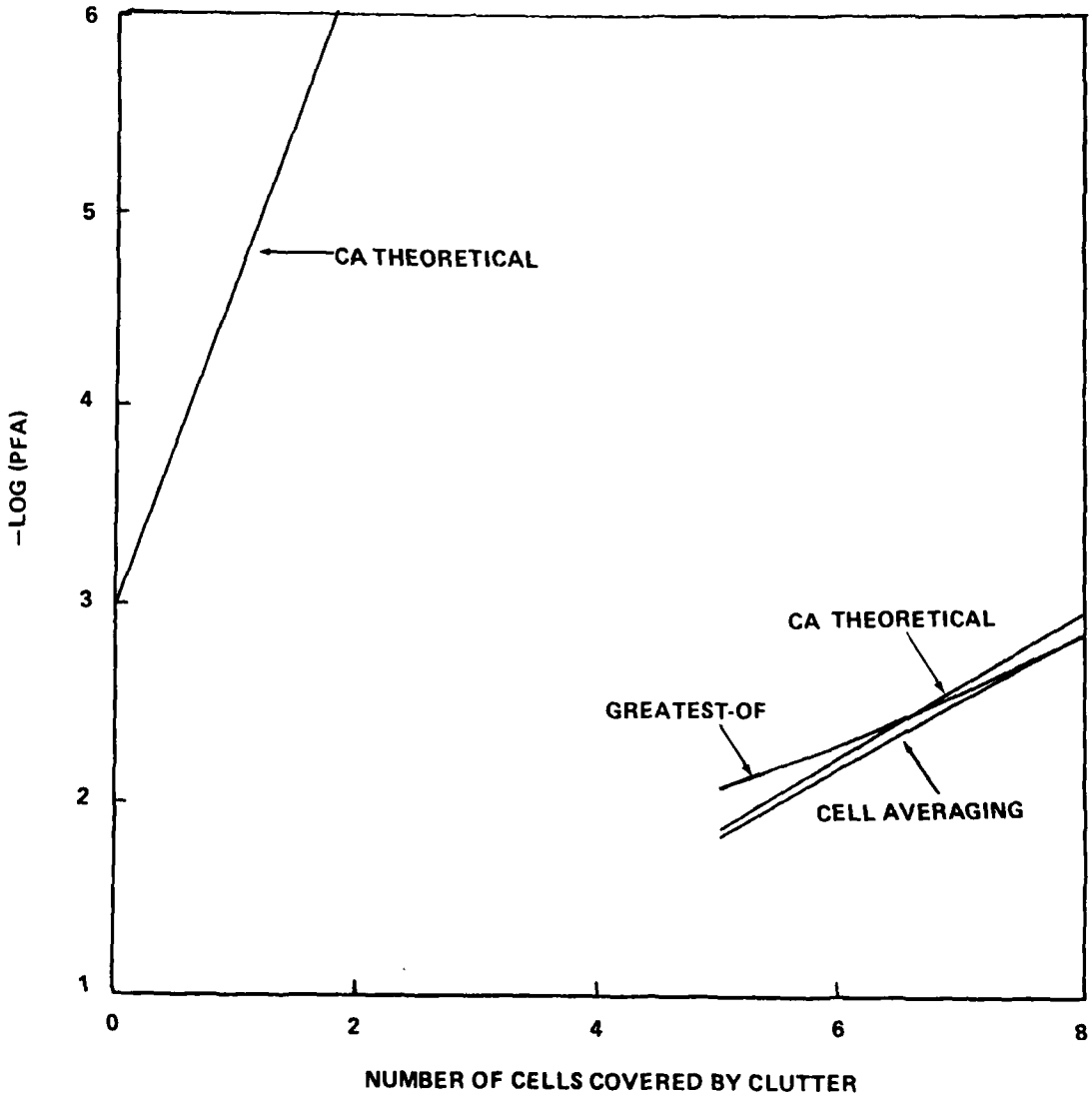

Figure 39. Clutter Edge Effects on Probability of False Alarm (N=8, τ_c = 100, $\overline{PFA}_D = 10^{-3}$)

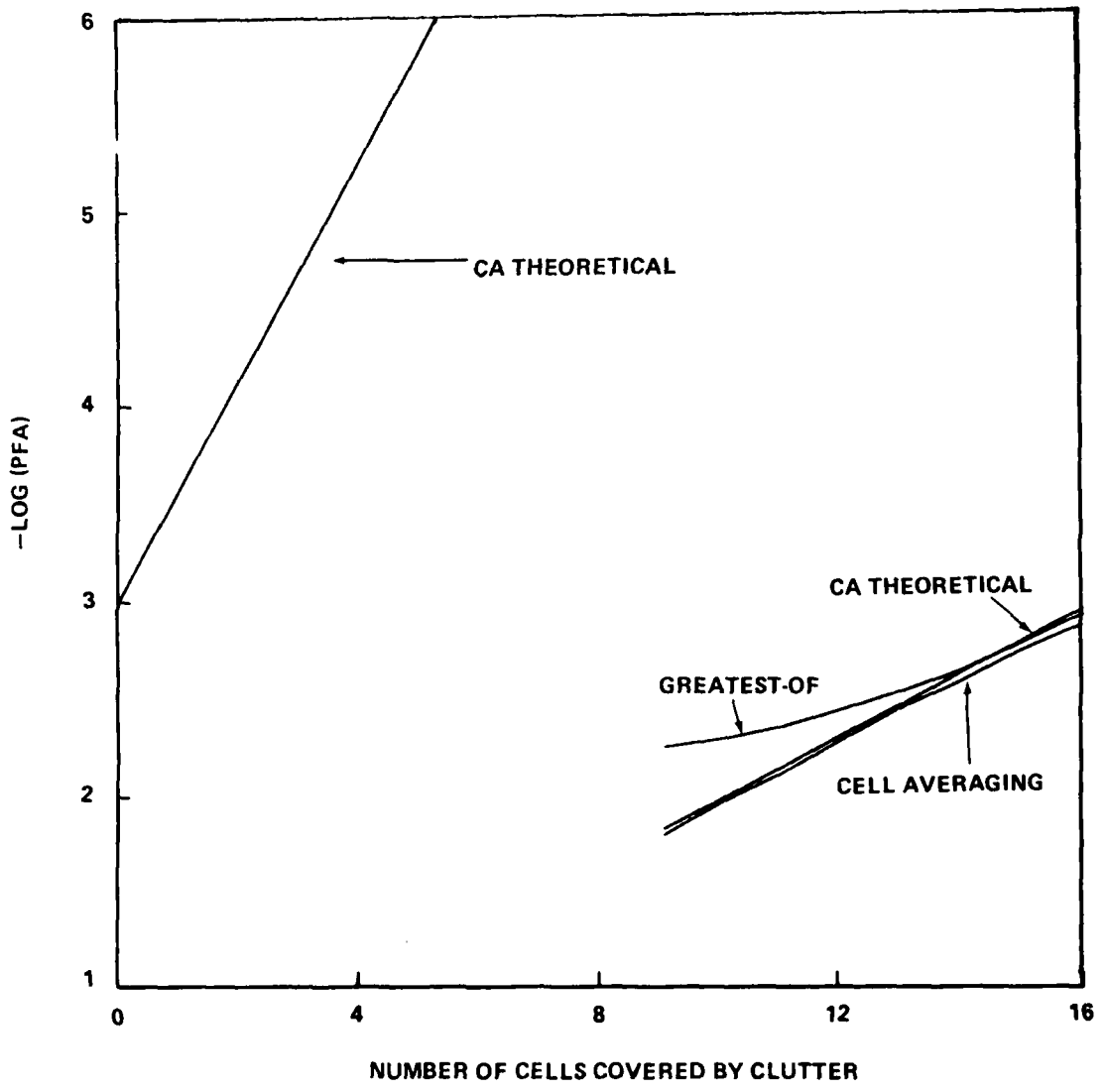

Figure 40. Clutter Edge Effects on Probability of False Alarm (N=16, τ_c = 10, $\overline{PFA}_D = 10^{-3}$)

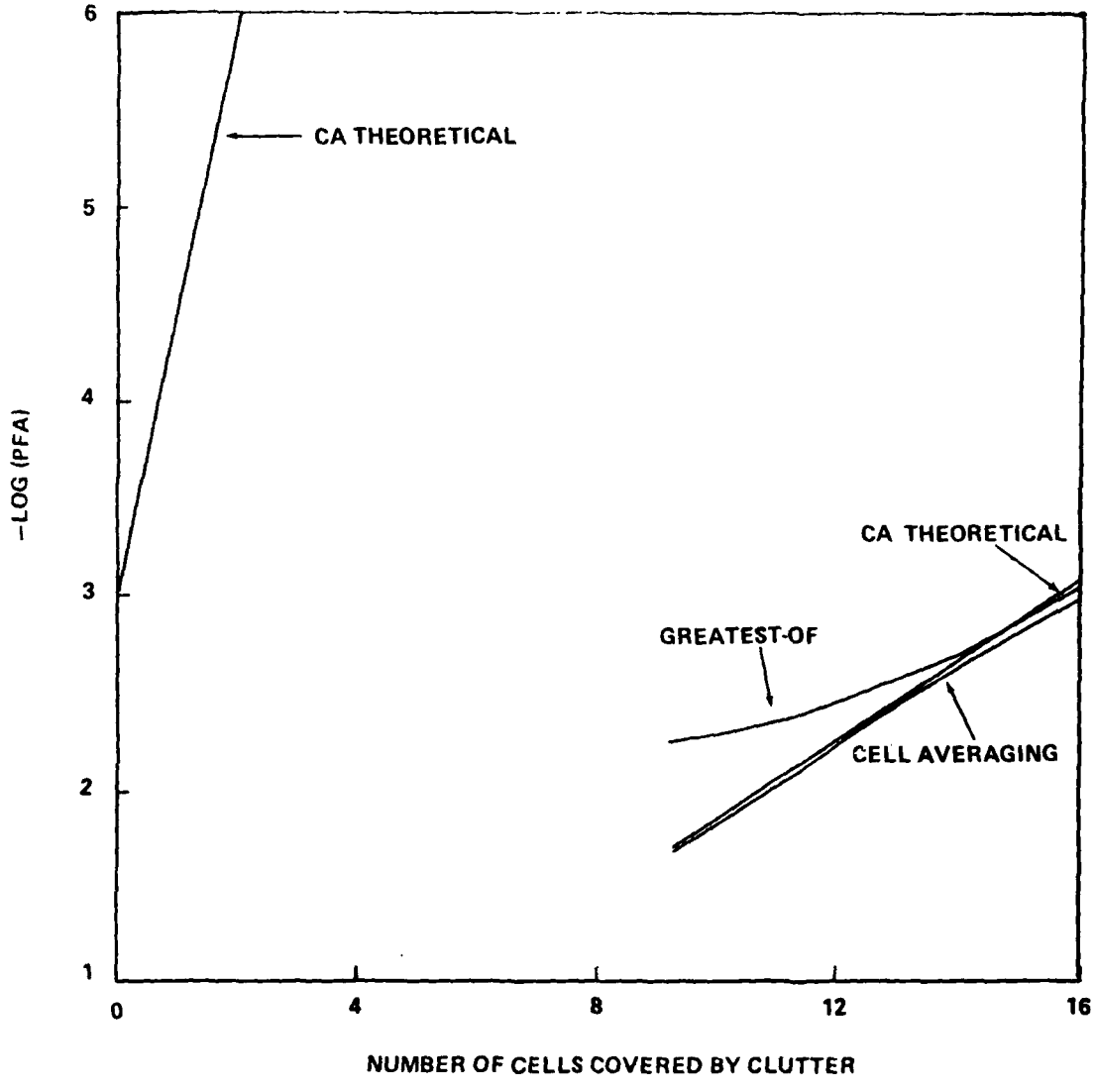

Figure 41. Clutter Edge Effects on Probability of False Alarm (N=16, τ_c = 100, $\overline{PFA}_D = 10^{-3}$)

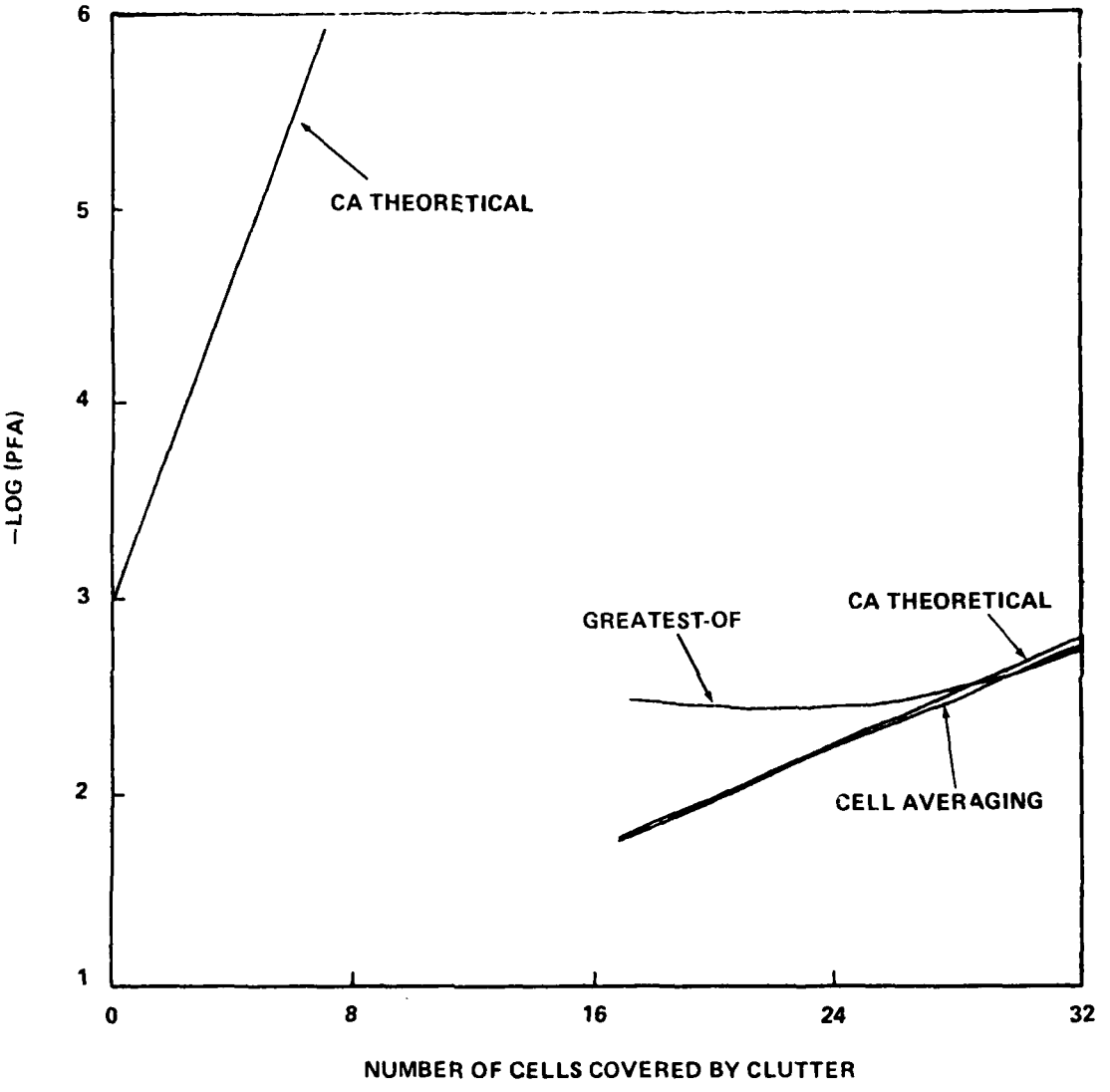

Figure 42. Clutter Edge Effects on Probability of False Alarm (N=32, τ_c = 10, $\overline{PFA}_D = 10^{-3}$)

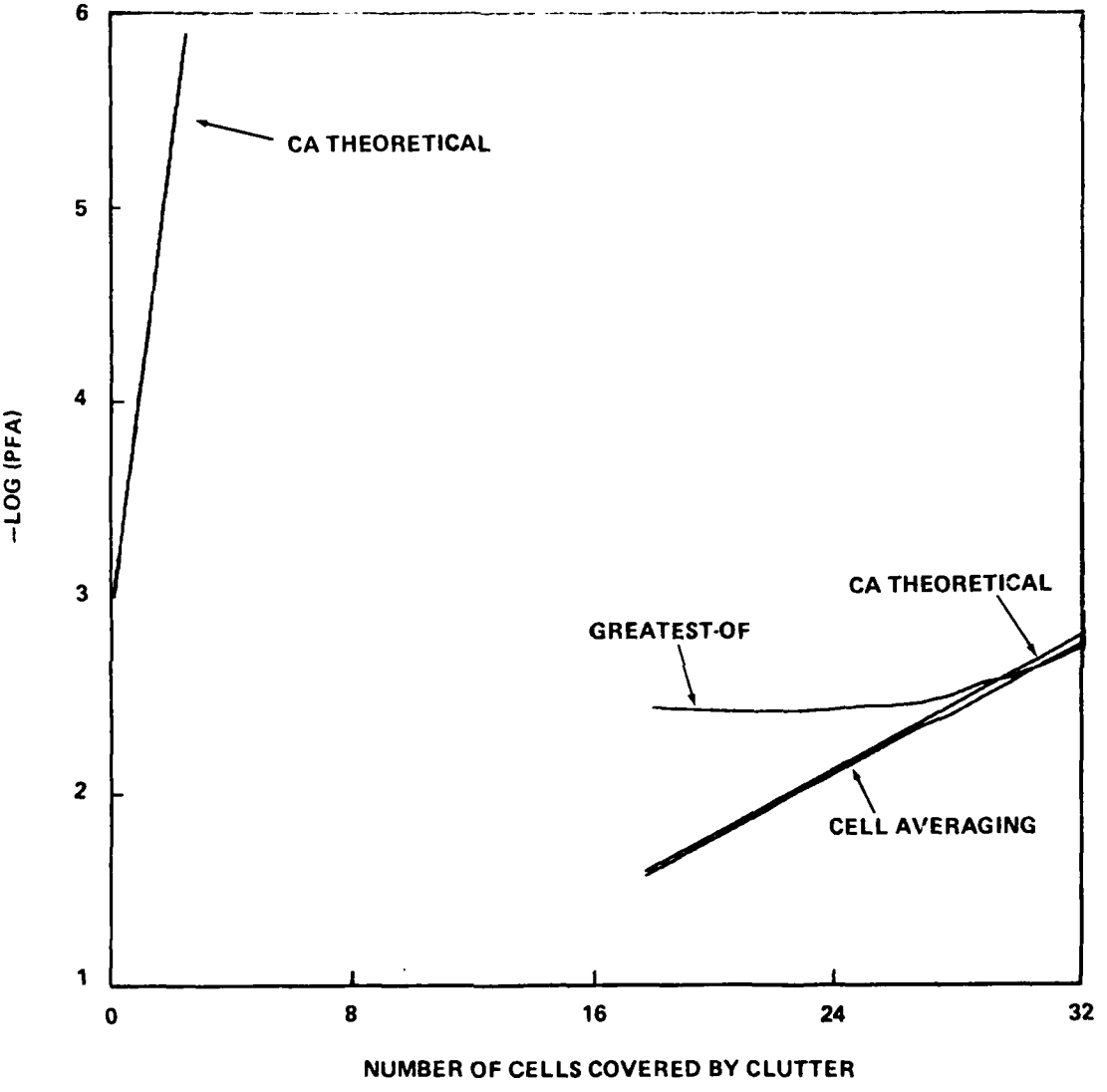

Figure 43. Clutter Edge Effects on Probability of False Alarm (N=32, τ_c = 100, $\overline{PFA}_D = 10^{-3}$)

"greatest-of" probabilities of false alarm. This factor, which shows the difference in performance, is a function of the design probability of false alarm. As shown in Moore and Lawrence [11], for a $\overline{PFA}_D = 10^{-6}$, N = 32 and τ_c = 100, the cell averaging CFAR probability of false alarm is 57.5 times greater than the "greatest-of" probability of false alarm. This feature is the primary advantage that the "greatest-of" CFAR has over the cell averaging CFAR.

Table 6. Comparison of Clutter Edge Probabilities of False Alarm ($\overline{PFA}_D = 10^{-3}$)

	τ_c			
	10		100	
N	$\overline{PFA}_{CA}$	$\overline{PFA}_G$	$\overline{PFA}_{CA}$	$\overline{PFA}_G$
8	0.93-2	0.66-2	0.14-1	0.77-2
16	0.15-1	0.54-2	0.21-1	0.56-2
32	0.18-1	0.35-2	0.26-1	0.35-2

5.6 Quantization Consideration

Recent radar signal processors are implemented digitally, hence, the effect of quantization noise must be considered when specifying a desired probability of false alarm. For this analysis the quantization or A/D conversion will occur after the detector with wordlengths of 6, 8, and 10 bits and the wordlength is not truncated in the CFAR processor. Since a given CFAR processor could have any combination of wordlengths, truncation schemes and assumed saturation level, no effort will be made to determine a general method to maintain a given false alarm.

The quantization errors for 8 and 10 bits wordlengths are negligible, thus, only the results for 6 bits are given in Tables 7

through 10. Tables 7 and 8 give the probabilities of false alarm for the two CFAR processors in homogeneous noise with $\sigma^2 = 1$ and $\sigma^2 = 2$ and 6 bits of quantization. Table 9 gives the average signal-to-noise difference, based on the cell averaging CFAR as described in this chapter, for both CFAR processors and 6-bit quantization. Table 10 gives probabilities of false alarm for both processors, linear detector, and 6 bits.

Table 7. Quantization Effects on Probability of False Alarm (Square Law; 6 bits, $\sigma^2 = 1$)

$\overline{PFA}_D$	N	$\overline{PFA}_{CA}$	$\overline{PFA}_G$
10^{-3}	8	0.55-3	0.52-3
	16	0.57-3	0.71-3
	32	0.78-3	0.82-3
10^{-4}	8	0.19-4	0.51-4
	16	0.51-4	0.57-4
	32	0.64-4	0.66-4
10^{-5}	8	---	0.27-5
	16	0.19-5	0.42-5
	32	0.36-5	0.64-5

Table 8. Quantization Effects on Probability of False Alarm (Square Law; 6 bits, $\sigma^2 = 2$)

$\overline{PFA}_D$	N	$\overline{PFA}_{CA}$	$\overline{PFA}_G$
10^{-3}	8	0.95-3	0.850-3
	16	0.94-3	0.103-2
	32	0.10-2	0.930-3
10^{-4}	8	0.68-4	0.910-4
	16	0.93-4	0.105-3
	32	0.106-5	0.112-3
10^{-5}	8	0.50-5	0.670-5
	16	0.77-5	0.860-5
	32	0.79-5	0.108-4

Table 9. Quantization Effects on Signal-to-Noise Ratio (Square Law, 6 bits)

$\overline{PFA}_D$	N	$\overline{\Delta}_{CA}$	$\overline{\Delta}_G$
10^{-3}	8	0.362	0.418
	16	0.286	0.116
	32	0.264	0.248
10^{-4}	8	0.460	0.256
	16	0.314	0.257
	32	0.280	0.217
10^{-5}	8	0.600	0.382
	16	0.365	0.276
	32	0.294	0.240

Table 10. Quantization Effects on Probability of False Alarm (Linear Detector, 6 bits $\sigma^2 = 1$)

$\overline{PFA}_D$	N	$\overline{PFA}_{CA}$	$\overline{PFA}_G$
10^{-3}	8	0.117-2	0.75-3
	16	0.107-2	0.89-3
	32	0.980-3	0.86-3
10^{-4}	8	0.124-3	0.101-3
	16	0.108-3	0.970-4
	32	0.108-3	0.100-3

It is observed from Table 7 that the probability of false alarm has decreased for both processors which is undesirable since this is not the original design value. Even if the CFAR scale factors K and K_G are adjusted to obtain the design probability of false alarm, the probability of false alarm would change if the standard deviation of the noise changed as shown in Table 8. Since the probability of false alarm (Table 7) decreased due to quantization, the probability of detection is also reduced. This is shown in Table 9 where the average signal-to-noise differences between no quantization and quantization

are given for both processors. Table 10 shows no real difference in probability of false alarm due to quantization because of the reduced dynamic range of the linear detector outputs.

The effects of A/D quantization and finite wordlengths must be considered when implementing a digital CFAR processor. Even though some analytical effort has been performed [20], a more complete study can be achieved only through simulation.

5.7 Non-Gaussian Interference Results

The cell averaging CFAR and "greatest-of" CFAR processors assume the noise amplitude distribution is Gaussian with an unknown power. In several instances this is not a valid assumption and a changing probability density function can be encountered due to a lack of clutter rejection by the MTI.

Several investigations of natural clutter characteristics have shown that clutter returns can be described by log-normal or Weibull [18] types of distributions where the Weibull pdf includes the Rayleigh pdf as a special case.

The Weibull pdf is a single variate function having two parameters, a and b, and is given by

$$p(\sigma^o) = \frac{b(\sigma^o)^{b-1}}{a} \exp\left[-(\sigma^o)^b/a\right] \tag{5.16}$$

where σ^o is the variate in terms of the clutter backscatter coefficient, b = 1/A (A = Weibull slope parameter) and

$$a = \frac{(\sigma_m^o)^b}{\ln 2} \tag{5.17}$$

where σ_m^o = median value of Weibull pdf.

The probability of false alarm performance against Weibull for A = 1, 2, 3 for both CFAR processors is given in Tables 11 through 13.

For A=1, the Weibull pdf reduces to the exponential pdf, therefore, the probability of false alarms obtained are the originally designed values.

For A=2 and A=3, which are representative of natural clutter [18], the probabilities of false alarm increase by a factor of approximately 100 and 1000, respectively, for both processors. This increase is unacceptable.

Table 11. Probabilities of False Alarm in Presence of Weibull Clutter (A=1)

$\overline{PFA}_D$	N	$\overline{PFA}_{CA}$	$\overline{PFA}_G$
10^{-3}	8	0.112-2	0.890-3
	16	0.117-2	0.118-2
	32	0.112-2	0.106-2
10^{-4}	8	0.119-3	0.125-3
	16	0.106-3	0.111-3
	32	0.110-3	0.129-3
10^{-5}	8	0.102-4	0.75-5
	16	0.133-4	0.142-4
	32	0.117-4	0.118-4

Table 12. Probabilities of False Alarm in Presence of Weibull Clutter (A=2)

$\overline{PFA}_D$	N	$\overline{PFA}_{CA}$	$\overline{PFA}_G$
10^{-3}	8	0.331-1	0.252-1
	16	0.298-1	0.250-1
	32	0.283-1	0.237-1
10^{-4}	8	0.170-1	0.136-1
	16	0.164-1	0.129-1
	32	0.154-1	0.125-1
10^{-5}	8	0.878-2	0.686-2
	16	0.916-2	0.699-2
	32	0.905-2	0.717-2

AD-A099 988 ARMY MISSILE COMMAND REDSTONE ARSENAL AL ADVANCED S--ETC F/G 17/9
PERFORMANCE COMPARISON OF CELL AVERAGING AND 'GREATEST-OF' CONS--ETC(U)
FEB 81 N B LAWRENCE
UNCLASSIFIED DRSMI-RE-81-9-TR SBIE-AD-E950 131 NL

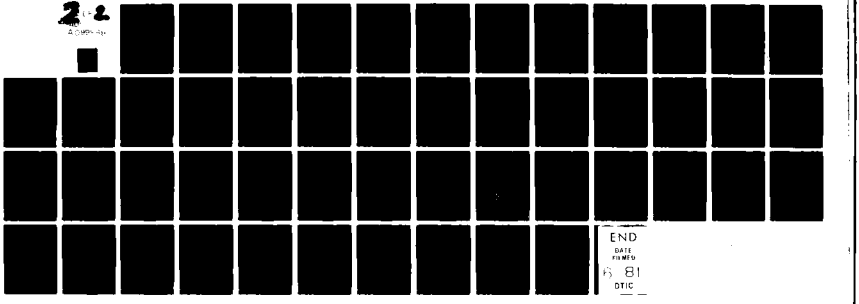

Table 13. Probabilities of False Alarm in Presence of Weibull Clutter (A=3)

$\overline{PFA}_D$	N	$\overline{PFA}_{CA}$	$\overline{PFA}_G$
10^{-3}	8	0.619-1	0.500-1
	16	0.498-1	0.410-1
	32	0.435-1	0.356-1
10^{-4}	8	0.431-1	0.355-1
	16	0.359-1	0.291-1
	32	0.307-1	0.248-1
10^{-5}	8	0.304-1	0.246-1
	16	0.265-1	0.210-1
	32	0.229-1	0.181-1

A CFAR processor has been designed which maintains false alarm regulation in log-normal and Weibull clutter [21]. Also, a Weibull loss has been presented for the cell averaging CFAR designed to maintain a constant false alarm rate in various Weibull clutter environments [16].

5.8 Interfering Target Results

The detection performance of both CFAR processors will be affected by a target or targets occupying the CFAR window when a target is in the cell of interest. The interfering target(s) can reduce the probability of detection to an unacceptable value as shown by Finn and Johnson [14] in their Figure 18 for a square law detector and a target pair using a cell averaging CFAR.

For a limited detection performance comparison, two Swerling I targets will be assumed: white Gaussian noise and a square law detector. Three cases will be simulated: 1) the target of interest is 10 dB above the noise and the interfering target is 7 dB above the noise, 2) the target of interest and the interfering target are both

10 dB above the noise, and 3) the target of interest is 10 dB above the noise and the interfering target is 13 dB above the noise.

The probabilities of detection, $\overline{PD}_{CA}$ and $\overline{PD}_{G}$, determined by the simulation are given in Tables 14 through 16. Using Equation (3.5) and the probabilities of detection, IF signal-to-noise ratios, SNR_{CA} for the cell averaging CFAR and SNR_{G} for the "greatest-of" CFAR are calculated. The last column, Δ_{SNR}, provides a measure of performance comparison between the two processors.

It is readily observed that the detection performance decreases as N decreases. Even for a large N, i.e., N=32, the cell averaging CFAR suffers a detectability loss of 0.7 dB, 1.2 dB, and 2.0 dB for cases 1, 2, and 3, respectively. The signal-to-noise difference, Δ_{SNR}, gives the amount the input SNR could be reduced for the cell averaging CFAR and maintain equivalent performance with the "greatest-of" CFAR. The range of Δ_{SNR} is from 0.3 dB to 0.7 dB.

While both processors are sensitive to an interfering target environment, the cell averaging CFAR is superior to the "greatest-of" in this type of environment. This advantage would have to be considered when designing a CFAR processor.

Table 14. Signal-to-Noise Ratio Comparison for a 7 dB Interfering Target

$\overline{PFA}_{D}$	N	$\overline{PD}_{CA}$	SNR_{CA}	$\overline{PD}_{G}$	SNR_{G}	Δ_{SNR}
10^{-3}	8	0.266	8.2	0.239	7.8	0.4
	16	0.381	8.9	0.357	8.5	0.4
	32	0.449	9.3	0.431	9.0	0.3
10^{-4}	8	0.140	8.3	0.124	8.0	0.3
	16	0.259	8.9	0.236	8.6	0.3
	32	0.334	9.4	0.317	9.1	0.3
10^{-5}	8	0.066	8.4	0.058	8.1	0.3
	16	0.166	9.0	0.148	8.6	0.4
	32	0.246	9.4	0.230	9.1	0.3

Table 15. Signal-to-Noise Ratio Comparison for a 10 dB Interfering Target

$\overline{PFA}_D$	N	$\overline{PD}_{CA}$	SNR_{CA}	$\overline{PD}_G$	SNR_G	Δ_{SNR}
10^{-3}	8	0.194	7.0	0.155	6.3	0.7
	16	0.318	8.0	0.278	7.4	0.6
	32	0.406	8.7	0.374	8.3	0.4
10^{-4}	8	0.097	7.3	0.081	6.8	0.4
	16	0.205	8.1	0.175	7.6	0.5
	32	0.294	8.8	0.264	8.4	0.4
10^{-5}	8	0.044	6.4	0.036	6.1	0.3
	16	0.126	8.2	0.106	7.8	0.4
	32	0.210	8.8	0.183	8.4	0.4

Table 16. Signal-to-Noise Ratio Comparison for a 13 dB Interfering Target

$\overline{PFA}_D$	N	$\overline{PD}_{CA}$	SNR_{CA}	$\overline{PD}_G$	SNR_G	Δ_{SNR}
10^{-3}	8	0.124	5.6	0.099	5.0	0.6
	16	0.243	6.9	0.196	6.1	0.8
	32	0.348	7.9	0.299	7.2	0.7
10^{-4}	8	0.056	3.5	0.046	2.8	0.7
	16	0.146	5.1	0.116	4.4	0.7
	32	0.242	6.3	0.201	5.7	0.6
10^{-5}	8	0.024	6.4	0.019	6.1	0.3
	16	0.085	7.2	0.066	6.2	0.5
	32	0.164	8.1	0.133	7.5	0.6

5.9 Summary

The detection performances of the cell averaging and "greatest-of" CFAR have been determined and presented. Both CFAR processors were designed for three common probabilities of false alarm and the actual probabilities of false alarm were obtained by the Monte Carlo simulation. For a given probability of false alarm, the two processors have essentially equivalent detection performance with the "greatest-of" having approximately 0.2 dB loss as compared to the cell averaging.

While both processors have only a slight degradation when a linear detector instead of a square law detector is used, their performance is unacceptable in Weibull clutter and is affected by finite wordlength processing.

The two main areas of performance comparison are the probability of false alarm regulation in clutter edges and the probability of detection in an interfering target situation. The "greatest-of" proved to regulate false alarms much better in the clutter edge environment while causing an additional detection loss, between 0.3 and 0.7 dB, in the interfering target environment as compared to the cell averaging method.

It is obvious that the selection of either the cell averaging CFAR or the "greatest-of" CFAR should be based on the expected radar environment. Due to similarity in their implementation, a combination of the two processors and supporting selection logic could provide an overall improved CFAR performance.

CHAPTER VI. SUMMARY, CONCLUSIONS, AND RECOMMENDATIONS

6.0 Summary

A computer simulation has been developed for a performance comparison of two commonly known CFAR techniques. The two techniques are the cell averaging and "greatest-of." The comparison is based on the probabilities of detection and the probabilities of false alarm obtained by performing Monte Carlo passes of the simulation.

The two CFAR processors were designed for average probabilities of false alarm of 10^{-3}, 10^{-4}, and 10^{-5}. These false alarm rates were verified by the simulation. Probability of detection versus input signal-to-noise ratio curves for each false alarm rate were generated for both processors. Two target models were used: the steady or non-fluctuating target and the Swerling I target. The probability of detection results were utilized to make a signal-to-noise ratio difference comparison and indicated that the cell averaging CFAR would require approximately 0.2 dB less input signal-to-noise ratio for equivalent performance to the "greatest-of" CFAR.

The detection performance for a linear detector system was determined for both CFAR processors and target models. Comparing the results to a square law detector system indicates that the detection performance is degraded by the use of a linear detector. However, this degradation is negligible, especially for a Swerling I target.

Two important analyses were performed: the clutter edge performance comparison and the interfering target results.

A clutter edge, i.e., residual clutter distributed in range, affects both CFAR processors by increasing the probability of false alarm above the design value. The amount the false alarm rate increases is a function of the design false alarm rate and the CFAR window size. The "greatest-of" technique provides better false alarm control than the cell averaging technique in a clutter edge condition.

An interfering target, i.e., a target which is in a reference cell of the CFAR processor, degrades the detection performance of both CFAR processors. In general, the amount of degradation is a function of the interfering target power, the design probability of false alarm and the CFAR window size. The cell averaging technique provides better detection performance than the "greatest-of" technique in an interfering target environment.

The quantization analysis demonstrated that the probability of false alarm and the probability of detection are affected by finite wordlength arithmetic. For some finite wordlength CFAR processors, the false alarm rate will change as the interference power changes.

The non-Gaussian interference analysis demonstrated the unacceptable false alarm rates obtained in Weibull interference for both CFAR processors.

6.1 Conclusions

The cell averaging and "greatest-of" CFAR processors can be designed to maintain a constant false alarm rate in homogeneous white Gaussian noise. The probability of detection obtained for a given probability of false alarm increases as the number of CFAR processor reference cells increase for both processors. The two CFAR

techniques have almost equivalent performance in white Gaussian noise with the cell averaging CFAR having a slight advantage.

The simulation results have shown a negligible improvement obtained for a square law detector over a linear detector. Hence, the analytical results developed for the two CFAR processors and a square law detector could be used to describe the performance for a linear detector system.

Whereas both processors fail to maintain the design probability of false alarm in a clutter edge environment, the "greatest-of" technique is affected less than the cell averaging technique and should be a prime CFAR candidate if such an environment is anticipated.

An interfering target will degrade the detection performance of both CFAR processors. The cell averaging technique is affected less than the "greatest-of" technique and should be a prime CFAR candidate if interfering targets are considered to be a dominant problem.

Finally, the performance of both processors is affected by finite wordlength arithmetic and the phenomenon should be analyzed when implementing either CFAR technique. The unacceptable false alarm rates obtained for both CFAR processors when Weibull clutter is in the reference cells requires utilization of a different CFAR if this is the expected environment.

The results agree with those previously available. But the interfering target performance comparison and the "greatest-of" performance in Weibull clutter and non-Gaussian interference represent results presently not available.

6.2 Recommendations

The recommendations for future work are to:

1) Improve the random number generator so that probabilities of false alarms less than 10^{-5} can be verified.

2) Use measured radar data as an input to the simulation to compare the CFAR processors.

3) Perform an extensive study of linear detector approximation algorithm's effect on CFAR performance.

4) Perform an extensive study of finite wordlength effect on design of and performance of CFAR processors.

5) Determine realistic models of jammers and perform a study.

6) Develop environmental models which contain clutter edges and interfering targets and determine selection logic for the "greatest-of" and cell averaging CFAR processors to optimize CFAR performance. Utilization of tracking information should be considered.

APPENDIX A

FIXED THRESHOLD PROBABILITY DENSITY FUNCTIONS DERIVATIONS

A.1 Introduction

This appendix gives derivations for the probability density functions for the square law or linear detected steady target and for the square law detected Swerling I target. These probability density functions are common equations and the derivations can also be found in Marcum [1] for the steady target and Swerling [2] for the Swerling I target.

The characteristic function approach is used to obtain the pdf for the square law detected output. The steady target is assumed to be distributed in the I and Q channels by

$$S_I = P \cos(\theta)$$
$$S_Q = P \sin(\theta) \tag{A.1}$$

and

$$y = (S_I + x_I)^2 + (S_Q + x_Q)^2$$

and this changes the pdf's for x_I and x_Q by a shift to these mean values, i.e., zero mean Gaussian

$$p(x_k) = \frac{1}{\sqrt{2\pi}\sigma} \exp\left[-\frac{(x_k - S_k)^2}{2\sigma^2}\right], \quad k = I, Q . \tag{A.2}$$

In the following derivation the subscript k will be dropped on x_k and S_k to simplify the equations.

The characteristic function for x^2 is

$$\phi_{x^2}(v) = E\{\exp(jvx^2)\} = \frac{1}{\sqrt{2\pi}\sigma}\int_{-\infty}^{\infty}\exp\left[-\frac{(x-S)^2 - jvx^2 2\sigma^2}{2\sigma^2}\right]dx$$

$$= \frac{1}{\sqrt{2\pi}\sigma}\int_{-\infty}^{\infty}\exp\left[-\frac{x^2(1-jv2\sigma^2) - 2Sx + S^2}{2\sigma^2}\right]dx \ . \qquad (A.3)$$

Now let $C = (1 - jv2\sigma^2)$ and complete the square,

$$\phi_{x^2}(v) = \frac{1}{\sqrt{2\pi}\sigma}\int_{-\infty}^{\infty}\exp\left[-\frac{x^2 - \frac{2S}{C}x + \frac{S^2}{C} - \frac{S^2}{C^2} + \frac{S^2}{C^2}}{(2\sigma^2/C)}\right]dx$$

$$= \frac{1}{\sqrt{C}}\exp\left[\frac{\frac{S^2}{C^2} - \frac{S^2}{C}}{(2\sigma^2/C)}\right]\frac{1}{\sqrt{2\pi}\,\frac{\sigma}{\sqrt{C}}}\int_{-\infty}^{\infty}\exp\left[-\frac{\left(x - \frac{S}{C}\right)^2}{(2\sigma^2/C)}\right]dx \ . \qquad (A.4)$$

After integration,

$$\phi_{x^2}(v) = \frac{1}{\sqrt{C}}\exp\left[\frac{S^2\left(\frac{1}{C} - 1\right)}{2\sigma^2}\right] .$$

Consequently, the characteristic function for y is

$$\phi_y(v) = \phi_{x_I^2}(v)\,\phi_{x_Q^2}(v) = \frac{1}{C}\exp\frac{\left(S_I^2 + S_Q^2\right)\left(\frac{1}{C} - 1\right)}{2\sigma^2}$$

$$= \frac{1}{C}\exp\left[-\frac{p^2}{2\sigma^2}\right]\exp\left[\frac{p^2}{2\sigma^2 C}\right] = \frac{\exp\left[-\frac{p^2}{2\sigma^2}\right]\exp\left[\frac{p^2}{2\sigma^2}\,\frac{1}{(1 - j2\sigma^2 v)}\right]}{1 - j2\sigma^2 v} \ . \qquad (A.5)$$

Let $x = p^2/(2\sigma^2)$ and $-v = u$, then

$$p(y) = \frac{\exp(-x)}{2\pi(2\sigma^2)}\int_{-\infty}^{\infty}\frac{\exp\left[\frac{x}{2\sigma^2}\,\frac{1}{ju + 1/2\sigma^2}\right]}{ju + \frac{1}{2\sigma^2}}\exp[juy]du$$

$$= \frac{\exp(-x)}{2\sigma^2}\exp\left[\frac{-y}{2\sigma^2}\right] I_0\left(2\sqrt{x\,\frac{y}{2\sigma^2}}\right)u(y)$$

$$= \frac{1}{2\sigma^2} \exp\left[-\frac{y^2 + P^2}{2\sigma^2}\right] I_o\left(2\frac{\sqrt{P^2 y}}{2\sigma^2}\right) u(y) \qquad (A.6)$$

This pdf is the well known Rician distribution [3]. A linear detector is given as $z = \sqrt{y}$ and by a change in variables the pdf for a linear detector can be obtained from Equation (A.6).

A.2 Derivation of Probability Density Function for a Square Law Detected Swerling I Target Plus Noise

When a Swerling I target is assumed, the results for the pdf are simplified. This type of target assumed that the group of N returns have a constant signal-to-noise ratio but that from group to group the pdf is

$$p(x) = \frac{1}{\bar{x}} \exp[-x/\bar{x}]u(x) \qquad (A.7)$$

where $x = P^2/(2\sigma^2)$ and $\bar{x}$ is the average signal-to-noise ratio. This is used with the characteristic function of Equation (A.5) to obtain

$$\bar{\phi}_y(v) = E\{\phi_y(v)\} = \int_{-\infty}^{\infty} \phi_y(v)p(x)dx$$

$$\bar{\phi}_y(v) = \int_0^{\infty} \frac{1}{C} \exp[-x] \exp\left[\frac{x}{C}\right] \frac{1}{\bar{x}} \exp\left[-\frac{x}{\bar{x}}\right] dx$$

$$= \frac{1}{c\bar{x}} \int_0^{\infty} \exp\left[x\left(-1 + \frac{1}{C} - \frac{1}{\bar{x}}\right)\right] dx$$

$$= \frac{1}{c\bar{x}\left(\frac{1}{C} - \frac{1}{\bar{x}} - 1\right)} [\exp(-\infty) - \exp(0)] = \frac{-1}{\bar{x} - c - c\bar{x}}$$

$$= \frac{-1}{\bar{x} - 1 + j2\sigma^2 v - \bar{x} + j2\sigma^2 v\bar{x}} = \frac{1}{1 - j2\sigma^2 v(1 + \bar{x})}$$

$$\bar{\phi}_y(v) = \frac{1}{2\sigma^2 (1 + \bar{x})} \frac{1}{-jv + \frac{1}{2\sigma^2 (1 + \bar{x})}} \qquad (A.8)$$

The pdf for y can be determined from this to be

$$p(y) = \frac{1}{2\sigma^2 (1+\bar{x})} \exp\left[-\frac{y}{2\sigma^2 (1+\bar{x})}\right] u(y) \ . \qquad (A.9)$$

APPENDIX B

DERIVATION OF THE GREATEST-OF CFAR PERFORMANCE EQUATIONS

B.0 Introduction

This appendix gives the derivations for the probability of false alarm and probability of detection equations for the "greatest of" CFAR. The derivations were originally derived by Moore [8]. It should be noted that in an independent concurrent effort, Hansen and Sawyer [13] have derived the same equations.

B.1 Derivations of the Greatest-Of CFAR Performance Equations

In the "greatest-of" CFAR method two independent thresholds are calculated, then the largest one is selected, viz.,

$$Y_1 = \frac{K}{M} \sum_{i=1}^{M} y_i$$

$$Y_2 = \frac{K}{M} \sum_{j=1}^{M} y_j$$

$$Y_{th} = MAX\ (Y_1, Y_2) \tag{B.1}$$

where a simplified notation is used for the subscripts on y and it is implied that the ranges of the summations are M but that i=j.

The pdf descriptions of Y_1 and Y_2 can be given by

$$P(Y) = \left(\frac{M}{K}\right) \frac{1}{2\sigma^2} \frac{1}{(M-1)!} \left(\frac{Y}{2\sigma^2}\right)^{M-1} exp\left[-\frac{MY}{K2\sigma^2}\right] u(Y)\ . \tag{B.2}$$

Papoulis [9] gives an expression for finding a pdf of the maximum of two random variables, cf., Equation (15), p. 193,

$$P_{GO}(Y_{th}) = 2F(Y)p(Y)\big|_{Y=Y_{th}} = 2F_Y(Y_{th})P_Y(Y_{th}) \tag{B.3}$$

where $F_Y(\cdot)$ is the cumulative distribution function for Y.

This could be used with fixed threshold probability of false alarm Equation (2.8) to obtain the expected PFA, i.e.,

$$\overline{PFA}_{GO} = \int_0^\infty \exp\left[\frac{-Y_{th}}{2\sigma^2}\right] P_{GO}(Y_{th})dY_{th}$$

$$= 2\int_0^\infty \exp\left[\frac{-Y_{th}}{2\sigma^2}\right] F_Y(Y_{th})F_Y'(Y_{th})dY_{th} \ . \qquad (B.4)$$

This can be integrated by parts as follows:

$$u = F_Y(Y_{th}) \qquad du = F_Y'(Y_{th})dY_{th}$$

$$dv = \exp\left[\frac{-Y_{th}}{2\sigma^2}\right] F_Y'(Y_{th})dY_{th}$$

$$v = \int \exp\left[\frac{-Y_{th}}{2\sigma^2}\right] p_Y(Y_{th})dY_{th} \ . \qquad (B.5)$$

Note that v is in the same form used to obtain PFA for a cell averaging CFAR Equation (3.3), but this is not a definite integral. *It follows* that

$$v = \frac{1}{\left(1 + \frac{K}{M}\right)^M (M-1)!} \int b^{M-1} \exp[-b]db$$

$$b = \frac{Y_{th}}{2\sigma^2}\left(1 + \frac{M}{K}\right)$$

$$v = \frac{-1}{\left(1 + \frac{K}{M}\right)^M} \exp\left[-\frac{Y_{th}}{2\sigma^2}\left(1 + \frac{M}{K}\right)\right] \sum_{m=0}^{M-1} \frac{\left[\frac{Y_{th}}{2\sigma^2}\left(1 + \frac{M}{K}\right)\right]^m}{m!}$$

$$v = -\overline{PFA} \exp\left[-\frac{Y_{th}}{2\sigma^2}\left(1 + \frac{M}{K}\right)\right] \sum_{m=0}^{M-1} \frac{\left[\frac{Y_{th}}{2\sigma^2}\left(1 + \frac{M}{K}\right)\right]^m}{m!} \qquad (B.6)$$

where $\overline{PFA}$ is the value associated with a conventional cell averaging CFAR of window size M. Thus

$$\overline{PFA}_{GO} = 2\left[uv\Big|_0^\infty - \int v\,du\right] = 2F_Y(Y_{th})v\Big|_0^\infty + 2\overline{PFA}\sum_{m=0}^{M-1}\frac{\left(1+\frac{M}{K}\right)^m}{m!}\int_0^\infty\left(\frac{Y_{th}}{2\sigma^2}\right)^m \exp\left[-\frac{Y_{th}}{2\sigma^2}\left(1+\frac{M}{K}\right)\right]p_Y(Y_{th})dY_{th}.$$

The first term, $F_Y(Y_{th})v$, yields 0, thus

$$\overline{PFA}_{GO} = 2\overline{PFA}\sum_{m=0}^{M-1}\frac{\left(1+\frac{M}{K}\right)^m}{m!}\int_0^\infty 2\sigma^2 a^m \exp\left[-a\left(1+\frac{M}{K}\right)\right]p_Y(2\sigma^2 a)da$$

$$= \overline{PFA}\left(\frac{M}{K}\right)^M \frac{2}{(M-1)!}\sum_{m=0}^{M-1}\frac{\left(1+\frac{M}{K}\right)^m}{m!}\int_0^\infty a^{m+M-1}\exp\left[-a\left(1+\frac{2M}{K}\right)\right]da$$

$$= \overline{PFA}\left(\frac{M}{K}\right)^M \frac{2}{(M-1)!\left(1+\frac{2M}{K}\right)^M}\sum_{m=0}^{M-1}\frac{(m+M-1)!}{m!\left(\frac{1+\frac{2M}{K}}{1+\frac{M}{K}}\right)^m}$$

$$= \frac{2\overline{PFA}}{(M-1)!\left(2+\frac{K}{M}\right)^M}\sum_{m=0}^{M-1}\frac{(m+M-1)!}{m!\left(\frac{2+\frac{K}{M}}{1+\frac{K}{M}}\right)^m} \qquad (B.7)$$

Since $\left(1+\frac{K}{M}\right) = \overline{PFA}^{-1/M}$, then

$$\overline{PFA}_{GO} = \frac{2\overline{PFA}}{(M-1)!\left(1-\overline{PFA}^{-1/M}\right)^M}\sum_{m=0}^{M-1}\frac{(m+M-1)!}{m!\left(1+\overline{PFA}^{-1/M}\right)^m} \qquad (B.8)$$

This relates the probabilities of false alarm.

The probability of detection for a Swerling I target with "greatest-of" CFAR is given by

$$\bar{P}_{D,GO} = \int_0^\infty \exp\left[-\frac{Y_{th}}{2\sigma^2(1+\bar{x})}\right] P_{GO}(Y_{th})dY_{th}$$

$$= 2\int_0^\infty 2\sigma^2 \exp\left[-\frac{a}{1+\bar{x}}\right] F_Y(2\sigma^2 a)\, p_Y(2\sigma^2 a)da \ . \qquad (B.9)$$

Integration by parts gives

$$u = F_Y(2\sigma^2 a) \qquad du = F_Y'(2\sigma^2 a)\, 2\sigma^2 da$$

$$dv = 2\sigma^2 \exp\left[\frac{-a}{1+\bar{x}}\right] p_Y(2\sigma^2 a)da$$

$$v = \left(\frac{M}{\bar{K}}\right)^M \frac{1}{(M-1)!}\int_0^\infty a^{M-1}\exp\left[-\left(\frac{M}{\bar{K}}+\frac{1}{1+\bar{x}}\right)a\right]da$$

$$= \left(\frac{M}{\bar{K}}\right)^M \frac{1}{(M-1)!}\,\frac{1}{\left(1+\frac{K}{M(1+\bar{x})}\right)^M}\int_0^\infty b^{M-1}\exp(-b)db$$

$$= \frac{-1}{(M-1)!}\,\frac{(M-1)!}{\left(1+\frac{K}{M(1+\bar{x})}\right)^M}\exp(-b)\sum_{m=0}^{M-1}\frac{b^m}{m!} \ , \qquad (B.10)$$

where

$$b = \left(\frac{M}{\bar{K}}+\frac{1}{1+\bar{x}}\right)a \ . \qquad (B.11)$$

Thus, using the probability of detection for an equivalent sized cell averaging CFAR,

$$v = -\bar{P}_D \exp(-b)\sum_{m=0}^{M-1}\frac{b^m}{m!} \qquad (B.12)$$

and

$$\bar{P}_{D,GO} = 2F_Y(2\sigma^2 a)v\Big|_0^\infty = 2\bar{P}_D\sum_{m=0}^{\infty} 2\sigma^2\int_0^\infty \exp(-b)\frac{b^m}{m!}\,p_Y(2\sigma^2 a)da$$

$$= \frac{2\bar{P}_D}{(M-1)!}\left(\frac{M}{\bar{K}}\right)^M \sum_{m=0}^{M-1}\frac{\left(\frac{M}{\bar{K}}+\frac{1}{1+\bar{x}}\right)}{m!}\int_0^\infty a^{m+M-1}\exp\left[-a\left(\frac{2M}{\bar{K}}+\frac{1}{1+\bar{x}}\right)\right]da$$

$$c = \left[\frac{2M}{K} + \frac{1}{(1+\bar{x})}\right] a$$

$$\bar{P}_{D,GO} = \frac{2\bar{P}_D}{(M-1)!}\left(\frac{M}{K}\right)^M \sum_{m=0}^{M-1} \frac{\left(\frac{M}{K} + \frac{1}{1+\bar{x}}\right)^m}{m!\left(\frac{2M}{K} + \frac{1}{1+\bar{x}}\right)^{M+m}} \int_0^\infty c^{m+N-1} \exp[-c]dc$$

$$= \frac{2\bar{P}_D}{(M-1)!} \frac{1}{\left(2 + \frac{K}{M(1+\bar{x})}\right)^M} \sum_{m=0}^{M-1} \frac{(m+M-1)!}{m!\left[\frac{2 + \frac{K}{M(1+\bar{x})}}{1 + \frac{K}{M(1+\bar{x})}}\right]^m}$$

$$= \frac{2\bar{P}_D}{(M-1)!} \frac{1}{\left(1 + \bar{P}_D^{-1/M}\right)^M} \sum_{m=0}^{M-1} \frac{(m+M-1)!}{m!\left(1 + \bar{P}_D^{-1/M}\right)^m} \qquad (B.13)$$

This is the desired expression for the probability of detection.

APPENDIX C

MONTE CARLO RUN ESTIMATION

The utilization of Monte Carlo simulations for estimation of probabilities of false alarm and probabilities of detection has a statistical uncertainty associated with it. This appendix determines values required to give a priori probabilities for a specified range of the estimated parameter.

Let y_n represent the nth target/no target decision for the cell of interest. Thus y_n will equal either 0 or 1. The probability that $y_n = 1$ will be denoted as p. Two cases are considered, viz., noise-only and signal-plus-noise.

Thus

$$\text{Prob}\,[y_n = 1 \mid \text{noise only}] = p = \text{PFA}$$
$$\text{Prob}\,[y_n = 1 \mid \text{signal-plus-noise}] = p = \text{PD} \qquad \text{(C.1)}$$

an estimate of p can be formed by calculating the arithmetic mean of N determinations, i.e.,

$$\bar{y} = \frac{1}{N} \sum_{n=1}^{N} y_n \ . \qquad \text{(C.2)}$$

This represents an unbiased, efficient and consistent estimator to the expected value of y_n. It is possible to obtain the mean and variance of $\bar{y}$ in terms of the mean and variance of y_n, i.e.,

$$E\{\bar{y}\} = \frac{1}{N} \sum_{n=1}^{N} E\{y_n\} = E\{y_n\} = p$$

$$E\{(\bar{y} - p)^2\} = \text{VAR}(\bar{y}) = \frac{\text{VAR}(y_n)}{N} = \frac{p(1-p)}{N} \ . \qquad \text{(C.3)}$$

One approach to finding the required value for N is to use Chebyshev's Inequality, i.e.,

$$P[|\bar{y} - E\{\bar{y}\}| \geq e] \leq \frac{VAR(\bar{y})}{2} = \frac{p(1-p)}{Ne^2} \tag{C.4}$$

letting the value of e depend on p, i.e.,

$$e = kp \tag{C.5}$$

yields

$$p[-e < \bar{y} - p < e] \geq 1 - \frac{(1-P)}{pNe^2} = K\,. \tag{C.6}$$

Thus if the estimate $(\bar{y})$ to p is to be within some specified range of $p(\pm e)$ with better than some specified probability (K) then Equation (C.6) can be used to determine the sufficient value for N. Typical results are given in Table C.1.

Table C.1. Values of N Obtained by Chebyshev's Inequality

	K = 0.5			K = 0.9		
P	k = 0.01	0.1	0.25	k = 0.01	0.1	0.25
10^{-6}	2×10^{10}	2×10^{8}	3.2×10^{7}	1×10^{11}	1×10^{9}	1.6×10^{8}
10^{-5}	2×10^{9}	2×10^{7}	3.2×10^{6}	1×10^{10}	1×10^{8}	1.6×10^{7}
10^{-4}	2×10^{8}	2×10^{6}	3.2×10^{5}	1×10^{9}	1×10^{7}	1.6×10^{6}
10^{-3}	2×10^{7}	2×10^{5}	3.2×10^{4}	1×10^{8}	1×10^{6}	1.6×10^{5}
0.5	2×10^{4}	200	32	1×10^{5}	1×10^{3}	160
0.6	1.33×10^{4}	133	21.3	6.67×10^{4}	667	107
0.7	8.57×10^{3}	85.7	13.7	4.29×10^{4}	429	68.6
0.8	5×10^{3}	50	8	2.25×10^{4}	250	40
0.9	2.22×10^{3}	22.2	3.56	1.11×10^{4}	111	17.8

APPENDIX D

FLOATING POINT SYSTEMS AP-120B

The Floating Point Systems AP-120B is a loosely coupled synchronous array processor which uses pipelined arithmetic elements. The array processor uses a 38-bit floating-point format and has a cycle time of 167 nsec. Figure D.1 shows the structure of the AP-120B, which consists of an interface to the host computer, a program memory, a 16-bit integer ALU, data memory, table memory, accumulators, I/O interface, and arithmetic elements.

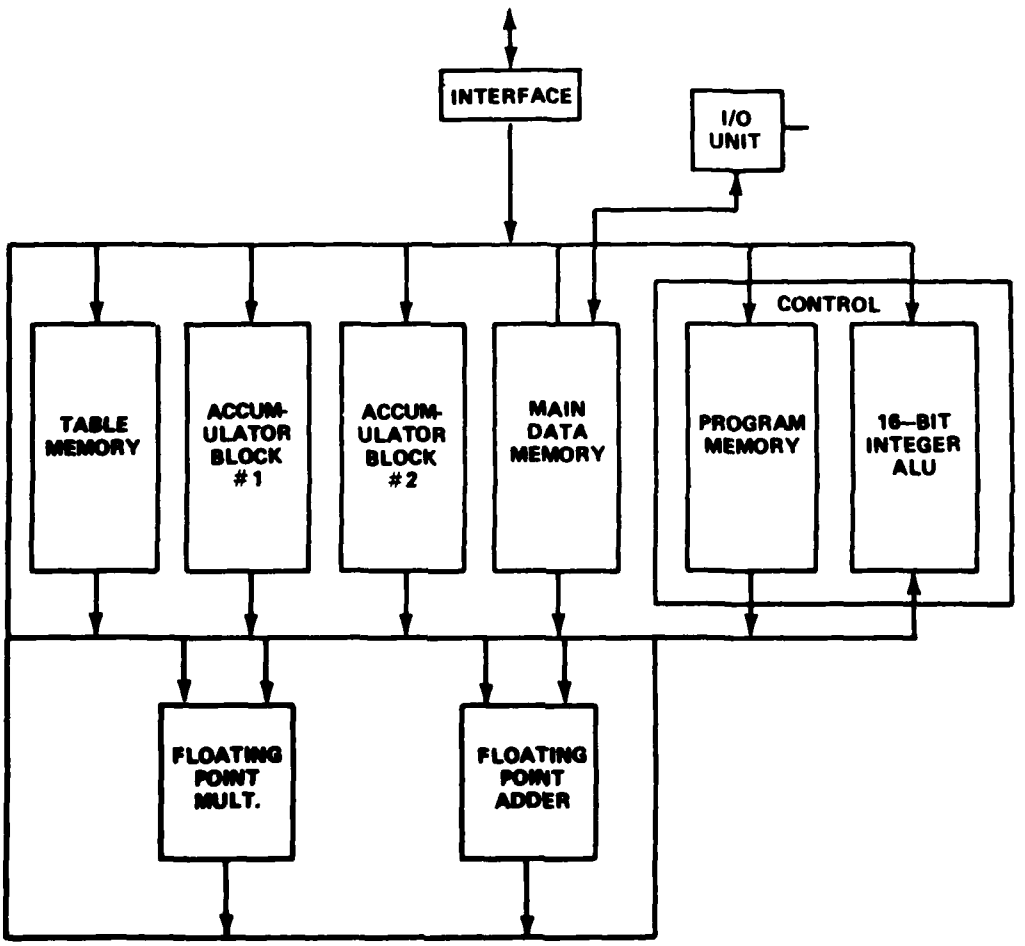

Figure D.1. AP-120B

The interface controls data, program transfer, and format conversion between the host and array processor.

Control consists of two elements: a 16-bit ALU which performs integer address indexing and loop counting for all of the memory elements. The second element is the program memory which contains the microcode to be executed in the array processor. This memory is 64 bits wide with each word being subdivided into 10 command fields. Each command field controls an element in the array processor, thus every element can be active in every machine cycle.

The main data memory is used for data; the table memory is used for storing constants and the accumulator blocks for intermediate result storage.

The AP-120B uses a unique bus structure in that there are dedicated paths between each memory and each arithmetic element, thus maximizing the flow of operands and resultants between functional elements.

The I/O interface allows the attachment of peripheral devices directly to the array processor.

The arithmetic elements consist of a 3-stage multiplier and a 2-stage adder, each stage running at the cycle time of the array processor (167 nsec), thus a multiply-add can be obtained in every cycle of the processor.

The software can be broken down into two categories:

a. Control Software - This software supplies the linkage between the host computer operating system and the array processor. It is usually in the form of a device driver.

b. User Software - This software enables a user to write programs for an array processor. Typically, this can be done at two

levels. A user can program in Fortran by writing a program for the host computer which consists of a series of calls to the array processor math library. This math library is supplied by the vendor and consists of a library of mathematical routines which have been coded for the array processor. Figure D.2 shows an example of such a program to compute a Fast Fourier Transform. Obviously, when the array processor is used in this manner, its internal structure is transparent to the user.

The second level of programming is to program the array processor directly in assembly language. Usually the vendor supplies an assembler, simulator and debug aids to assist the programmer. Figure D.3 shows such a program written in the assembly language for the FPS AR-120B. This program calculates $Ci - Ai^2 + Bi^2$ where i ranges from 1 to N. The y axis of the figure represents machine cycles, while the x axis represents flow through the pipelines. The program reduces to a 4-cycle loop. However, this loop does demonstrate the parallel structure of array processors, for example, on the first cycle of loop, a memory fetch, a floating multiply, a memory save and floating add are all in progress on the same machine cycle (contrast this with a conventional computer). At this level, the programmer has to be aware of the internal structure of the array processor to maximize performance.

CALL APCLR	Clear array processor
CALL APPUT	Transfer data to array processor
CALL CFFT	Perform complex FFT
CALL APGET	Transfer results to front-end computer

Figure D.2. AP Fortran

	FETCH STAGE	MULTIPLY STAGE	ADD STAGE
	FETCH A		
	FETCH B		
	NOP		
	SAVEX		
	FETCH A;	FMUL A, A, SAVEY B	
	FETCH B;	FMUL B, B	
	NOP;	FMUL	
	SAVEX A;	FMUL; SAVEY A^2	
LOOP:	FETCH A;	FMUL A, A, SAVEY B	FADD B, A
	FETCH B;	FMUL B, B	FADD
	NOP;	FMUL;	DEC N
	SAVEX A;	FMUL: SAVEY A^2	STORE C; BGT LOOP
DONE:	RETURN		

Figure D.3. AP Assembly

Table E.1. Main CFAR Simulation Program

```
C
C     PROGRAM TO SIMULATE A CELL-AVERAGING
C     AND GREATEST OF CFAR FOR COMPARISON OF THE TWO
C     ALGORITHMS BY MONTE CARLO TECHNIQUES. THE
C     COMPARISON CAN BE MADE FOR VARIOUS
C     ENVIRONMENTS AND WORD LENGTHS.
C
C           INPUTS
C
C        SEED  -  UNIFORM RANDOM NO. GENERATOR SEED
C        STDV  -  STANDARD DEVIATION OF GAUSSIAN NOISE
C        MEAN  -  MEAN VALUE OF GAUSSIAN NOISE
C        SNRI  -  INPUT SIGNAL-TO-NOISE RATIO
C        NTAR  -  TARGET MODEL NO.
C        NDET  -  DETECTOR LAW: SQ. LAW=0,LINEAR=1
C        NUD2  -  HALF OF CFAR WINDOW WIDTH
C        PFDCA -  DESIRED CFAR PROBABILITY OF FALSE ALARM
C        PFDGO -  DESIGN GO PROBABILITY OF FALSE ALARM
C        NMCR  -  NUMBER OF MONTE CARLO RUNS
C        IPDF  -  RUN INDEX: PFA=0,PD=1
C        NSN   -  NO. OF SNR RUNS
C        NC    -  NO. OF CELLS COVERED
C        TAU   -  RATIO COVERED/NON-COVERED
C        ISKP  -  CELLS SKIPPED BY CFAR
C        IQ    -  QUANTIZATION: YES>0
C        NBIT  -  NO. OF BITS
C        IWEI  -  WEIBULL CLUTTER: NO=0,YES=1
C        A     -  WEIBULL PARAMETER
C        CPOW  -  WEIBULL CLUTTER POWER
C        IDCG  -  DISK INDEX: CA=0,GO=1
C
C
C           CALCULATED INPUTS
C
C        CKCA  -  CA THRESHOLD CONSTANT
C        CKGO  -  GO THRESHOLD CONSTANT
C        AMPI  -  INPUT AMPLITUDE AT IF
C
C           OUTPUTS
C
C
C        PFCA  -  CA PROBABILITY OF FALSE ALARM OBTAINED
C        PFGO  -  GO PROBABILITY OF FALSE ALARM OBTAINED
C        PDCA  -  CA PROBABILITY OF DETECTION OBTAINED
C        PDGO  -  GO PROBABILITY OF DETECTION OBTAINED
C
      DIMENSION PFDCA(9),PFDGO(9),NUD2(9),NMCR(9)
      DIMENSION DUM(4),PDCA(100),PDGO(100)
      EQUIVALENCE (CA,DUM(1)),(GO,DUM(2)),(DCA,DUM(3)),(DGO,DUM(4))
      REAL MEAN,NMCR
      DATA PFDCA/3*1.E-3,3*1.E-4,3*1.E-5/
      DATA PFDGO/0.8773E-2,0.5069E-2,0.3181E-2,
     1  0.2227E-2,0.1043E-2,0.5318E-3,
     1  0.5998E-3,0.2297E-3,0.9409E-4/
      DATA NUD2/4,8,16,4,8,16,4,8,16/
      DATA NMCR/3*1.0E8,3*1.0E9,3*1.E10/
      CALL ASSIGN(3,'DK1:CFAR.PLT',0,'NEW')
      DEFINE FILE 3(200,128,U,JJ)
      SEED=0.2510483945

      STDV=1.
      MEAN=0.
      SNRI=0.
      NTAR=1
```

Table E.1 (cont'd)

```
      NDET=0
      IPDF=0
      TAU=1.
      TAUSR=SQRT(TAU)
      ISKP=1
      IQ=0
      NBIT=8
      IWEI=0
      A=1.
      CPOW=1.
      IDCG=0
      ICI=1
      IF(NDET.EQ.0) Q=IQ**2/2.**NBIT
      IF(NDET.EQ.1) Q=IQ/2.**NBIT
      CALL APCLR
      CALL VCLR(0,1,32767)
      CALL APUR
      CALL APPUT(A,13,1,2)
      CALL APPUT(CPOW,14,1,2)
      CALL APPUT(SEED,16,1,2)
      CALL APPUT(STDV,5,1,2)
      CALL APPUT(MEAN,6,1,2)
      CALL APPUT(TAUSR,11,1,2)
      CALL APPUT(Q,12,1,2)
      CALL APUD
      IF(IPDF.EQ.1) WRITE(6,102)
  102 FORMAT(/1H1,2H N,6X,4HSNRI,13X,5HPFDCA,13X,4HPDCA,
     1 13X,4HPDGO)
      IF(IPDF.EQ.0) WRITE(6,103)
  103 FORMAT(/1H1,2H N,6X,5HPFDCA,13X,4HPFCA,
     1 13X,5HPFDGO,13X,4HPFGO)
      IF(IPDF.EQ.2) WRITE(6,105)
  105 FORMAT(/1H1,2H N,3X,2HNC,6X,5HPFDCA,13X,5HPFTCA,13X,4HPFCA,
     1 13X,5HPFDGO,13X,4HPFGO)
C     MAIN LOOP
      DO 2 J=3,9,3
      SNRI=0.
      NU=NUD2(J)
      NU2=NU**2
      NCLU=0
      IF(IPDF.EQ.2) NCLU=NU2+14
      CKCA=(PFDCA(J)**(-1./NU2)-1.)
      CKGO=(PFDGO(J)**(-1./NU)-1.)
      IF(NDET.EQ.1) CKCA=SQRT(CKCA*NU2)*1.14/NU2
      IF(NDET.EQ.1) CKGO=SQRT(CKGO*NU)*1.14/NU
      CALL APPUT(CKCA,8,1,2)
      CALL APPUT(CKGO,9,1,2)
      CALL APUR
      FNMCR=NMCR(J)
      IF(IPDF.EQ.1) FNMCR=1.E5
      NMON=INT(FNMCR/(1.E5/FLOAT(ISKP)-1.))
      NSN=21
      IF(IPDF.NE.1) NSN=1
C     SIGNAL-TO-NOISE LOOP
      DO 3 I=1,NSN
      AMPI=STDV*SQRT(2.*10.**(SNRI/10.))
      CALL APPUT(AMPI,10,1,2)
      CALL APUR
      NU1=NU+1
      NU14=NU1+14
      NC=0
C     NONSTATIONARY CLUTTER LOOP
      DO 5 ICLU=1,NCLU
      IF(ICLU.GT.NU1)GO TO 11
```

Table E.1 (cont'd)

```
            PFTCA=PFDCA(J)**(FLOAT(NW2-NC)/FLOAT(NW2))
            PFTCA=PFTCA*(1.+TAU*(PFDCA(J)**(-1./NW2)-1.))**(-NC)
            GO TO 99
   11       IF(ICLU.LT.NW14) GO TO 5
            PFTCA=PFDCA(J)**(FLOAT(NC)/FLOAT(NW2))
            PFTCA=PFTCA*(1.+(PFDCA(J)**(-1./NW2)-1.)/TAU)**(NC-NW2)
   99       CONTINUE
            CALL APPUT(SEED,4,1,2)
            CALL APPUT(SEED,7,1,2)
            CALL APWR
            CALL UCLR(0,1,4)
            CALL THLN(NW,NMON,NTAR,NDET,ICLU,ISKP,IQ,IWEI)
            CALL APWR
            CALL APGET(DUM,0,4,2)
            CALL APWD
            IF(NCLU.NE.0) GO TO 10
C           PFA AND PD CALCULATION
            PFCA=CA/(FNMCR)
            PFGO=GO/(FNMCR)
            PDCA(I)=(DCA-CA)/FNMCR
            PDGO(I)=(DGO-GO)/FNMCR
            IF(IPDF.EQ.1) WRITE(6,101)NW2,SNRI,PFDCA(J),PDCA(I),PDGO(I)
            IF(IPDF.EQ.0) WRITE(6,101)NW2,PFDCA(J),PFCA,PFDGO(J),PFGO
  101       FORMAT(2X,I2,3XE12.5,4(5X,E12.5))
            GO TO 5
C           NONSTATIONARY CLUTTER PFA AND PD CAL.
   10       NC1=NC+1
            PDCA(NC1)=CA/FNMCR
            PDCA(NC1+NW2+1)=GO/FNMCR
            NC2=NC1+(NW2+1)*2
            PDCA(NC2)=PFTCA
            WRITE(6,104) NW2,NC,PFDCA(J),PFTCA,PDCA(NC1),PFDGO(J)
     1      ,PDCA(NC1+NW2+1)
  104       FORMAT(2X,I2,3X,I2,3X,E12.5,4(5X,E12.5))
            NC=NC+1
    5       CONTINUE
            SNRI=SNRI+1.
    3       CONTINUE
C           DISK WRITE
            IF(IPDF.EQ.0) GO TO 2
            IF(IPDF.EQ.2) NSM=3*(NW2+1)
            IF(IDCG.EQ.0) WRITE(3'ICI) (PDCA(IP),IP=1,NSM)
            IF(IDCG.EQ.1) WRITE(3'ICI) (PDGO(IP),IP=1,NSM)
            ICI=ICI+1
    2       CONTINUE
            STOP
            END
*
```

SUBROUTINE THLN

PURPOSE: To generate target noise and clutter inputs to CFAR program.

FORTRAN CALL: Call THLN (NWD2, NMON, NTAR, NDET, ICLU, ISKP, IQ)

PARAMETERS: NWD2 = Half of CFAR window width

NMON = Number of program passes

NTAR = Target model number

NDET = Detector law: Square Law = 0; Linear = 1

ICLU = Number of cells covered

ISKP = Cells skipped by CFAR

IQ = Quantization: No = 0; Yes = 1

IWEI = Weibull Clutter: No = 0, Yes = 1

EXTERNALS: VSQRT, VRAND, VLN, VFILL, QUANT, RANDM, VSQ, VMVL, VADD, CFR, VNEG, WEIBULL

SCRATCH: SP (0-6, 12-14), DPX (-4, 3), DPY (0, 1)

Table E.2. Subroutine THLN

```
$TITLE THLN
*       AP PROGRAM TO GENERATE TARGET AND
*       NOISE INPUT FOR CFAR PROGRAM
*       THERE ARE EIGHT INPUTS:
*         NWD2  -  HALF OF CFAR WINDOW WIDTH
*         NMON  -  NO. OF PROGRAM RUNS
*         NTAR  -  TARGET MODEL NO.
*         NDET  -  DETECTOR LAW:SQ. LAW=0;LINEAR=1
*         ICLU  -  NO. OF CELLS COVERED
*         ISKP  -  CELLS SKIPPED BY CFAR
*         IQ    -  QUANTIZATION: NO=0,YES=1
*         IWEI  -  WEIBUL: NO=0,YES=1
*
$ENTRY THLN,8
$EXT  VSIN,VCOS
$EXT  VSQRT,VRAND,VLN,VFILL,QUANT,VMUL
$EXT RANDM,VSQ,VSMUL,VADD,CFAR,VNEG
        NWD2  $EQU 0
        NMON $EQU 1
        NTAR $EQU 2
        NDET $EQU 3
        ICLU $EQU 4
        ISKP $EQU 5
        IQ $EQU 6
        IWEI $EQU 7
        ICLA $EQU 13
        N100 $EQU 14
        ICLT $EQU 12
 THLN:LDDPA; DB=13.
        MOV NTAR,NTAR; DPX(0)<SPFN
        MOV NWD2,NWD2;DPY(0)<SPFN
        MOV NMON,NMON;DPX(1)<SPFN
        MOV NDET,NDET;DPX(2)<SPFN
        MOV ICLU,ICLU;DPX(-1)<SPFN
        MOV ISKP,ISKP;DPX(-2)<SPFN
        MOV IQ,IQ;DPX(3)<SPFN
        MOV IWEI,IWEI;DPY(3)<SPFN
        LDSPI 14,DB=10.
        MOV N100,N100;DPY(1)<SPFN
        LDSPI 13,DB=493.
        SUB NWD2,ICLA;DPX(-3)<SPFN
        MOV NMON,NMON;DPX(-4)<SPFN
 LOOP: LDDPA; DB=13.
*       GUASSIAN RANDOM NO.GENERATOR
        LDSPI 0,DB=4.
        LDSPI 1,DB=400.
        LDSPI 2,DB=20400.
        LDSPI 3,DB=6.
        LDSPI 4,DB=5.
        LDSPI 5,DB=21000.
        LDDPA; DB=4.
        JSR RANDM
        LDDPA; DB=13.
        LDSPI 7,DB=DPY(3)
        MOV IWEI,IWEI
        BNE LWEI
        JMP LNWEI
  LWEI: LDSPI 0,DB=4.
        LDSPI 1,DB=21400.
*       LDSPI 2,DB=14.
        LDSPI 2,DB=1.
        LDSPI 3,DB=10200.
*       LDSPI 4,DB=13.
```

Table E.2 (cont'd)

```
LDDPA; DB=4.
JSR VRAND
LDDPA; DB=13.
LDSPI 0,DB=21400.
LDSPI 1, DB=1.
LDSPI 2,DB=21400.
LDSPI 3,DB=1.
LDSPI 4,DB=10200.
LDDPA; DB=4.
JSR VLN
LDDPA; DB=13.
LDSPI 0,DB=21400.
LDSPI 1,DB=1.
LDSPI 2,DB=21400.
LDSPI 3,DB=1.
LDSPI 4,DB=10200.
LDDPA; DB=4.
JSR VSQRT
LDDPA; DB=13.
LDSPI 0,DB=4.
LDSPI 1,DB=400.
LDSPI 2,DB=1.
LDSPI 3,DB=10200.
LDDPA; DB=4.
JSR VRAND
LDDPA; DB=13.
LDSPI 0,DB=400.
LDSPI 1,DB=1.
LDSPI 2,DB=15.
LDSPI 3,DB=400.
LDSPI 4,DB=1.
LDSPI 5,DB=10200.
LDDPA; DB=4.
JSR VSMUL
LDDPA; DB=13.
LDSPI 0,DB=400.
LDSPI 1,DB=1.
LDSPI 2,DB=10600.
LDSPI 3,DB=1.
LDSPI 4,DB=10200.
LDDPA; DB=4.
JSR VSIN
LDDPA; DB=13.
LDSPI 0,DB=400.
LDSPI 1,DB=1.
LDSPI 2,DB=400.
LDSPI 3,DB=1.
LDSPI 4,DB=10200.
LDDPA; DB=4.
JSR VCOS
LDDPA; DB=13.
LDSPI 0,DB=400.
LDSPI 1,DB=1.
LDSPI 2,DB=21400.
LDSPI 3,DB=1.
LDSPI 4,DB=400.
LDSPI 5,DB=1.
LDSPI 6,DB=10200.
LDDPA; DB=4.
JSR VMUL
LDDPA; DB=13.
LDSPI 0,DB=10600.
LDSPI 1,DB=1.
LDSPI 2,DB=21400.
```

Table E.2 (cont'd)

```
        LDSPI 3,DB-1.
        LDSPI 4,DB-10600.
        LDSPI 5,DB-1.
        LDSPI 6,DB-10200.
        LDDPA; DB-4.
        JSR UMUL
LNWEI:  LDDPA; DB-13.
        LDSPI 2,DB-DPX(0)
        MOV NTAR,NTAR
        BEQ CAS0
        JMP CAS1
*       CASE 0 TARGET GENERATOR
CAS0: LDDPA; DB-13.
        LDSPI 0,DB-10.
        LDSPI 1,DB-30000.
        LDSPI 2,DB-1.
        LDSPI 3,DB-10000.
        LDDPA; DB-4.
        JSR UFILL
        LDDPA; DB-13.
        JMP QCH
*       CASE 1 TARGET GENERATOR
CAS1: LDDPA; DB-13.
        LDSPI 0,DB-7.
        LDSPI 1,DB-30000.
        LDSPI 2,DB-1.
        LDSPI 3,DB-10000.
        LDDPA; DB-4.
        JSR URAND
        LDDPA; DB-13.
        LDSPI 0,DB-30000.
        LDSPI 1,DB-1.
        LDSPI 2,DB-30000.
        LDSPI 3,DB-1.
        LDSPI 4,DB-10000.
        LDDPA; DB-4.
        JSR ULN
        LDDPA; DB-13.
        LDSPI 0,DB-30000.
        LDSPI 1,DB-1.
        LDSPI 2,DB-30000.
        LDSPI 3,DB-1.
        LDSPI 4,DB-10000.
        LDDPA; DB-4.
        JSR UNEG
        LDDPA; DB-13.
        LDSPI 0,DB-30000.
        LDSPI 1,DB-1.
        LDSPI 2,DB-30000.
        LDSPI 3,DB-1.
        LDSPI 4,DB-10000.
        LDDPA; DB-4.
        JSR USORT
        LDDPA; DB-13.
        LDSPI 0,DB-30000.
        LDSPI 1,DB-1.
        LDSPI 2,DB-10.
        LDSPI 3,DB-30000.
        LDSPI 4,DB-1.
        LDSPI 5,DB-10000.
        LDDPA; DB-4.
        JSR USMUL
QCH: LDDPA; DB-13.
*       NOISE + TARGET
```

Table E.2 (cont'd)

```
        LDSPI 0, DB=30000.
        LDSPI 1,DB=1.
        LDSPI 2,DB=500.
        LDSPI 3,DB=1.
        LDSPI 4,DB=30000.
        LDSPI 5,DB=1.
        LDSPI 6,DB=10000.
        LDDPA; DB=4.
        JSR VADD
        LDDPA; DB=13.
        LDSPI 0,DB=30000.
        LDSPI 1,DB=1.
        LDSPI 2,DB=30000.
        LDSPI 3,DB=1.
        LDSPI 4,DB=10000.
        LDDPA; DB=4.
        JSR VSQ
*       NOISE ONLY
        LDDPA;DB=13.
        LDSPI 0,DB=DPX(0)
        LDSPI 13,DB=493.
        SUB NUD2,ICLA;DPX(-3)<SPFN
        LDSPI 12,DB=DPX(-1)
CLU:    LDDPA;DB=13.
        LDSPI 0,DB=DPX(-3)
        LDSPI 1,DB=DPX(-2)
        LDSPI 2,DB=11.
        LDSPI 3,DB=DPX(-3)
        LDSPI 4,DB=DPX(-2)
        LDSPI 5,DB=200.
        LDDPA; DB=4.
        JSR VSMUL
        LDDPA; DB=13.
        LDSPI 13,DB=DPX(-3)
        INC ICLA;DPX(-3)<SPFN
        DEC ICLT
        BEQ NOIS
        JMP CLU
NOIS:   LDDPA; DB=13.
        LDSPI 0,DB=400.
        LDSPI 1,DB=1.
        LDSPI 2,DB=400.
        LDSPI 3,DB=1.
        LDSPI 4,DB=20400.
        LDDPA; DB=4.
        JSR VSQ
        LDDPA; DB=13.
        LDSPI 0,DB=30000.
        LDSPI 1,DB=1.
        LDSPI 2,DB=10700.
        LDSPI 3,DB=1.
        LDSPI 4,DB=30000.
        LDSPI 5,DB=1.
        LDSPI 6,DB=10000.
        LDDPA; DB=4.
        JSR VADD
        LDDPA; DB=13.
        LDSPI 0,DB=400.
        LDSPI 1,DB=1.
        LDSPI 2,DB=10600.
        LDSPI 3,DB=1.
        LDSPI 4,DB=400.
        LDSPI 5,DB=1.
        LDSPI 6,DB=10200.
```

Table F.2 (cont'd)

```
        LDDPA; DB=4.
        JSR VADD
*       DETECTOR LAW
        LDDPA; DB=13.
        LDSPI 3,DB=DPX(2)
        MOV NDET,NDET
        BNE END
        JMP SLD
*       LINEAR
END: LDDPA; DB=13.
        LDSPI 0,DB=30000.
        LDSPI 1,DB=1.
        LDSPI 2,DB=30000.
        LDSPI 3,DB=1.
        LDSPI 4,DB=10000.
        LDDPA; DB=4.
        JSR VSQRT
        LDDPA; DB=13.
        LDSPI 0,DB=400.
        LDSPI 1,DB=1.
        LDSPI 2,DB=400.
        LDSPI 3,DB=1.
        LDSPI 4,DB=10200.
        LDDPA; DB=4.
        JSR VSQRT
*       SQUARE LAW
SLD: LDDPA; DB=13.
*       QUANTIZATION
        LDSPI 6,DB=DPX(3)
        MOV IQ,IQ
        BNE LOOP2
        JMP LOOP1
LOOP2: LDDPA; DB=13.
        LDSPI 0,DB=400.
        LDSPI 1,DB=12.
        LDSPI 2,DB=10200.
        LDDPA;DB=4.
        JSR QUANT
        LDDPA; DB=13.
        LDSPI 0,DB=30000.
        LDSPI 1,DB=12.
        LDSPI 2,DB=10000.
        LDDPA;DB=4.
        JSR QUANT
*       NOISE ONLY CFAR
LOOP1: LDDPA; DB=13.
        LDSPI 0,DB=DPY(0)
        LDSPI 1,DB=10000.
        LDSPI 2,DB=0.
        LDSPI 6,DB=493.
        LDSPI 7,DB=507.
        LDSPI 15,DB=500.
        LDSPI 13,DB=DPX(-2)
        LDDPA; DB=4.
        JSR CFAR
*       TARGET + NOISE CFAR
        LDDPA; DB=13.
        LDSPI 0,DB=DPY(0)
        LDSPI 1,DB=10000.
        LDSPI 2,DB=2.
        LDSPI 6,DB=493.
        LDSPI 7,DB=507.
        LDSPI 15,DB=30000.
        LDSPI 13,DB=DPX(-2)
```

Table E-2 (cont'd)

```
        LDDPA; DB=4
        JSR CFAR
        LDDPA; DB=13
        LDSPI 1,DB=DPX(1
        DEC NMON;DPX(1),<SPFN
        BEQ FIN
        JMP LOOP
FIN:    LDDPA; DB=13.
        LDSPI 1,DB=DPX(-4.
        MOV NMON,NMON;DPX(1)<SPFN
        LDSPI 14,DB=DPX(1)
        DEC M100;DPX(1),<SPFN
        BEQ FIN1
        JMP LOOP
FIN1: LDDPA;DB=4.
        RETURN
$END
$
```

SUBROUTINE CFAR

PURPOSE: To simulate two CFAR algorithms: Cell averaging and greatest-of

FORTRAN CALLS: Call CFAR (NWD1, NT, OA, NN, TB, TA, TCI)

PARAMETERS:
NWD1 = Half of CFAR window width
NT = Total number of inputs
OA = AP output address
NN = Number of cells skipped
TB = AP address before cell of interest
TA = AP address after cell of interest
TCI = AP address for cell of interest

EXTERNALS: None

SCRATCH: SP (0-2, 6-7, 13-15)

Table E.3. Subroutine CFAR

```
$TITLE CFAR
*       AP PROGRAM TO SIMULATE TWO CFAR
*       ALGORITHMS: CELL AVERAGING AND
*       GREATEST-OF. THERE ARE SEVEN
*       INPUTS:
*         NWD2  -  HALF OF CFAR WINDOW WIDTH
*         NT    -  TOTAL NO. OF INPUTS
*         OA    -  AP OUTPUT ADDRESS
*         NN    -  NO. OF CELLS SKIPPED
*         TB    -  AP ADDRESS BEFORE CELL OF INTEREST
*         TA    -  AP ADDRESS AFTER CELL OF INTEREST
*         TCI   -  AP ADDRESS FOR CELL OF INTEREST
$ENTRY CFAR,7
   NWD2 $EQU   0
   NT   $EQU   1
   OA   $EQU   2
   NN   $EQU  13
   TB   $EQU   6
   TA   $EQU   7
   TCI  $EQU  15
   NS   $EQU  14
 CFAR:  MOV NWD2,NS
        DEC NS
        SUB NS,TB
        LDTMA; DB=!ONE
        NOP
        DPX(2)<TM
        MOV OA,OA; SETMA
        NOP
        NOP
        DPY(3)<MD;INCMA
        NOP
        NOP
        DPY(-4)<MD
        LDSPI 10,DB=8.
        MOV 10,10; SETMA
        NOP
        NOP
        DPY(0)<MD;INCMA
        NOP
        NOP
        DPY(-3)<MD
*   LOOP FOR ADDING N PREVIOUS  CELLS
LOOP4:  FADD ZERO,ZERO;MOV TB,TB;SETMA
        FADD
        MOV NWD2,NS
LOOP1:  INCMA;DPX<MD
        FADD DPX,FA;DEC NS
        FADD ;BGT LOOP1
        DPX(-2)<FA
*   LOOP FOR ADDING N FORWARD  CELLS
        FADD ZERO,ZERO;MOV TA,TA;SETMA
        FADD
        MOV NWD2,NS
LOOP2:  INCMA;DPX<MD
        FADD DPX,FA;DEC NS
        FADD ;BGT LOOP2
        DPY(1)<FA
*   ADDING SUMS AND STORING IN DPX(0)
        FADD DPY(1),DPX(-2)
        FADD
        DPX<FA
*   FINDING LARGEST SUM AND STORING IN DPX(-3)
```

Table E.3 (cont'd)

```
        FSUB DPX(-2),DPY(1)
        FSUB
        DPX(-3)<DPX(-2)
        BFGT LOOP3
        DPX(-3)<DPY(1)
LOOP3:  ADD NN,TA
        ADD NN,TB
*    MULTIPLY SUMS BY K/N
        FMUL DPX(0),DPY(0)
        FMUL DPX(-3),DPY(-3)
        FMUL
        FMUL;DPX<FM
        FMUL; DPX(-3)<FM
        MOV TCI,TCI;SETMA
        NOP
        NOP
        DPY(2)<MD
*    PERFORM CA THRESHOLD COMPARE
        FSUB DPY(2),DPX(0)
        FADD
        NOP
        BFGE CROSS
        BR FIN
CROSS:  FADD DPX(2),DPY(3)
        FADD
        DPY(3)<FA
*    PERFORM GO THRESHOLD COMPARE
FIN:    FSUB DPY(2),DPX(-3)
        FADD
        NOP
        BFGE CROS1
        BR FIN1
CROS1:  FADD DPX(2),DPY(-4)
        FADD
        DPY(-4)<FA
FIN1:   ADD NN,TCI
        SUB NN,NT
        BEQ FIN2
        JMP LOOP4
*    STORE NO. OF DETECTIONS
FIN2:   MOV 0A,0A
        MI<DPY(3);SETMA
        NOP
        MI<DPY(-4);INCMA
        NOP
        LDDPA; DB-4.
        RETURN
@END
$
```

SUBROUTINE VRANDX

PURPOSE: To generate an array of random numbers uniformly distributed between 0 and 1.

FORTRAN CALL: Call VRANDX (A,X,I,N)

PARAMETERS: A = Address of starting seed

X = Base address of output array

I = Increment between elements of output array

N = Number of output samples desired

FORMULA: Technique used is multiplicative congruential method.

X(0) = MOD(B*A,1·0) where B = 27.0

X(M) = MOD(B*X(M-1), 1.0) for M=1,2...,N-1

EXTERNALS: None

SCRATCH: SP (0-3, DPX (0-2), DPY (0)

NOTES: 1. Preferred starting seed is 0.2510637948.

2. At completion the seed is set for the last number generated.

Table E.4. Subroutine VRANDX

```
*##### VRANDX - VECTOR RANDOM NUMBERS /COMMON/ - REL 3.0, AUG 77 #####
*       FOR EITHER MEMORY
        $TITLE VRANDX
        $ENTRY VRANDX,4
*
*       ---ABSTRACT---
*FILLS VECTOR C WITH A SEQUENCE OF FLOATING POINT RANDOM NUMBERS
*UNIFORMLY DISTRIBUTED BETWEEN 0.0 AND 1.0.  SEQUENCE IS GENERATED
*USING A SEED A.  FOLLOWING GENERATION THE SEED IS SET TO THE LAST
*RANDOM NUMBER GENERATED, THUS ALLOWING THE SEQUENCE TO BE CONTINUED
*IN THE NEXT CALL TO VRAMP. SUGGESTED SEED FOR FIRST CALL IS 0.2510637948.
*
*TECHNIQUE USED IS MULTIPLICATIVE CONGRUENTIAL METHOD.
*FORMULA:  C(0)=MOD(B*A,1.0)          WHERE B=27.0
*          C(K)=MOD(B*C((K-1)K),1.0)  FOR K=1 TO N-1
*       AND  A = C((N-1)K)
*
*       ---STATISTICS---
*LANGUAGE: APAL
*EQUIPMENT: AP-120 WITH EITHER MEMORY
*SIZE: 16 LOCATIONS
*SPEED: INTRO: 5 CYCLES
*       LOOP:  7-8  CYCLES (7.1 CYCLES AVERAGE)
*       COLUMNS/LOOP: 1
*       FLOPS/LOOP:   3
*       1.19N + 0.83 USEC, FOR 167 NSEC CLOCK
*       MEGAFLOPS: 2.52
*SUBROUTINES USED: NONE
*AUTHOR: R.S. NORIN
*DATE:   JAN 77
*
*       ---USAGE---
*FORTRAN: CALL VRANDX(A,C,K,N)
*APAL:    JSR VRANDX
*S-PAD PARAMETERS
*   NAME     NUMBER
     A  SEQU  0                  *ADDRESS OF SEED
     C  SEQU  1                  *BASE ADDRESS OF DESTINATION VECTOR C
     K  SEQU  2                  *INCREMENT BETWEEN ELEMENTS OF C
     N  SEQU  3                  *NUMBER OF ELEMENTS IN C
*TABLE MEMORY
 ONE  SEQU  !ONE
*
*SCRATCH:  SP(1,3), DPX(0-2), DPY(0), DPA UNCHANGED
*
*
VRANDX:  MOV A,A; SETMA          *GET SEED A
         RPSF B; DPX<DB          *GET MULTIPLIER B
        LDTMA;DB=ONE
         RPSF FMASK; DPX(2)<DB   *GET FRACTION MASK
         FMUL DPX,MD;            *B*A
             DPX(1)<TM;          *SAVE 1.0
             SUB K,C             *BACK UP DESTINATION ADDRESS
LOOP:    FMUL                    *PUSH
         FMUL                    *PUSH
         FSUB FM,DPX(1);         *FORM B*A-1 SINCE METHOD OF
                                 *EXTRACTING FRACTION WILL BE DIFFERENT
                                 *IF B*A<1.0
             DPY<FM              *SAVE B*A FOR LATER
         FADD                    *PUSH
         FAND DPX(2),DPY         *ASSURE B*A>1 SO
                                 *FRACTION CAN BE EXTRACTED WITH MASK
         FADD ZERO,DPY;          *GET FRACTION DIRECTLY IF B*A<1
```

Table E.4 (cont'd)

```
            DEC N;                  'DECREMENT COUNT
            BFGT GT1                'GET FRACTION IMMEDIATELY FROM
                                    'FA IF B#A>1
        FADD; MOV N,N               'THIS IS AN EXTRA CYCLE
                                    'IN LOOP IF B#A<1
GT1:    ADD K,C;SETMA;MI<FA;        'STORE RANDOM NUMBER
            FMUL DPX,FA;            'START FORMING NEXT NUMBER
            BNE LOOP                'CONTINUE UNTIL
DONE:   MOV A,A; SETMA; MI<FA;      'DONE. THEN STORE LAST RANDOM
                                    'NUMBER AS THE NEW SEED.
        RETURN                      'THEN EXIT.
B:  $FP  27.0                       'MULTIPLIER CONSTANT
FMASK:  $FP  0.9999999925           'FRACTION MASK
        $END
$
```

SUBROUTINE RANDM

PURPOSE: Generates an array of random numbers which are independent and have a Gaussian distribution.

FORTRAN CALL: Call RANDM (A, X, N, MEAN, STD, SCR)

PARAMETERS:

A = Address of starting seed

X = Base address of output array

N = Number of samples desired

MEAN = Location of the desired mean value

STD = Location of the desired standard deviation

SCR = Base address of scratch storage (N words of scratch storage are required)

FORMULA: Starting from two random numbers u_1 and u_2 which are uniformly distributed between 0 and 1, two Gaussian numbers with desired mean and standard deviation are obtained as

$$m_1 = n_1 \sigma + \mu$$

$$m_2 = n_2 \sigma + \mu$$

where

$$n_1 = \sqrt{-2 \ln u_1} \cos (2\pi u_2)$$

$$n_2 = \sqrt{-2 \ln u_1} \sin (2\pi u_2)$$

EXTERNALS: VRANDX, LN, SQRT, COS, SIN

SCRATCH: SP (0-9), DPX (-3, -2, 0-2), DPY (-3, -2, 0)

NOTES: N words of scratch storage are required

Table E.5. Subroutine RANDM

```
$TITLE RANDM
$ENTRY RANDM,6
$EXT VRANDX,LN,SQRT,COS,SIN
  SEED $EQU 0
     X $EQU 1
     N $EQU 2
  MEAN $EQU 3
  STDV $EQU 4
     Z $EQU 5
    MS $EQU 6
    XS $EQU 7
    N2 $EQU 10
     Y $EQU 11
    X1 $EQU 3
    X2 $EQU 4
RANDM: MOV MEAN,MEAN; SETMA
       MOV N,MS
       MOV STDV,STDV; SETMA
       INC N; DPX(-3)<MD
       MOVR N,N2; LDTMA; DB='TWOPI
       MOV X,Y; DPY(-3)<MD
       MOV X,XS; DPX(-2)<TM
       ADD N2,Y
       MOV N,3
       LDSPI 2,DB=1.
       JSR VRANDX
       MOV XS,X;SETMA
       MOV XS,X1
       DEC X1
       MOV N2,N
LOOP1: DPX<MD; JSR LN
       JSR SQRT
       INC X;SETMA
       DEC N
       INC X1; SETMA; MI<DPX; BNE LOOP1
       MOV N2,N
       MOV Y,X;SETMA
       MOV Z,X1
       DEC X1
LOOP2: FMUL DPX(-2),MD
       FMUL; MOV X1,X2
       FMUL; ADD N2,X2
       DPY(-2)<FM
       DPX<FM; JSR COS
       INC X1; SETMA; MI<DPX
       DPX<DPY(-2); JSR SIN
       INC X;SETMA
       DEC N
       INC X2; MI<DPX; SETMA; BNE LOOP2
       MOV N2,N
       DEC Y
       MOV XS,X; SETMA
       MOV XS,X2
       MOV Z,X1; SETMA
       DPX<MD; DEC X2
       ADD N2,X1; SETMA
LOOP3: FMUL DPX,MD
       FMUL; INC X; SETMA
       FMUL DPX,MD
       INC X2; SETMA; MI<FM; FMUL
       FMUL; DPX<MD
       INC Y; SETMA; MI<FM
       NOP
       INC Z; SETMA
```

Table E.5 (cont'd)

```
        DEC N; LDTMA; DB<SQRT2
        INC XI; SETMA; BNE LOOP3
        FMUL TM,DPY(-3), MOV XS,X; SETMA
        FMUL; DEC XS
        FMUL; INC X; SETMA
        DPY(-3)<FM; FMUL FM,MD
        FMUL
LOOP4:  FMUL DPY(-3),MD
        FADD FM,DPX(-3); INC X; SETMA
        FADD; FMUL; DEC NS
        INC XS; SETMA; MI<FA; BNE LOOP4
        RETURN
$END
$
```

SUBROUTINE WEIBUL

PURPOSE: To generate an array of clutter amplitudes (one for each clutter cell of interest) where the spatial statistics of clutter power are described by a Weibull distribution and zero correlation.

FORTRAN CALL: Call WEIBUL (S,X,B,NC,A)

S = Address of seed for random number generation

X = Base address of output array

B = Base address of array [B(i)] containing the median powers from each clutter cell

NC = Number of samples (clutter cells) desired

A = Address of Weibull parameter, a

FORMULA:

$$X(i) = \sqrt{B(i)\left[\left(\ln \frac{1}{u(i)}\right)\right]^{a}} \quad i=0.1,\ldots,(NC-1)$$

where [u(i)] is a set of random numbers which are uniformly distributed between 0 and 1.

EXTERNALS: VRANDX, LN, EXP, VSQRT

SCRATCH: SP (0-8, 13-15), DPX (-4-3), DPY (-4-3)

NOTES: The array [B(i)], which is prestored, must reflect the variation of clutter power between different clutter cells.

Table E.6. Subroutine WEIBUL

```
$TITLE WEIBUL
$ENTRY WEIBUL,5
$EXT VRANDX,LN,EXP
  SEED $EQU 0
   CON $EQU 2
     K $EQU 1
     N $EQU 3
     A $EQU 4
  CONS $EQU 5
    KS $EQU 6
    NS $EQU 7
   KSS $EQU 4
WEIBUL:MOV A,A; SETMA
       MOV CON,CONS
       MOV N,NS
       MOV K,KS; DPY(-3)<MD
       LDSPI 2.DD-1.
       JSR VRANDX
       DEC CONS
       MOV KS,KSS
       MOV KS,K; SETMA
       DEC KS
       MOV NS,N
  LOOP:DPX(0)<MD; JSR LN
       JSR LN
       FMUL DPX(0),DPY(-3); MOV CONS,CONS; SETMA
       FMUL
       FMUL
       DPY(-2)<MD
       DPX(0)<FM;JSR EXP
       FMUL DPX(0),DPY(-2)
       FMUL; INC K; SETMA
       FMUL; DEC N
       INC KS; SETMA; MI<FM; BNE LOOP
       NOP
       RETURN
  $END
```

SUBROUTINE QUANT

PURPOSE:	To truncate detector outputs
FORTRAN CALL:	Call QUANT (X,Q,N)
PARAMETERS:	X = Base address of input and output
	Q = Base address of LJB level
	N = Number of inputs
EXTERNALS:	Div
SCRATCH:	SP (0-4), DPX (-1, 0, 1, 3), DPT (-1, -2)

Table E.7. Subroutine QUANT

```
$TITLE QUANT
$ENTRY QUANT,3
$EXT DIV
    X $EQU 0
    Q $EQU 1
    N $EQU 2
    Y $EQU 3
    T $EQU 4
QUANT:MOV X,Y; SETMA
      LDTMA; DB=!ONE
      MOV Q,Q; SETMA
      DEC Y; DPX(-1)<MD
      FABS DPX(-1); DPY(0)<TM
      FADD; DPY(1)<MD; DPX(0)<MD
      DPY(-1)<FA
      JSR DIV
      FMUL DPX(0),DPY(-1)
      LDTMA; DB=!HALF
      FMUL; DPY(0)<DPX(-1)
      FMUL; DPX(1)<TM
      LDSPI T; DB=27.; DPX(2)<FM
 LOOP:FIXT DPX(2)
      FADD
      DPX(3)<FA; INC X; SETMA
      FADD ZERO,MDPX(3); MOV T,T
      FADD
      FADD DPX(1),FA; DPY(0)<MD
      FABS DPY(0)
      FMUL DPY(1),FA; FSUB DPX(-1),ZERO
      FMUL DPX(0),FA; FADD
      FMUL; DPX(-1)<DPY(0)
      DPY(2)<FM; BFGT POS
      FSUBR DPY(2),ZERO
      FADD
      DPY(2)<FA
  POS:FMUL; DEC N
      INC Y;SETMA; MI<DPY(2); BNE LOOP; DPX(2)<FM
      RETURN
 $END
$
```

REFERENCES

1. J. I. Marcum, "A Statistical Theory of Detection by Pulsed Radar and a Mathematical Appendix," IRE Trans. Vol. IT-6, April 1960, pp. 59-308.
2. P. Swerling, "Probability of Detection for Fluctuating Targets," Rand Corporation, Research Memorandum RM-1217, 17 Mar 1954.
3. J. O. Rice, "Mathematical Analyses of Noise," Bell System Tech. J. 23, 1944, pp. 282-332.
4. G. M. Watson, A Treatise on the Theory of Bessel Functions, MacMillan, New York, 1944.
5. P. Beckmann, Probability in Communications Engineering, Harcourt, Brace and World, Inc., New York, 1967.
6. R. Nitzberg, "Constant-False-Alarm-Rate Signal Processors for Several Types of Interference," IEEE Trans. AES-8, January 1972, pp. 27-34.
7. D. P. Meyer and M. A. Mayer, Radar Target Detection, Academic Press, New York, 1973.
8. J. D. Moore, "Performance Analysis for Radars Utilizing a Multiple CFAR Processor," Final Report on D.O. 1079, Battelle Columbus Laboratories, August 1979.
9. A. Papoulis, Probability, Random Variables, and Stochastic Processes, McGraw-Hill, New York, 1965.
10. V. G. Hansen, "Constant False Alarm Rate Processing in Search Radars," IEEE 1973 International Radar Conference, London, England, 23-25 October 1979, pp. 325-332.

REFERENCES (cont'd)

11. J. D. Moore and N. B. Lawrence, "Comparison of Two CFAR Methods Used with Square Law Detection of Swerling I Targets," IEEE 1980 International Radar Conference, 28-30 April 1980, pp. 403-408.

12. V. G. Hansen and H. R. Ward, "Detection Performance of the Cell Averaging Log/CFAR Receiver," IEEE Trans. AES-8, September 1972, pp. 648-652.

13. V. G. Hansen and J. H. Sawyer, "Detectability Loss Due to 'Greatest-of' Selection in Cell Averaging CFAR," IEEE Trans. AES-16, January 1980, pp. 115-118.

14. H. M. Finn and R. J. Johnson, "Adaptive Detection Mode with Threshold Control as a Function of Spatially Sampled Clutter-Lead Estimates," RCA Rev. Vol. 29, September 1968, pp. 414-464.

15. H. M. Finn, "Adaptive Detection in Clutter," Proc. of National Electronics Conference, Vol. 22, 1966, pp. 562-567.

16. L. Novak, "On the Detection Performance of a Cell-Averaging CFAR in Non-Stationary Weibull Clutter," 1974 IEEE International Symposium on Information Theory, 27-31 October 1974, pp. 998-1031.

17. M. Abramowitz and I. A. Stegun, Handbook of Mathematical Functions with Formula, Graphs, and Mathematical Tables, US Department of Commerce, Bureau of Standards, Applied Math Series No. 55, US Government Printing Office, Washington, DC June 1964.

18. R. R. Boothe, "The Weibull Distribution Applied to the Ground Clutter Backscatter Coefficient," Technical Report RE-69-15, US Army Missile Command, Redstone Arsenal, Alabama, June 1969.

REFERENCES (cont'd)

19. A. E. Gibson, "Adaptive Detection Probabilities for Fluctuating Target Models in Nonhomogeneous Gaussian Noise," IEEE Trans. AES-9, January 1973, pp. 113-115.

20. P. S. Tong and P. E. Steichen, "Performance of CFAR Devices in ECM Environments," Technology Services Corporation Internal Memo TSC-W4-65, 17 February 1976.

21. G. B. Goldstein, "False-Alarm Regulation in Log-Normal and Weibull Clutter," IEEE Trans. AES-9, January 1973, pp. 84-92.

DISTRIBUTION

	No. of COPIES
Commander US Army Materiel Development & Readiness Command ATTN: DRCCG DRCRD 5001 Eisenhower Avenue Alexandria, VA 22333	 1 1
Commander Ballistic Missile Defense Systems Command ATTN: BMDSC-HR P. O. Box 1500 Huntsville, AL 35807	1
Director Ballistic Missile Defense Advanced Technology Center ATTN: ATC-R P. O. Box 1500 Huntsville, AL 35807	2
Commander US Army Electronics Research & Development Command ATTN: DRSEL, Mr. Fishbien DRCPM-MALR Fort Monmouth, NJ 07703	 1 1
US Army Materiel Systems Analysis Activity ATTN: DRXSY-MP Aberdeen Proving Ground, MD 21005	1
IIT Research Institute ATTN: GACIAC 10 West 35th Street Chicago, IL 60616	1
DRCPM-MDE, Mr. Evans	1
-HAE, Mr. Ams	1
-ROL, Mr. Bishop	1
DRSMI-R, Dr. McCorkle	1
-RE, Mr. Lindberg	1
-REO	1
-REG	1
-RER, Mr. Low	1
Mr. Lawrence	25
-RE, Record Set	1
-RG	1
-RD	1
-LP, Mr. Voigt	1
-RPR	15
-RPT, Record Copy	1
Reference Copy	1